

**Neuronal correlates of visuo-motor
integration: modulation of oscillatory
activity due to cortical stimulation and age**

Dissertation

zur Erlangung des Grades eines Doktors
der Naturwissenschaften

der Fakultät für Biologie
und
der Medizinischen Fakultät
der Eberhard-Karls-Universität Tübingen

vorgelegt

von

Carola Renate Ilse Arfeller

aus Leipzig

29. 10. 2010

Tag der mündlichen Prüfung:

17. 12. 2010

Dekan der Mathematisch-
Naturwissenschaftlichen Fakultät:

Prof. Dr. Wolfgang Rosenstiel

Dekan der Medizinischen Fakultät:

Prof. Dr. Ingo B. Autenrieth

1. Berichterstatter:

Prof. Dr. Christoph Braun

2. Berichterstatter:

PD Dr. Michael Schrauf

Prüfungskommission:

Prof. Dr. Christoph Braun

PD Dr. Michael Schrauf

Prof. Dr. Gerhard Eschweiler

PD Dr. Ingo Hertrich

Prof. Dr. Dirk Wildgruber

Eidesstattliche Erklärung

Hiermit versichere ich, dass ich die hier vorliegende zur Promotion eingereichte Arbeit mit dem Titel „*Neuronal correlates of visuo-motor integration: modulation of oscillatory activity due to cortical stimulation and age*“ selbstständig verfasst, nur die angegebenen Quellen und Hilfsmittel benutzt und wörtlich oder inhaltlich übernommene Stellen als solche gekennzeichnet habe. Ich versichere an Eides statt, dass diese Angaben wahr sind und dass ich nichts verschwiegen habe. Mir ist bekannt, dass die falsche Abgabe einer Versicherung an Eides statt mit Freiheitsstrafe bis zu drei Jahren oder mit Geldstrafe bestraft wird.

Tübingen, den 29.10.2010

Unterschrift

Für den Mann mit den schönsten braunen Augen der Welt

If the brain were simple enough for us to understand it, we would be too simple to understand it.

Ken Hill

Danksagung

Ich möchte an dieser Stelle die Gelegenheit nutzen, all denen meinen herzlichsten Dank auszusprechen, die direkt und indirekt dazu beigetragen haben, dass ich dieses Mammutprojekt stemmen konnte.

Zu aller erst möchte ich mich bei meinem Doktorvater Prof. Dr. Christoph Braun bedanken, dafür dass er mich in einer anfangs ausweglos erscheinenden Situation unterstützt und die Finanzierung, um die Arbeit zu Ende bringen zu können, sichergestellt hat. Darüber hinaus möchte ich mich auch für die äußerst kompetente Betreuung bedanken, ohne die ich die Studien nicht hätte durchführen können. Kein geringerer Dank gebührt Dr. Hubert Preissl, der mir während der gesamten Arbeit unzählige Male nicht nur computer- und technische Probleme aus dem Weg geräumt und mir die Fortsetzung meiner Arbeit im MEG-Zentrum überhaupt ermöglicht hat. Bei Prof. Dr. Eschweiler bedanke ich mich ganz herzlich für die Beratung bei der Studie über die altersbedingten Veränderungen und Unterstützung bei der Probandenrekrutierung.

Ich möchte mich ganz herzlich bei den Mitgliedern meines Advisory Boards, Prof. Dr. Christoph Braun, PD Dr. Michael Schrauf und Prof. Dr. Gerhard Eschweiler für ihr Interesse an meiner Arbeit und ihre Unterstützung bedanken.

I cordially thank Dr. Christos Papadelis who developed the strategy for the data analysis of the MEG study, and who did not only teach me analyzing data but a lot more things important in life. Without him I would never have been able to continue my work on the MEG project. Thank you SO much!

I would like to express my sincere gratitude to my current supervisor, Dr. Luigi Cattaneo, for his patience and support in finishing my thesis.

Ganz herzlich bedanken möchte ich mich auch bei der ehemaligen Arbeitsgruppe „Hirnstimulation“ an der Klinik für Psychiatrie und Psychotherapie. Das sind im Einzelnen: Dr. Albrecht Rilk, der mir mit einem unerschütterlichen Glauben in meine Fähigkeiten gezeigt hat, dass das Wasser nicht so tief ist, wie ich anfangs befürchtet hatte. Maren Reinl, die zu allen möglichen und unmöglichen Zeiten mit kreativen Ideen aufwartet. Dr. Sarah Schlipf, die unermüdliche Aufbauarbeit geleistet hat und selbst aus dem Krankenbett heraus noch die medizinische Beratung für die Studie mit den älteren Leuten übernommen hat. Sowie Dr. Surjo Soekadar, der mich mit den „richtigen“ Leuten bekannt gemacht hat und auf den ich v. a. immer dann zählen kann, wenn die Zeit ganz knapp ist. Prof. Dr. Christian Plewnia danke ich für meinen Start in Tübingen und die Freiheit, meine Doktorarbeit selbst in die Hand zu nehmen.

Nicht weniger herzlich möchte ich mich bei dem Team vom MEG-Zentrum bedanken. Dr. Anja Wühle, die mich beim Antragschreiben sehr unterstützt hat, die meisten meiner Probanden mit mir im Kernspin gemessen hat und mir in den letzten Zügen des Schreibens geholfen

hat, meine Gedanken zu strukturieren. Krunoslav Stíngl und Matthias Witte, die mir oft bei technischen Problemen während der Messungen geholfen haben. Gabi Walker-Dietrich und Maike Borutta, die mich gelehrt haben, MEG-Messungen korrekt durchzuführen. Sabine Frank und Dr. Ralf Veit danke ich für das Messen der Probanden im Kernspin. Gabi, Tanja, Anja und Sabine, danke für die vielen Gespräche nicht über die Arbeit! Und Tanja herzlichen Dank, dass Du mir in Deinem Büro Asyl gewährt hast. Jürgen Dax sei gedankt für das Programmieren des experimentellen Setups sowie für die vielen verlängerten Arbeitstage, um mich nicht mit der Technik allein zu lassen.

Sincere thanks are also given to Andrea Mognon and to Emanuele Olivetti for never getting tired of discussing ways to analyze the data and coming up with very helpful advices.

I would also like to thank the MEG team at the CIMeC in Trento. Gianpaolo Demarchi for never getting tired of answering questions, and Gianpiero Monittola, Luigi Tamé, and Elisa Leonardelli for the fun we share.

Prof. Dr. Horst Herbert und PD Dr. Annette Werner möchte ich ganz herzlich für ihren Einsatz danken, das Stipendium zu bekommen.

Meinen Eltern, Renate und Armin Arfeller, bin ich zutiefst dankbar dafür, dass sie neben den finanziellen v. a. die ideellen Voraussetzungen dafür geschaffen haben, einen solchen Ausbildungsweg einzuschlagen. Meinem Bruder und dem Rest meiner Familie - allen voran meiner Tante Uli und meiner Cousine Beate - danke ich für den Rückhalt und das Vertrauen in mich, das Richtige zu tun.

Meinen Freunden möchte ich meinen allerherzlichsten Dank aussprechen, dafür, immer ein offenes Ohr zu haben, mich bei meinen Vorhaben zu unterstützen und für die schönen Zeiten, die wir teilen. Das sind v. a.: Sabine Bosch, Ute Heinemeyer, Sophie Kappich, Klara Müller, Simone und Matthias Schmauch, Sarah Schlipf, Surjo Soekadar, Gabrielle Travers-Podmaniczky, Sandy Wildau.

Bei den Mitgliedern des RV Pfeil Tübingen bedanke ich mich für die wunderbare Zerstreung und dafür, dass sie mir gezeigt haben, dass man jeden Berg bezwingen kann und immer ans Ziel kommt.

Last but not least möchte ich meinem Freund und Lebensgefährten Christoph Linnemann danken. Dafür, einfach immer da zu sein, an mich zu glauben und mich bedingungslos zu lieben. Danke!

Carola Arfeller

Contents

List of Abbreviations	iii
Zusammenfassung	1
Abstract	3
1 Introduction	5
1.1 Oscillatory Activities	5
1.2 Age Dependent Alterations	7
1.3 Electroencephalography and Magnetoencephalography	8
1.4 Transcranial Magnetic Stimulation	10
1.5 The Aims of the Thesis	12
1.5.1 First Study	12
1.5.2 Second Study	14
2 First Study: Visuo-motor Integration and Aging	15
2.1 Introduction: Aims and Hypotheses	15
2.2 Methods	15
2.2.1 Subjects and experimental Setup	16
2.2.2 Behavioural Tasks	17
2.2.3 Data Acquisition	19
2.2.4 MEG Data Analysis	20
2.2.5 EEG Data Analysis	25
2.2.6 Statistical Analysis	26
2.3 Results	28
2.3.1 Alertness and Tiredness	29
2.3.2 Performance	29
2.3.3 MEG Data	29
2.3.4 EEG Data	39
2.3.5 Summary of Results	41
2.4 Discussion	44

3	Second Study: Asynchronous Bifocal Stimulation	51
3.1	Introduction: Aims and Hypotheses	51
3.2	Methods	51
3.2.1	Subjects	52
3.2.2	Stimuli and Procedure	52
3.2.3	EEG Recording	54
3.2.4	Offline Analysis	55
3.2.5	Statistical Analysis	57
3.3	Results	58
3.3.1	Alertness and Tiredness	59
3.3.2	Power Spectra	59
3.3.3	Coherence	61
3.3.4	Summary of Results	66
3.4	Discussion	68
4	Conclusion	71
	Bibliography	75
	List of Figures	89
	List of Tables	91
	Personal Contribution to the Studies	93
	Curriculum Vitae	95

List of Abbreviations

ANOVA	Analysis of Variance
APB	M. abductor pollicis brevis
AR	autoregressive modeling
BOLD	blood oxygen level dependent
ECD	Equivalent Current Dipole
ECR	extensor carpi radialis
EEG	Electroencephalography
EMG	Electromyogram
EOG	Electrooculogram
FFT	Fast Fourier Transformation
IFG	Inferior frontal gyrus
ICA	Independent Component Analysis
LTD	Long Term Depression
M	motor
M1	Primary Motor Cortex
MEG	Magnetoencephalography
MEP	Motor Evoked Potential
MNE	Minimum Norm Estimation
MNI	Montreal Neurological Institute
MSE	mean square error

LIST OF ABBREVIATIONS

MSR	magnetically shielded room
MT	Motor Threshold
PLV	phase locking value
PMv	ventral Premotor Cortex
ppTMS	paired pulse TMS
PSP	Postsynaptic Potential
PT	Phosphene Threshold
RMSE	root mean square error
ROI	Region of Interest
ROIs	Regions of Interest
ROP	right opponens pollicis
rTMS	repetitive Transcranial Magnetic Stimulation
SI	Primary sensory cortex
SII	Secondary somatosensory cortex
SAM	Synthetic Aperture Magnetometry
SE	Standard Error of the Mean
SnPM	Statistical nonParametric
SQUID	Superconducting Quantum Interference Device
SRCoh	Stimulation Related Coherence
SRN	signal to noise ratio
SRPower	Stimulation Related Power
TMS	Transcranial Magnetic Stimulation
V	visual
V1	Primary Visual Cortex

VM	continuous visuo-motor
V + M	visual plus motor
VRS	Visual Rating Scale

Zusammenfassung

Frühere Ergebnisse zeigten, dass das Netzwerk für visuomotorische Integration hauptsächlich aus präzentralen und occipito-parietalen Arealen besteht. Die „Binding“ Theorie vermutet, dass die Integration von räumlich verteilter Information in eine kohärente Wahrnehmung auf die Bildung vorübergehender funktioneller Netzwerke basiert. Basierend darauf wird hypothetisiert, dass die Integration von multimodalen sensorischen Eingängen und motorischer Kontrolle erreicht wird, indem die verschiedenen darin involvierten Hirnareale durch phase locking miteinander gekoppelt werden. Es ist ebenfalls weithin bekannt, dass sich die Morphologie und Neurophysiologie des Gehirns im Verlauf des Alterns verändern. Das Ziel der hier vorliegenden Dissertation war (1.) die neuronalen Mechanismen, die der visuomotorischen Integration unterliegen, weiter zu beleuchten, (2.) zu untersuchen, welche altersabhängigen Veränderungen auftreten und (3.) zu erforschen, ob es möglich ist, kortiko-kortikale Kopplung durch *repetitive transkranielle Magnetstimulation (rTMS)* simultan appliziert auf zwei kortikale Areale zu modulieren. Dafür wurden zwei Studien entworfen. Das Ziel der ersten Studie dieser Arbeit war es, die Mechanismen, die zur visuomotorischen Integration beitragen und altersbedingte Veränderungen zu untersuchen. Vier verschiedene Altersgruppen (25 Jahre, 40 Jahre, 60 Jahre und 80 Jahre) wurden rekrutiert und kombiniert *Magneto-enzephalographie (MEG)/ Elektroenzephalographie (EEG)* aufgezeichnet, während die Probanden eine *visuomotorische (VM)*, rein *visuelle (V)*, rein *motorische* oder eine *visuell + motor (V + M)* Aufgabe (ohne Feedback) ausführten. Mit Hilfe von *Synthetic Aperture Magnetometry (SAM)*, einer Beamformertechnik für die MEG Quellenlokalisierung, und einer Gruppenanalyse der lokalisierten Quellen wurden die Regionen, die zum Netzwerk der visuomotorischen Integration gehören, identifiziert. In einem zweiten Schritt wurden Powerspektrum und Kohärenz, ein Maß für kortiko-kortikale Kopplung, für die MEG- und die EEG-Daten berechnet. Wir konnten frühere Ergebnisse replizieren, die besagen, dass das Netzwerk für visuomotorische Integration occipito-parietale und präzentrale Regionen beinhaltet. Wir fanden die früher beschriebene Verschiebung der Hirnaktivität zu mehr präfrontale Arealen in den älteren Probanden. Die Älteren zeigten eine insgesamt höhere neuronale Aktivität, ausgeprägter im Betafrequenzbereich, verglichen mit den jungen Probanden. Wir fanden einen Trend für eine erhöhte Aktivität

des Parietalkortex bei den älteren Probanden. Wir fanden eine Tendenz in Richtung früherer Berichte, dass das Altern einhergeht mit der fortschreitenden Beeinträchtigung motorischer Leistung, die ebenfalls mit früheren Ergebnissen korrespondiert. Und wir konnten frühere Ergebnisse über kortiko-kortikale Kopplung zwischen den Arealen, die in visuomotorische Integration involviert sind, nicht replizieren und wir konnten auch eine Abnahme der Kohärenz während dem Ausführen der visuomotorischen Aufgabe bei einem Vergleich der jungen und alten Probanden nicht bestätigen.

Das Ziel der zweiten Studie war es, die Ergebnisse zu erweitern, dass rTMS simultan appliziert auf zwei unterschiedliche Hirnregionen, kortiko-kortikale Kopplung gemessen mit EEG-Kohärenz erhöht. Dafür wurden vier Bedingungen von bifokal angewendeter rTMS entworfen. Eine synchrone Stimulation, und drei asynchrone Stimulationen, d. h. es war eine kurze zeitliche Verzögerung zwischen den beiden abgegebenen Pulsen über *V1* (*primärer visueller Kortex*) und *M1* (*primärer motorischer Kortex*): entweder 3 ms, 7 ms oder eine zufällige Verzögerung zwischen 0 ms und 7 ms. Die synchrone Stimulation erwies sich als diejenige, die die Kohärenz zwischen M1 und V1 unmittelbar nach der Stimulation erhöhte. Dieser Effekt verschwand nach 15 Minuten.

Die Ergebnisse lassen darauf schließen, dass Quellenlokalisierung mit MEG-Daten unter Verwendung einer Beamformertechnik eine zuverlässige Methode darstellt, um kortikale Netzwerke, die in multimodale Integration involviert sind sowie altersbedingte Veränderungen zu identifizieren. Weiterführende Analysen des zeitlichen Verlaufes der Aktivität in diesen identifizierten Regionen würden Einblick in die Zeitskala integrativer neuronaler Prozesse geben. Bisher gibt es unterschiedliche Ansätze um kortiko-kortikale Kopplung zu analysieren, aber weiterführende methodische Entwicklungen sind notwendig, um diese Analysestrategien zum extrahieren der synchronisierten Aktivitäten zu verbessern.

Abstract

Previous findings showed that the network for visuo-motor integration comprises mainly precentral and occipito-parietal regions. The binding theory assumes that the integration of spatially distributed information into a coherent percept is based on transiently formed functional networks. Based on that it is hypothesized that the integration of multimodal sensory input and motor control is achieved by linking the various involved brain areas by phaselocked oscillatory activity. It is also widely known that the morphology and neurophysiology of the brain changes along the course of aging. The present thesis aimed (1.) to further elucidate the neuronal mechanisms underlying visuo-motor integration, (2.) to investigate which alterations occur depending on aging and (3.) to explore whether it is possible to modulate cortico-cortical coupling using *repetitive Transcranial Magnetic Stimulation (rTMS)* applied simultaneously to two cortical sides. Therefore, two studies were designed. The first study of this thesis aimed to investigate mechanisms contributing to visuo-motor integration and changes occurring during healthy aging. Four different age groups (25 years, 40 years, 60 years, and 80 years) were recruited and combined *Magnetoencephalography (MEG)/ Electroencephalography (EEG)* was recorded while subjects performed a *continuous visuo-motor (VM)*, *visual (V)*, *motor (M)*, or *visual plus motor (V+M)* (without feedback) task. Using *Synthetic Aperture Magnetometry (SAM)*, a beamformer technique for MEG source localization, and performing a group level analysis of the localized sources, the regions contributing to the network for visuo-motor integration were identified. In a second step, the power spectra and coherence, a measure for cortico-cortical coupling, were computed for MEG and EEG data. We could replicate former results stating that the network for visuo-motor integration comprises occipito-parietal and precentral cortices. We found the formerly described shift of brain activity to more prefrontal areas in the elderly subjects. The elderly showed an overall higher neuronal activity, yet more pronounced in the beta frequency, compared to young adults. We found a tendency in an increased activity of the parietal cortex in the elderly. We found a tendency towards previous reports that aging is accompanied by progressing impairment of motor performance which also corresponds to previous findings. And we could not replicate previously reported results on cortico-cortical coupling between the areas involved in

visuo-motor integration, nor could we confirm the decrease of coherence in the VM task when comparing young and elderly subjects.

The second study that aimed to extend the findings that rTMS applied simultaneously to two distinct brain regions increases cortico-cortical coupling as measured with EEG coherence. Four conditions of bifocally applied rTMS were designed. A synchronous stimulation, and three asynchronous stimulation, i. e. there was a short delay between the two pulses given to *Primary Visual Cortex (V1)* and *Primary Motor Cortex (M1)*: either 3 ms, 7 ms or a random delay between 0 ms and 7 ms. The synchronous stimulation proved to be the one to increase the coherence between M1 and V1 immediately after stimulation. This effect vanished after 15 minutes.

The findings suggest that source localization of MEG data using a beamformer technique is a reliable tool to identify cortical networks involved in multimodal integration and to identify aging related alterations. Further analysis of the time course of these identified regions would give an inside on the temporal scale of integrative neuronal processing. To date, there are several approaches to analyze cortico-cortical coupling, but further methodological developments are necessary to improve analysis strategies for extracting the synchronized activities.

1 Introduction

An apparently simple everyday action, like goal directed grasping of a certain object, is in fact a highly complex procedure involving multimodal sensory and motor processes. But how does the human brain integrate the sensory information such as visual and haptic input, and simultaneously controls the motor system? This question can be answered in a few words:

„The anatomical structure and functional mechanisms in the human brain are governed by two conflicting principles: specialization and integration. Both principles are optimally implemented by complex, modular, and highly interconnected networks of neurons.“

(Schnitzler and Gross 2005a, p. 175)

The functioning of both principles acting in concert is crucial for all actions requiring goal-directed motor behaviour. Identifying the brain regions and functional networks involved in sensorimotor integration is therefore important not only for understanding „normal“ functioning but also age related changes and pathological conditions. So far, it is widely accepted that a cortical network comprising posterior parietal (occipito-parietal) and premotor areas (precentral cortices) accounts for visuo-motor integration processes (Andersen and Buneo 2002, Battaglia-Mayer and Caminiti 2002, Caminiti et al. 1998, Kalaska et al. 1997, Medendorp et al. 2008, Thoenissen et al. 2002, Wise et al. 1997).

1.1 Oscillatory Activities

For integrating information it is not sufficient to activate or deactivate specialized brain regions (Belardinelli et al. 2006). In addition to changes in activation, dynamic and coordinated interactions between various cortical and subcortical neuronal assemblies are assumed. Similar to multi-sensory integration in object recognition where different features are processed at different spatially distributed brain locations and subsequently

merged to an object representation, also sensory-motor tasks require the integration of sensory information and forwarding it to premotor and motor areas. In object recognition the binding theory (Singer 1993, Singer and Gray 1995) assumes that the integration of spatially distributed information into a coherent percept is based on transiently formed functional networks. The integration is achieved by linking the various brain areas by phaselocked oscillatory activity. This model has been adopted for other sensory modalities as well as for sensorimotor integration. Synchronized oscillatory activity of distant cortical regions as measured by cortico-cortical coherence has been put forward as an index for the coupling and integration of activity (for review see Engel et al. 2001, Fries 2005, Schnitzler and Gross 2005b).

Coherence reflecting the spatio-temporal correlation between two oscillatory signals (Engel and Singer 2001) can be quantified using methods providing high temporal resolution, such as *Magnetoencephalography (MEG)* and *Electroencephalography (EEG)* (Gross et al. 2003, Belardinelli et al. 2006).

Over the past decade, several findings led to controversial attribution of information processes and oscillatory activity in distinct frequency ranges. Some studies show the occurrence of high frequency oscillations (gamma [30 - 90 Hz]) over short distances, while long range synchrony is mostly observed in lower frequency ranges (theta [3 - 8 Hz], alpha [8 - 13 Hz], beta [13 - 30 Hz]) (Kopell et al. 2000, von Stein and Sarnthein 2000, for review see Schnitzler and Gross 2005b). Depending on task demands, it has been shown that large scale synchrony also appears in the alpha band when mastering higher cognitive tasks, such as mental calculation, and working memory tasks (Palva and Palva 2007). Other results suggest that higher cognitive and perceptual processes are associated with higher frequencies such as gamma (Miltner et al. 1999, Keil et al. 2001). Moreover, long range synchronization was found in different frequency ranges in the motor system (for review see Tallon-Baudry and Bertrand 1999, Schnitzler and Gross 2005b). Cell assemblies comprising more neurons are believed to oscillate slowly (Singer 1993) and are likely to be spatially more extended than rapidly oscillating cell assemblies, a notion that has also been supported by modeling studies (da Silva 1991, 1996, Traub et al. 1996). Multimodal integration tasks such as visuomotor tracking were associated with enhanced interregional synchronization predominantly in the lower beta (13-21 Hz) frequency range (Classen et al. 1998). Accordingly, it is hypothesized that each frequency band contains distinct components, which in turn reflect specific functions (Kolev et al. 2002, Klimesch et al. 2007). However, looking at the literature, a coherent picture is still missing: for instance, Miltner et al. (1999), Keil et al. (2001) show that higher cognitive tasks are processed in higher frequency bands while Palva and Palva (2007)

demonstrates the opposite. The discrepancy might be explained by the weakness of the network-related oscillatory activities with respect to cerebral background activity. But also methodological issues referring to the recording modality and the signal analysis may account for the differences.

1.2 Age Dependent Alterations

It is well known that the neurophysiology of the brain changes along the course of aging. For example, motor related activity has been shown to undergo age dependent alterations. In the healthy adolescents, activity in the motor cortex is associated with contralateral effector movement (Kolb and Wishaw 1996, Graziadio et al. 2010), while in childhood as well as in elderly there is no such lateralization (Graziadio et al. 2010).

With respect to task related changes of oscillatory activity three alterations occurring in the alpha range are mainly described: general decrease of spectral alpha power, foremost in occipital regions; alpha slowing due to reduction of dominant alpha frequency; shift in the distribution of alpha spectral power and alpha incidence from posterior to anterior areas (Kolev et al. 2002, for review see Niedermeyer 1997, Palva and Palva 2007, Rossini et al. 2007). In addition, there is evidence that the spatial distribution of EEG activity becomes unified in elderly subjects, and thereby, the hemispheric specialization is abandoned. Generally, the progressive loss of interhemispheric inhibition is thought to cause this „blurring“ of cortical activation in the elderly (Labyt et al. 2006). It might well be that the „blurring“ of the topography of oscillatory activity could be a correlate of the age related degradation of cortical networks. Alternatively, it has been speculated that topographic flattening might reflect a compensatory process by which the decline of specific neuronal connections is counterbalanced by an increase of the general coupling between cortical regions (Babiloni et al. 2000, Rossini and Forno 2004).

To date, there are more studies investigating oscillatory activities in pathological aging processes such as Alzheimer's Disease and Parkinson (e. g. Maestú et al. 2004, 2006, Moazami-Goudarzi et al. 2008, Montez et al. 2009, Stoffers et al. 2007) than in normal aging. So far, there are a few studies on oscillatory activities and age dependent alterations in healthy elderly people. For example, using EEG and a visuo-motor task (Labyt 2003, Labyt et al. 2004, 2006), whereby in this case the visually presented target was a fixed point and the subjects had to perform a self-initiated brief wrist extension (*contraction*) or a voluntary *relaxation* of maintained moderate contraction of the *extensor carpi radialis (ECR)*. They (Labyt 2003) reported a decrease of coherence

in the elderly compared to younger subjects. In a very recent study, subjects were asked to maintain a steady, low level isometric contraction of the *right opponens pollicis (ROP)* by opposing the right thumb and index finger against the resistance of a compliant object (Graziadio et al. 2010) while EEG was recorded. There are even less studies on MEG, oscillatory activity and age dependent alterations in healthy people. One study used a combined cognitive-motor task in which subjects had to respond to a specific colour–letter combination in a *go/nogo* task while recording (Vallesi et al. 2010). In another study, spontaneous oscillations in the *Primary sensory cortex (SI)* were investigated by means of tactile evoked responses (Ziegler et al. 2010).

Taken together, to our knowledge there are so far no studies examining oscillatory activity in healthy elderly people using MEG, nor combined MEG and EEG in a continuous visuo-motor task.

1.3 Electroencephalography and Magnetoencephalography

For studying the dynamics of information processing in the human brain, *Electroencephalography (EEG)* and *Magnetoencephalography (MEG)* are very well suited non-invasive methods taking advantage of the electrophysiological properties of the brain by measuring neuronal activity. While EEG measures the differences of the electric potential on the scalp, MEG captures the magnetic fields accompanying the current flow generated by thousands of neurons acting in concert (Hämäläinen et al. 1993, Diekmann et al. 1999). According to Biot-Savart’s law (the right-hand rule), any electrical current (in this case: the neuronal activity) causes a circular magnetic field that is orthogonal to the orientation of the current.

For the acquisition of EEG, electrodes are attached to the surface of the scalp and connected to a differential amplifier (Lutzenberger et al. 1985). What we call EEG is the pattern of variation in voltage over time that is displayed as curves in the output of the amplifier. The amplitude usually varies between approximately -100 and $+100 \mu\text{V}$, and the frequency ranges up to 40 Hz or more (Coles and Rugg 1995).

The weak magnetic field caused by the current flowing in the brain can be detected using highly sensitive, i. e. helium cooled superconducting sensors, so called *Superconducting Quantum Interference Devices (SQUIDs)* magnetometers (Hämäläinen et al. 1993,

Diekmann et al. 1999). In a so called whole-head MEG system, the SQUIDS are arranged in a dewar in whose vicinity the subject's head is placed during MEG recording.

While MEG most likely picks up the magnetic field of only the intracellular (mainly intradendritic) currents, EEG is also sensitive to the extracellular current distribution. It is assumed that the intradendritic currents originate from *Postsynaptic Potentials (PSPs)* in the dendrites of cortical pyramidal neurons (Diekmann et al. 1999). Therefore, the dendrites have to be oriented parallel to each other and perpendicular to the cortical surface in order to contribute to the field picked up by the MEG. If the orientation of dendrites differs from a parallel arrangement, their fields partially cancel each other and no activity can be captured (Diekmann et al. 1999).

The main problem one has to face when working with MEG is the low *signal to noise ratio (SRN)*, because the brains' signals are very weak and there are many sources of interference. In Figure 1.1 the magnitudes of various magnetic fields appearing in natural, technical, and physiological environments are displayed. Given the ratio between the spontaneous brain activity that is for alpha activity about 1 pT, and for evoked brain activity even less (about 0.1 pT), and the magnitude of the earth's steady field for example which is about eight to ten orders of magnitude higher, the necessity of a shielded room attenuating external magnetic fields and other noise suppression strategies, such as the usage of 3rd order gradiometers, hardware filtering, and background noise outprojection becomes obvious (Diekmann et al. 1999).

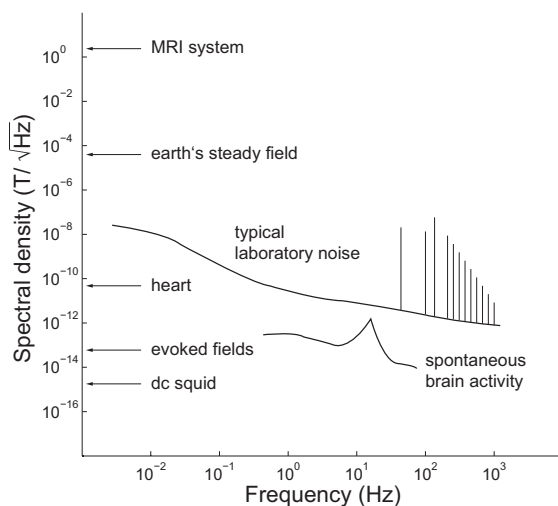


Figure 1.1: Examples of the magnitude of various magnetic fields as a function of frequency (i. e. spectral density). The peak of the spontaneous brain activity at ~ 10 Hz corresponds to alpha activity. The spectral lines on laboratory noise reflect the main frequency and it's harmonics. Considering the ratio between the magnitude of the brain activity and the earth's steady field, for example, a shielded room for the acquisition of MEG is essential. Graphic according to Diekmann et al. (1999).

Both techniques, EEG and MEG, provide a very high temporal resolution in the millisecond range which is perfect for studying oscillatory activities. However, MEG has a higher spatial resolution compared to EEG (Belardinelli et al. 2006), and is convenient for threedimensional source localization (Cuffin and Cohen 1979). While

EEG captures also radial sources, MEG is essentially sensitive to tangential sources only. Radial sources stem from regions of the cortex oriented tangentially to the scalp, i. e. in the gyri (Baule and McFee 1965, Vrba 2001). Tangential sources, can be imagined as current elements tangential to the surface of an imaginary sphere that comprises that brain.

The most common use of the MEG is like EEG the measurement of the time course of cortical activity by means of evoked responses, i. e. analysis on the *sensor level* (Hansen et al. 2010). However, to gain insight which brain region causes the captured cortical activity, the analysis on the *source level* is required. Source localization can only be calculated by an inverse solution which does not provide an unique solution (Helmholtz 1853) due to the infinite number of source configurations that constitute the same magnetic field pattern. Therefore, it is necessary to introduce further constraints and to include a priori information about the brain physiology and anatomy in order to solve the inverse problem.

In recent years, several approaches have been developed in order to reliably localize sources in the human brain. In general, there are two strategies. One is localizing discrete sources, by means of e. g. *Equivalent Current Dipoles (ECDs)* assuming a limited number of focal sources. The alternative is the localization of many distributed sources. *sLORETA* (Pascual-Marqui 2002), *Minimum Norm Estimation (MNE)* (e. g. Molins et al. 2008), and *Beamformers* (for an overview see e. g. Brookes et al. 2008, Papadelis et al. 2009) are some of the techniques.

1.4 Transcranial Magnetic Stimulation

Transcranial Magnetic Stimulation (TMS) is a well established method used for non-invasively stimulate cortical areas. Thereby, cortical neurons are depolarized based on the principle of electromagnetic induction (Barker et al. 1985, George et al. 1999), i. e. a short electric impulse is sent through a coil which causes – according to Faraday’s law – a magnetic field. The alteration of the magnetic field causes in the surrounding electric conductive tissue – in this case: brain tissue – a current, which activates the cortex depending on its current status of excitability. The advantage of the application of an external magnetic field compared to an electric field is that it passes the scalp and the liquor almost unimpeded (Epstein et al. 1990, Rudiak and Marg 1994). Placing the coil during TMS over the motor cortex activates neurons which trigger a response

in a muscle on the contralateral body site. The muscle response can be measured, e. g. in a small finger muscle, as a *Motor Evoked Potential (MEP)*.

Applying series of rapid consecutive single stimuli is called rTMS. rTMS causes activity changes in regions interconnected with the stimulated area through mono- or polysynaptic connections (Hayashi et al. 2004), modulates subcortical transmitter concentrations (Strafella et al. 2003), and induces morphological modifications in stimulated areas as well as in areas linked to them (May et al. 2007). These effects persist after the stimulation (Chen et al. 1997), are not restricted to the stimulated area (Lee et al. 2003, Plewnia et al. 2003b), and affect behaviour (Kobayashi et al. 2004).

Low frequency rTMS (≤ 1 Hz) has been shown to decrease the excitability of the motor cortex (Chen et al. 1997) in a LTD-like (Long Term Depression) manner, whereas high frequency rTMS (≥ 5 Hz) produces the direct opposite effect (Berardelli et al. 1998). It has been demonstrated that coherence can be differentially modulated by applying rTMS to the motor and premotor cortex with frequencies of 10 Hz (Jing and Takigawa 2000), 5 Hz (Serrien et al. 2002, Oliviero et al. 2003, Fuggetta et al. 2008), and 1 Hz (Strens et al. 2002, Chen et al. 2003). High as well as low frequency rTMS proved to be very useful investigating functional relevance of cortical activity. Based on these findings, rTMS is used experimentally to treat a wide range of clinical disorders that may involve altered states of cortical excitability (Hoffman and Cavus 2002), such as Tinnitus (Plewnia et al. 2003a, Folmer et al. 2006, Plewnia et al. 2007, Arfeller et al. 2009), major depression (Herwig et al. 2007, O'Reardon et al. 2007), auditory hallucinations (Aleman et al. 2007), and stroke (Talelli et al. 2007). Stefan et al. (2000) combined peripheral electrical stimulation of the median nerve and rTMS of the primary motor cortex that led rapidly (after just 90 stimuli) to an effect persisting at least 30 to 60 minutes. It can be assumed that a lasting, yet reversible, and topographically specific increase of neuronal activity was induced by the converging transsynaptic activation of cortical output neurons by rTMS and somatosensory afferent information by median nerve stimulation (Stefan et al. 2000, Wolters et al. 2003). For the interregional communication of neuronal cell assemblies for integrating multimodal sensory information and controlling the motor system accordingly, Hebb (Hebb 1949) suggested a mechanism whereby an increase in synaptic efficacy arises from the presynaptic cell's repeated and persistent stimulation of the postsynaptic cell.

The question arises whether combining stimulation of two cortical sides could also increase the effect on neuronal activity and functional connectivity. While a few groups used *paired pulse TMS (ppTMS)*, i. e. two consecutive single pulses, on different cortical sites, e. g. on *ventral Premotor Cortex (PMv)* and M1 (Koch et al. 2006, O'Shea et al.

2007, Davare et al. 2009, Mars et al. 2009, Buch et al. 2010) in order to investigate the functional role of these areas in the execution of specific tasks, e. g. grasping, Plewnia et al. (2008) were the first to apply synchronous bifocal rTMS to the motor and visual cortex, respectively. The effects of synchronous bifocal *vs.* monofocal rTMS on long-range synchronization of human brain activity were compared using coherence measured with EEG. In the bifocal condition, the cortico-cortical coherence, serving as a measure of functional connectivity, between the sensorimotor and the visual cortex on the stimulated (left) side increased within two minutes after the train of rTMS. The effect could be observed up to 10 minutes after stimulation. In the monofocal condition, i. e. stimulation of the primary motor cortex alone, were no effects on coherence. The authors concluded that synchronous bifocal rTMS applied over two cortical sides enhance cortico-cortical coupling. The question remained whether a short temporal delay between the pulses given to M1 and V1, i. e. an asynchronous bifocal stimulation, would be more or less effective compared to the simultaneous stimulation.

1.5 The Aims of the Thesis

The aim of the thesis was threefold:

1. to investigate the neuronal mechanisms underlying multimodal integration processes using the visuomotor system as an example
2. to examine the age dependent alterations of oscillatory brain activity occurring in the visuomotor system
3. to explore whether it is possible to modulate those mechanisms.

Therefore, two studies were designed.

1.5.1 First Study

The first study aimed to further elucidate the processes involved in visuomotor integration. Thereby, two main questions arised: what are the general mechanisms underlying these processes, and could age dependent alterations be observed?

Oscillatory Activities and Visuomotor Integration

According to previous findings, i. e. that the network involved in visuo-motor integration comprises mainly precentral (premotor and motor areas) and occipito-parietal (visual areas and parietal cortex) regions (Andersen and Buneo 2002, Battaglia-Mayer and Caminiti 2002, Caminiti et al. 1998, Kalaska et al. 1997, Medendorp et al. 2008, Thoenissen et al. 2002, Wise et al. 1997) and that large scale oscillatory activities are mainly found in alpha and beta frequency ranges (Classen et al. 1998, Kopell et al. 2000, von Stein and Sarnthein 2000), we designed the present study in order to replicate the findings and to extend these results. In particular, we predicted to confirm the findings of Classen et al. (1998) using EEG, that is cortico-cortical coupling of EEG channels covering the motor/premotor area and the visual cortex. In order to extend these findings, we combined MEG and EEG, since MEG provides a better spatial resolution than EEG (Belardinelli et al. 2006), and is better suited for threedimensional source localization (Cuffin and Cohen 1979). We hypothesized that analyzing MEG on the source level using a beamformer technique, would provide more detailed spatial information about the regions involved in the visuo-motor integration task and about their cortico-cortical coupling.

The well established *continuous visuo-motor (VM)* task used here, required the tracking of a visual target changing continuously in size by adapting the force of a pinch grip (Belardinelli et al. 2007, Braun et al. 2007, Gerloff et al. 2006). This task is a good example of functional cooperation between visual and motor areas, since it poses a demand on the brain to continuously analyze the visual signal showing the discrepancy between requested and actually generated force and to produce an adequate force accordingly. The specificity of the functional network was studied in control tasks according to the study of Classen et al. (1998). Therefore, our subjects performed additionally to the VM task a pure motor *motor (M)*, a pure visual *visual (V)*, and a *visual plus motor (V+M)* task. In the latter, the task was the same as in the VM condition, but no feedback about the performance was given.

Visuomotor Integration and Age Dependent Alterations

Given the few known age dependent alterations and frequency component's organization, we hypothesized firstly, an age dependent shift of the frequency component reflecting multimodal integration processes, i. e. a more pronounced activation in the beta range

compared to the alpha range. The second hypothesis stated that the hemispheric lateralization of motor-related activity will be found in the younger group, but not in the elderly. The third prediction was to find a decrease of coherence in the VM task when comparing the younger group with the elderly.

1.5.2 Second Study

In order to extend the finding that coupling of oscillatory activity can be selectively enhanced by synchronous rTMS given to two distinct brain areas (Plewnia et al. 2008), the present study was designed to compare the effects of three different asynchronous bifocal rTMS stimulations *vs.* the synchronous bifocal stimulation.

2 First Study: Visuo-motor Integration and Age Dependent Alterations

The study described in the following chapter is about the dynamic changes of functional connectivity underlying visuo-motor integration and about possible changes in connectivity patterns depending on the age.

2.1 Introduction: Aims and Hypotheses

The present study aimed: to confirm the findings of Classen et al. (1998) using EEG, that is cortico-cortical coupling of EEG channels covering the motor/premotor area and the visual cortex. To gain a more detailed insight in the processes, we combined MEG and EEG. We hypothesized that analyzing MEG on the source level using a beamformer technique, would provide more detailed spatial information about the regions involved in the visuo-motor integration task. With respect to age dependent alterations, we expected to find a gradual course of the changes that have been described in several studies. These are the shift of activity from posterior to more frontal areas, a „blurring“, i. e. an increasing reduction of hemispheric lateralization from the young to the oldest group, and a decrease in task specific coherence.

2.2 Methods

In this section, the details of the experimental procedure and the steps of data analysis will be described. The experiment was conducted at the MEG-Center of the University of Tübingen.

2.2.1 Subjects and experimental Setup

In total, 44 volunteers participated in the study. They were recruited among the student population in Tübingen, the University hospital staff, and via announcement in the local newspapers. The study was approved by the ethics committee of the Medical Faculty of the University of Tübingen. All subjects gave written informed consent prior to the experiment according to the Declaration of Helsinki and received monetary compensation. Participants were assigned to four different age groups ranging from 25 to 85 years (see Table 2.1).

Table 2.1: Participants

Group	Mean Age (Std)	N	Gender Ratio
Group I	24.60 (± 1.8)	12	6 females
Group II	39.89 (± 3.0)	11	5 females
Group III	57.68 (± 2.7)	12	6 females
Group IV	79.75 (± 4.4)	9	5 females

All participants were right handed according to the Edinburgh handedness inventory (Oldfield 1971) and were free of known past or present mental health or neurological problems. Additionally, all subjects of Group III and Group IV were screened for indications of dementia using the *DemTect* (Kessler et al. 2000, Kalbe et al. 2004). The *DemTect* a questionnaire designed to evaluate the functioning of verbal memory, verbal fluency, intellectual flexibility, and attention. The raw scores are coded according to different age groups and are therefore comparable between groups independent from age and education. The scale ranges from „0“ to „18“, 13 and above indicate normal cognitive abilities. Within Group III the mean score was 17.1 (± 1.5) and in Group IV 16.6 (± 1.5).

During the experiment, the participants were seated comfortably inside a light dimmed *magnetically shielded room (MSR)*. They were asked to fixate on a stationary cross displayed in the middle of a screen placed ~ 1 m in front of them (see Figure 2.1 on page 17) in order to maintain central fixation. To reduce the number of eye-blinks during recordings, participants were also asked to refrain from blinking as much as possible.



Figure 2.1: Experimental Setup of the study on visuomotor integration. Inside a magnetically shielded room, subjects were placed with their head carrying the EEG cap in a helmet shaped dewar. The screen displaying the feedback and the fixation cross was ~ 1 m in front of the subject and the pinch grip to the subject's right side.

2.2.2 Behavioural Tasks

Participants accomplished four tasks in total. In the VM integration task, participants tracked a sinusoidally-varying target stimulus by exerting force isometrically using their thumb and second digit to press against a force sensor pinch grip (Figure 2.2).

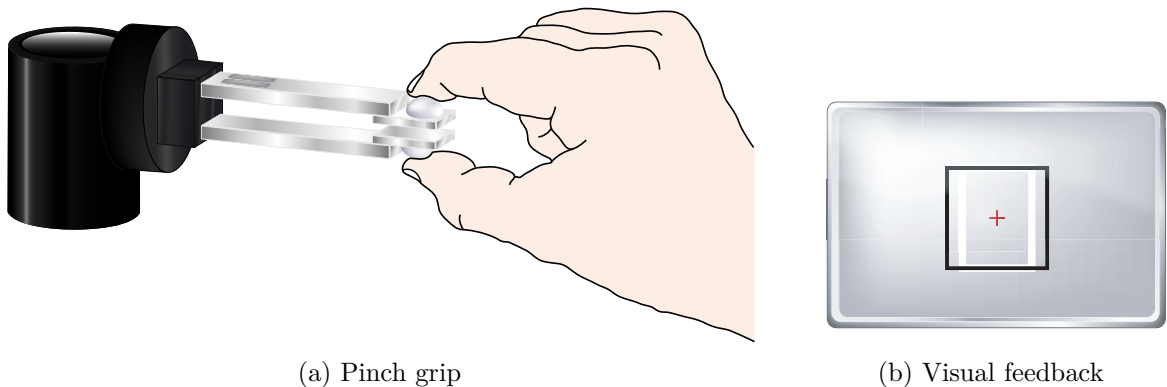


Figure 2.2: (a) Pinch grip, i. e. a force transducer that measures the isometric contraction applied to a manipulandum. (b) The visual feedback about the requested (black rectangle) and the actual, from the subject produced force (white rectangle), is shown.

The force of the isometric contraction was measured by a force transducer, designed and constructed at the University of Tübingen (Belardinelli et al. 2007, Braun et al. 2007, Gerloff et al. 2006), using strain gauges affixed to the upper and lower surface of

a manipulandum. The difference between the requested and the actually produced force was continuously visualised by a white rectangle changing its size horizontally with a frequency of 0.3 Hz projected on the screen in front of the participant (Figure 2.1 on the previous page).

A black stationary rectangle on the screen served as reference (Figure 2.2 on the preceding page) and participants were asked to align both rectangles as precisely as possible. The visual feedback was projected in the middle of the screen by using a projector (PLC-XP41, Sanyo) standing outside the magnetically shielded room. The projector provided the visual feedback on the screen through a cut-away portal in the shield. The screen size was 1024×768 pixels and the monitor refresh rate was 60 Hz. The extreme positions of the target beam subtended a visual angle of 4° . To avoid learning effects and to gain a relatively stable intra-individual performance, participants became familiar with the *continuous visuo-motor (VM)* task in a training session preceding the MEG recordings.

In the *visual plus motor (V + M)* task, participants were instructed to produce the same sinusoidal isometric finger activation as in *continuous visuo-motor (VM)*, but were not provided with visual feedback about their force production. In the *visual (V)* task, the participants watched the sinusoidally-varying target and the stationary stimulus without performing the pinch grip task. In the *motor (M)* task, the participants were instructed to imagine a metronome implying a pulse every other second and press the manipulandum correspondingly with half the amount of their maximum force. In this condition, both rectangles remained stationary and aligned on the screen. The order of the tasks was randomized between subjects. Each subject performed five blocks in total: two blocks of VM, and one of V, M, and V + M each. The experimental procedure for each block is depicted in Figure 2.3 on the next page. Each block took 10 min and 30 s and consisted of three trials and each trial lasted 3 min and 30 s. Each trial started with 1 min of baseline recording during which the participants fixated the stationary cross without performing any motor task. Then subjects performed the task (either VM, V, M or V + M) for 2 min. The task was followed by a 30 s interval during which the participants could relax their eyes from fixation and blink if necessary (see Figure 2.3 on the facing page). Before each block and after the last block *Alertness* and *Tiredness* were assessed by means of a *Visual Rating Scale (VRS)*. Subjects were asked to rate their current status of alertness (*extremely bad* \leftrightarrow *extremely good*) and tiredness (*none* \leftrightarrow *extremely tired*) on a scale ranging from 0 to 10.

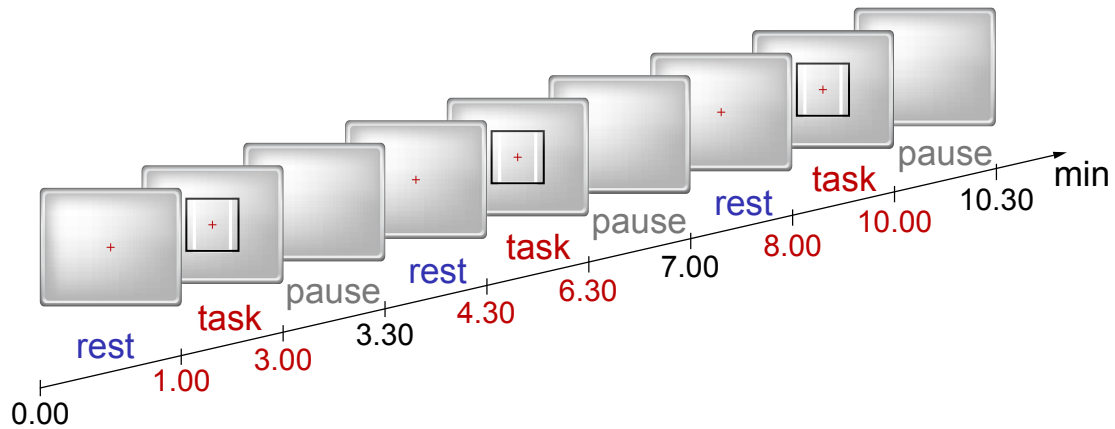


Figure 2.3: Schematic representation of the experimental procedure. Each block of either VM, V, M or V + M lasted 10 min, 30 s and consisted of three trials. Each trial started with 1 min baseline, followed by 2 min task performance and ended with 30 s pause during which participants could relax their eyes.

2.2.3 Data Acquisition

Whole head MEG was recorded simultaneously with combined EEG and *Electromyogram (EMG)*.

MEG Recordings Whole-head MEG recordings were acquired using a 275-channel axial gradiometer system (VSM MedTech Ltd) sampled at 585.93 Hz and band-passed at 0-200 Hz. An additional 29 reference channels were recorded for noise cancellation purposes. The signals recorded by the axial gradiometers were analyzed as synthetic third order gradiometers (Vrba and Robinson 2001). To enable the coregistration of MEG data with the anatomical brain scans, three coils were placed at the nasion and pre-auricular points prior to MEG data acquisition. The coils at the fiducial localisation served to continuously monitor the position of the subjects' head relative to the MEG sensors. After each acquisition, the coils were removed and on their locations were carefully placed radio-opaque washers for off-line coregistration of the recorded MEG data with the structural MR images obtained from each subject. Participants' performance was also continuously recorded with the same sampling rate as MEG (Figure 2.4 on the next page).

Standard CTF software was used to filter offline the MEG data by using a 3 Hz high pass filter, a 50 Hz notch filter (and its harmonics), and by removing the DC offset. The recorded MEG signal was visually inspected for possible artifacts.

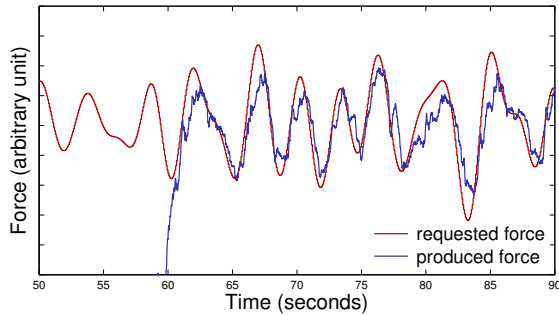


Figure 2.4: Example of 30 seconds performance of the visuo-motor integration task of one subject. Each trial started with one minute rest, at 60 seconds the screen switched from the fixation cross to the task, where the requested and the produced force was displayed.

EEG Recordings EEG was recorded from 33 scalp positions (Ag-AgCl electrodes) according to the standard 10-20 system referenced to the left and right mastoids and grounded to FPz (see Figure 2.7 on page 26). The recording parameters were the same as for the MEG data. Electrode impedances were kept below 5 k Ω . The *Electrooculogram (EOG)* was recorded at FP1 and FP2 in order to exclude trials contaminated with eye movements from further analysis. Electromyographic activity was recorded bipolarly from the *M. abductor pollicis brevis (APB)* of the right hand. The filter parameters of the MEG data were also applied to the EEG data.

Exclusion of Datasets In total, 220 datasets were collected, five datasets for each subject. Datasets from five subjects were excluded from further analysis due to the following reasons:

Group I	one	low performance
Group II	one	low signal to noise ratio
Group III	two	heavy artifact contamination in MEG data
Group IV	one	no structural MR image, because the subject was afraid that the noise during scanning would increase her tinnitus

2.2.4 MEG Data Analysis

In the following section the MEG data analysis will be described.

MEG Source Activity Estimation

Source activity was estimated using the *Synthetic Aperture Magnetometry (SAM)* (Robinson and Vrba 1998), a well-established spatial filtering tomographic scanning technique based on the nonlinear constrained minimum-variance beamformer. Volumetric images of source power (pseudo z-statistics) were estimated by sequentially applying the

beamformer to a number of locations placed on a regular grid spanning the whole brain. Task-related changes in brain activity were assessed by differential estimates of power integrated over pre-defined time windows for both active and baseline activity. The detailed algorithm is described elsewhere (Vrba and Robinson 2001). The *active* state was defined as the 30 s following the onset of the VM task according to the participants' performance recordings, or in case of artifacts, as 30 s free of artifacts within the time window of task performance. The *baseline* states (rest) were defined as the 30 s windows preceding the VM onset, or in case of artifacts, an artifact free period within the time window of the baseline state. The transition period, i. e. ~ 3.5 s when subjects reached the pinch grip to start performance were excluded at the end of the baseline state and the beginning of the active state. The source power difference was calculated between VM and rest (active *vs.* baseline) for each 2 mm cubic volume element within the conducting volumes. The spatial filters were calculated for the VM condition. These filters were later also used to estimate the brain activity during V, M, and V + M. A multiple local-sphere model served as head model. Pseudo-z statistical parametric images were computed on a voxel-by-voxel basis from the difference in source power between VM and rest. Broadband brain activity ranging from 0 to 70 Hz entered the analysis. Negative and positive pseudo-z values indicate source power decreases and increases respectively. The resultant volumetric maps were overlaid on the individual participant's structural MRI based on coregistration results. Details of the calculation of SAM pseudo-T source image statistics have been described in a number of reports (Brookes et al. 2007).

Group Level Analysis of MEG Source Activity

Each subject's MRI was spatially normalized into the *Montreal Neurological Institute (MNI)* template space using SPM5 (<http://www.fil.ion.ucl.ac.uk/spm/>) and the resulting normalization parameters were applied to the volumetric SAM images. Hence, all of the volumetric images were then in the same threedimensional coordinate space and could be carried forward into a group statistical analysis using the *Statistical nonParametric (SnPM)*. Within SnPM, analysis at the voxel level was performed using a multi-subject one-sample *t* test design. For group analysis of the MEG data, non-parametric permutation tests were conducted using for each group the full permutation set with 10 mm variance smoothing and thresholded at $P \leq 0.05$ (corrected, two-tailed) (Nichols and Holmes 2002, Singh et al. 2003). The permutation test statistical results were visualized using both SPM5 and xjview (<http://www.alivelearn.net/xjview8/>) on a the *avg152T1* MNI template. Individual spatial *Regions of Interest (ROIs)* were

identified by scanning individuals volumetric images resulting from the SAM analysis. In total, 12 ROIs were selected for each subject (see Table 2.2).

Table 2.2: Selected ROIs

Left Side, ROI number	ROI	Right Side, ROI number
1	prefrontal cortex	7
2	SII	8
3	IFG	9
4	M1/SI	10
5	parietal cortex	11
6	visual area	12

Estimation of Virtual Sensors' Time Courses

For each subject's ROI, the time course of source activity was estimated for the active state, i. e. the same time window used for the estimation of the source activity for each trial, as if a sensor was placed at that position in the brain (virtual sensor), using the individual's VM condition covariance matrices for the time window of the active state (Robinson and Vrba 1998, Cheyne et al. 2006). The virtual sensors' time-courses were FFT band-pass filtered (2-45 Hz), downsampled and normalized (zero-mean). In order to analyze the frequency domain features of the signals, 10s segments fulfilling the requirement of stationarity were selected for each trial and condition (i. e. three segments per condition of active and three segments of baseline activity for each condition).

Cross-Spectral Analysis of MEG Source Activity

The source activity signals were then stored in a $M \times N$ data matrix

$$Y = \{ym(n)\}, \quad n = 1, \dots, N, \quad m = 1, \dots, M \quad (2.1)$$

where M is the number of virtual sensors ($M=12$) and N the number of samples ($N=5632$) per segment.

The *Fast Fourier Transformation (FFT)* was computed using non overlapping segments of 1024 data points. For coherence analysis the magnitude squared cross spectrum (P) of the frequency range of interest (f , in our case: alpha range from 8-13 Hz and

lower beta band from 13.7- 24 Hz) was divided by the power spectra of both time series (Schnitzler and Gross 2005a).

$$Coh_{xy}(f) = \frac{|P_{xy}(f)|^2}{P_{xx}(f)P_{yy}(f)} \quad (2.2)$$

The power spectra and the coherence was calculated for the three 10 s windows which were treated as if being one 30 s window, since this has been shown to be the minimum time to provide reliable coherence values Terry and Griffin (2008).

In order to assess pure effects when comparing conditions and age groups, the power spectra of the active state was subtracted from the power spectra of the baseline (rest) state for each virtual channel. Figure 2.5 on the following page shows an example of the power spectra for the baseline (*rest*) state, the active state (*task*) as well as for the subtracted mean Δ Power for the two extreme age groups, i. e. Group I and Group IV. Any further analysis was done using the *Rest-Task* values.

Analogue, for the coherence anylsls the baseline state was subtracted from the active state for each virtual channels and for all further analysis the *Task-Rest* values were used. In Figure 2.6 on page 25 an example channel combination (left M1/SI – left visual area) is displayed showing the coherence values for the rest and the task activity averaged across groups (left side) and the mean Δ Coherence of rest subtracted from task activity.

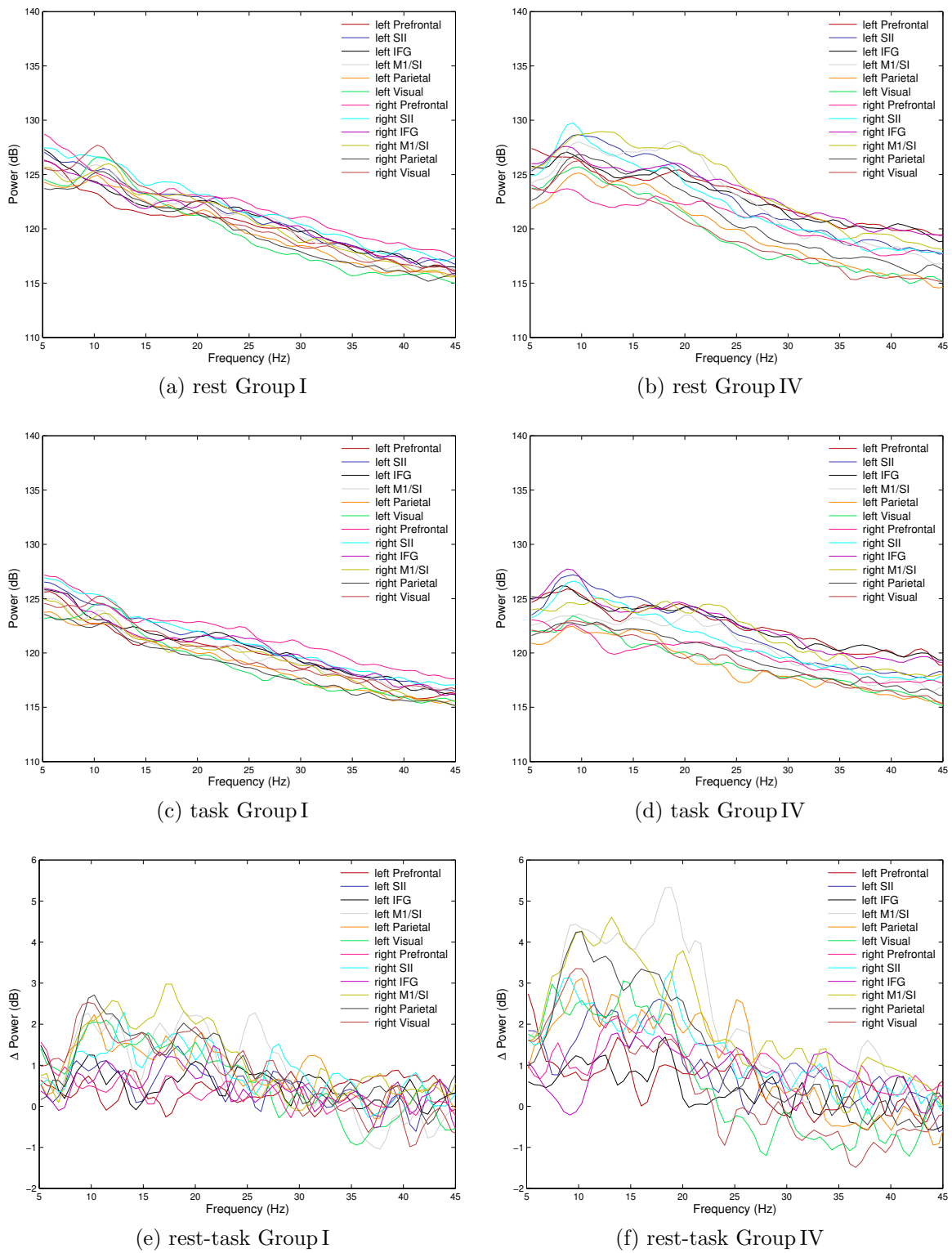


Figure 2.5: Power spectra of rest (top row) and task (middle row), and the mean Δ Power of task subtracted from rest (bottom row) activity for Group I (left column) and Group IV (right column) in the condition VM are shown.

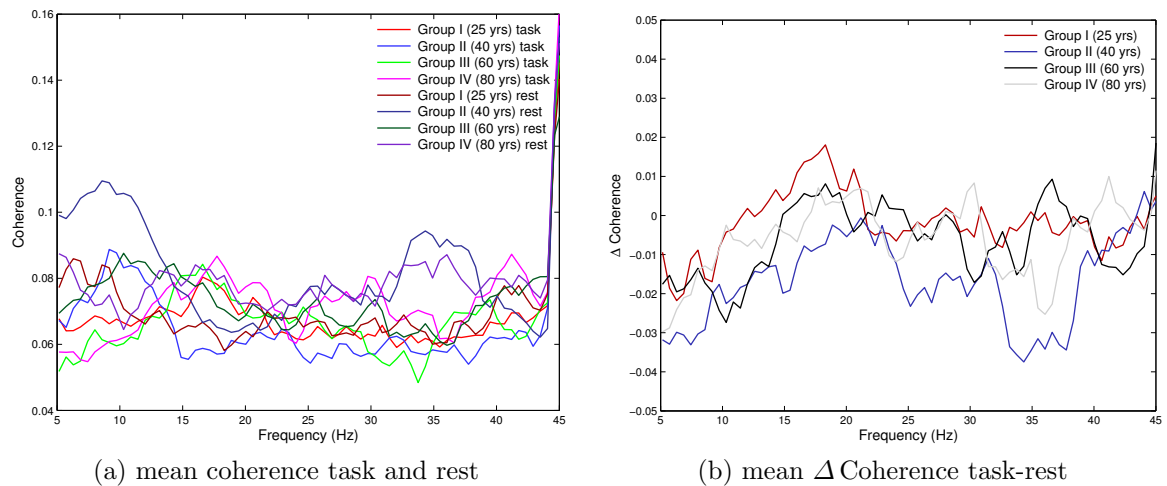


Figure 2.6: (a) The mean coherence of rest and task and (b) the mean Δ Coherence of rest subtracted from task activity for all age groups in the condition VM at the virtual channel combination left M1/ SI – left visual area are displayed.

2.2.5 EEG Data Analysis

The same segments of active and baseline periods as from the MEG data were extracted from the EEG data. In order to minimize effects of an active reference arising from spontaneous activity, channels of interest were bipolarized by subtracting the activity from two neighbored channels. Thereby, the channels were chosen according to the ROIs selected for the MEG data (see Table 2.2 on page 22). The following channels have been selected: left/ right prefrontal cortex: F3-Fz/ F4-Fz, left/ right M1/ SI: FC3-CP3/ FC4-CP4, left/ right SII: T7-TP7/ T8-TP8, left/ right parietal cortex: P7-P3/ P8-P4, and left/ right visual area: PO7-PO3/ PO8-PO4 (see also Figure 2.7 on the next page). The power spectra and the coherence of the EEG data were then calculated according to the formulas described in the previous section (see section 2.2.4 on page 22 starting on page 22).

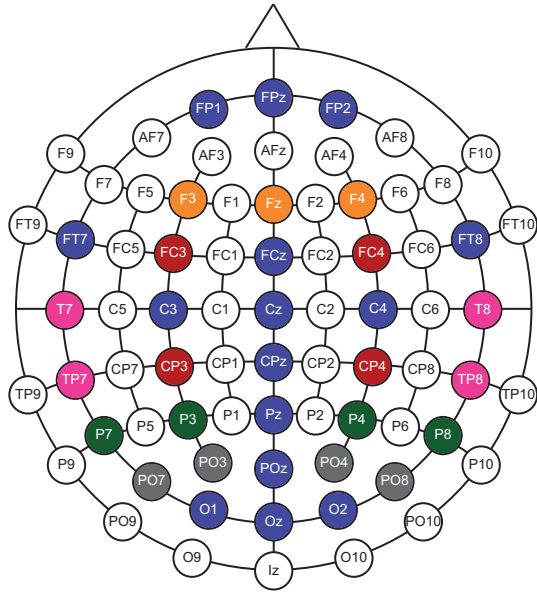


Figure 2.7: The scalp positions were chosen according to the standard 10-20 system. Channels were referenced to left and right mastoids, and grounded to FPz. The red marked channels are the ROIs according to the virtual channels of the MEG data. Therefore, two channels were bipolarized by subtracting one from another. For the left side: F3-Fz ($\hat{=}$ prefrontal cortex), FC3-CP3 ($\hat{=}$ M1/SI), T7-TP7 ($\hat{=}$ SII), P7-P3 ($\hat{=}$ parietal cortex), and PO3-PO7 ($\hat{=}$ visual area). Accordingly, F4-Fz, FC4-CP4, T8-TP8, P8-P4, and PO4-PO8 were bipolarized for the right side.

2.2.6 Statistical Analysis

For statistical analysis *Analysis of Variances (ANOVAs)* with repeated measurements, oneway ANOVAs, two-tailed paired *t* tests, and independent samples *t* tests have been computed using PASW Statistics 18 (SPSS Inc., Chicago, Illinois, USA) and MATLAB® R2009b (The MathWorksTM, Natick, MA, USA). If not noted otherwise, the results of multiple pairwise comparisons were corrected using the Bonferroni-Holm procedure (Holm 1979).

Alertness and Tiredness

Since each condition poses a different demand on attention, for the analysis of the alertness and tiredness ratings an oneway ANOVA with a four-level between factor *Age Groups* was computed for each condition and rating. In total, ten ANOVAs were calculated.

Performance

The performance how well the subject accomplished the task was continuously assessed during the recording of the MEG/EEG data. In a preceding training session, subjects became familiar with the VM task by performing two blocks (six trials) of the VM condition in order to avoid learning effects and to achieve a relatively stable intra-individual performance.

During Training For the performance assessed during the training session the *root mean square error (RMSE)* was calculated. The *mean square error (MSE)* quantifies the difference between an estimator and the true value of the quantity that is estimated. MSE corresponds to the expected value of the squared error loss, whereby the error is defined as the amount by which the estimator differs from the quantity to be estimated (Lehmann and Casella 1998). Therefore, the MSE represents the variance of the difference between the estimator and the quantity to be estimated. Calculating the square root of the variance, i. e. computing the RMSE results in the standard error of the difference between the requested force (estimator) and the actual force (quantity to be estimated). An oneway ANOVA with a six-level within factor *Trials* was calculated for each age group and a 4×6 ANOVA (*Age Groups* and *Trials*) with repeated measurements.

During MEG/ EEG Recording For the performance that was recorded during the MEG/ EEG session, the correlation between the two channels – one recording the requested and one recording the actual force – was calculated for the condition VM and an oneway ANOVA with a four-level between factor *Age Groups* was computed. Additionally, an independent samples *t* tests between Group I and Group IV was calculated.

MEG and EEG Data

The overall aim of the study was to investigate the course of the age dependent alterations on oscillatory activity. For this reason we recruited four age groups. Accordingly, we computed for each virtual/ EEG channel and for each virtual/ EEG channel combination, a 4×4 ANOVA with the four-level between factor *Age Groups* and the four-level within factor *Conditions*. These ANOVAs did not yield any significant differences. However, not detecting any statistically significant overall age effect does not imply that there are no differences when comparing pairs of groups. We simulated data (see Figure 2.8 on the next page) in order to depict such a scenario. The simulated data resemble the MEG/ EEG data, respectively. The simulated data were created using the MATLAB command `randn()`. Absolute values were computed, and an offset and some variance added in order to simulate the MEG/ EEG data of four groups in one condition. An example oneway ANOVA with a four-level between factor was calculated. There was no statistically significant difference ($P = 2.65$). However, an independent samples *t* test between the variables *G1* and *G4* which represent our extreme groups, i. e. the youngest and the eldest, revealed a significant difference of $P \leq 0.05$.

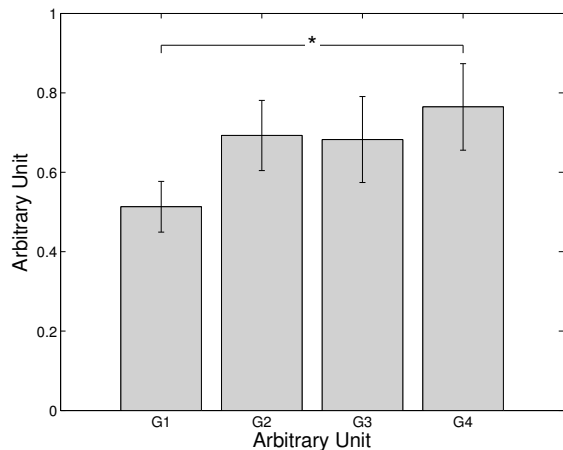


Figure 2.8: Simulated data, created using the MATLAB command `randn()`. Absolute values were computed, and an offset and some variance added in order to simulate the MEG/EEG data of four different groups in one condition. The data were averaged and the error bars indicate standard error of the mean. An Oneway ANOVA with a four-level between factor revealed no significant result ($P = 2.65$). But an independent samples t test between the variables $G1$ and $G4$ showed a significant difference ($*P \leq 0.05$).

According to the second aim of the current study, that is investigating whether there are age dependent alterations, and taking into account that so far there is no study on healthy elderly people and oscillatory activities associated with a continuous visuo-motor task performed during MEG recording, we compared the youngest (Group I) and the oldest group (Group IV).

Power Spectra At first the youngest group (aged ~ 25 years) was statistically analyzed with respect to the power spectra of each of the virtual channels (MEG data) and the bipolarized EEG channels for the conditions VM *vs.* V and V + M *vs.* V in the alpha (8-13 Hz) and the beta (13.7-24 Hz) range using two-tailed paired t tests. The same procedure was applied to the data of the eldest age group (Group IV). For the comparison between the two extreme age groups (Group I *vs.* Group IV), independent samples t tests were computed for the condition VM in both frequency ranges. There was a 2×2 ANOVAs (*Age Groups*: Group I, Group IV; *Conditions* VM, V + M) calculated for the virtual channel over SII.

Coherence There were 4×4 ANOVAs (*Age Groups* \times *Conditions*) calculated for several virtual (MEG data) and bipolar (EEG data) channel combinations.

2.3 Results

In the following section, all the results will be described starting from the ratings of alertness and tiredness, the performance during the training session and during the MEG/EEG recordings, and the power spectra and cross-spectral analysis (coherence) of the MEG and EEG data.

2.3.1 Alertness and Tiredness

There were no statistically significant differences between the four age groups with respect to alertness and tiredness. Also pairwise comparisons of Group I and Group IV using independent samples *t* tests did not reveal any statistically significant effects.

2.3.2 Performance

During Training Neither the oneway ANOVAs with a six-level within factor *Trials* for each age group nor the 4×6 ANOVA (*Age Groups* and *Trials*) with repeated measurements did reveal any statistically significant differences. Comparing Group I and Group IV using independent samples *t* tests did also not reveal any statistically significant effects.

During MEG/ EEG Recording The mean correlation (\pm *Standard Error of the Mean (SE)*) between the requested and the actual force, i. e. the performance, decreased gradually from the youngest (Group I) to the eldest (Group IV) group.

Group I	Group II	Group III	Group IV
0.74 (± 0.06)	0.70 (± 0.06)	0.62 (± 0.07)	0.58 (± 0.06)

The differences between the age groups were not statistically significant.

2.3.3 MEG Data

In the following section there will be first the results of the group level analysis of MEG source activity displayed. In the second part, the results of power spectra and the coherence of the MEG data will be described.

Group Level Analysis of MEG Source Activity

Figure 2.9 on the following page shows the results of the SnPM group level analysis for Group I (left side) and Group IV (right side). The main commonly activated regions are the prefrontal area, M1/SI, *Secondary somatosensory cortex (SII)*, parietal cortex, and visual cortex, whereby the M1/SI go in line with the precentral region of the network for visuo-motor integration, and the parietal cortex and the visual represent

the parietal-occipito region of this network (Andersen and Buneo 2002, Battaglia-Mayer and Caminiti 2002, Caminiti et al. 1998, Kalaska et al. 1997, Medendorp et al. 2008, Thoenissen et al. 2002, Wise et al. 1997). The activated regions of Group I (25 years) are more discrete compared to the more widespread („blurring“) activity in Group IV (80 years).

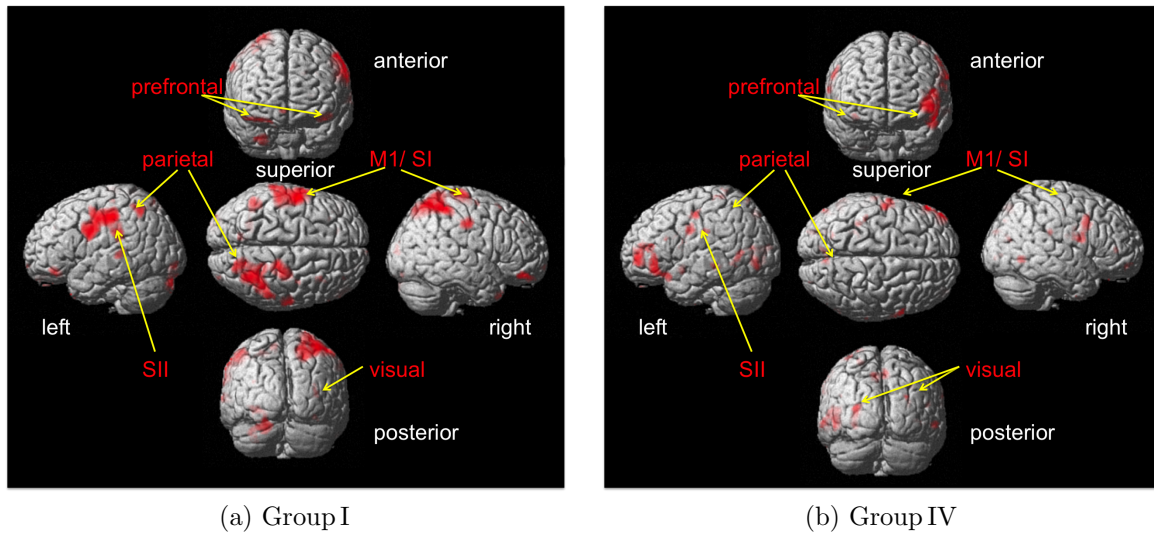


Figure 2.9: The results of the group level analysis MEG source activity are shown for (a) Group I and (b) Group IV. The anterior, superior, posterior, left, and right view are displayed. The main commonly activated regions are prefrontal area, M1/ SI, SII, parietal cortex, and visual cortex.

Power Spectra

The results of the power spectra will be described first for the within group analysis of the two extreme age groups (Group I and Group IV) and then the results for the between group analysis of Group I *vs.* Group IV.

Within Group Results The two-tailed paired *t* tests between the conditions VM *vs.* V and V + M *vs.* V for the first age group (Group I: 25 years) in the alpha range (8-13 Hz) for the virtual channel placed over the left M1/ SI revealed a significant difference between the conditions VM and V ($P=0.0013$) and between V + M and V ($P=0.0181$). In the beta range (13.7-24 Hz), the two-tailed paired *t* tests showed significant differences between the conditions VM and V for the left M1/ SI ($P=0.0187$) and the right M1/ SI ($P=0.007$). In Figure 2.10 on the next page the mean Δ Power for Group I in the alpha (top row) and beta range (bottom row) for the left (left column)

and right M1/ SI (right column) is displayed. The mean Δ Power is lowest for the visual condition compared to the complex conditions VM and V + M.

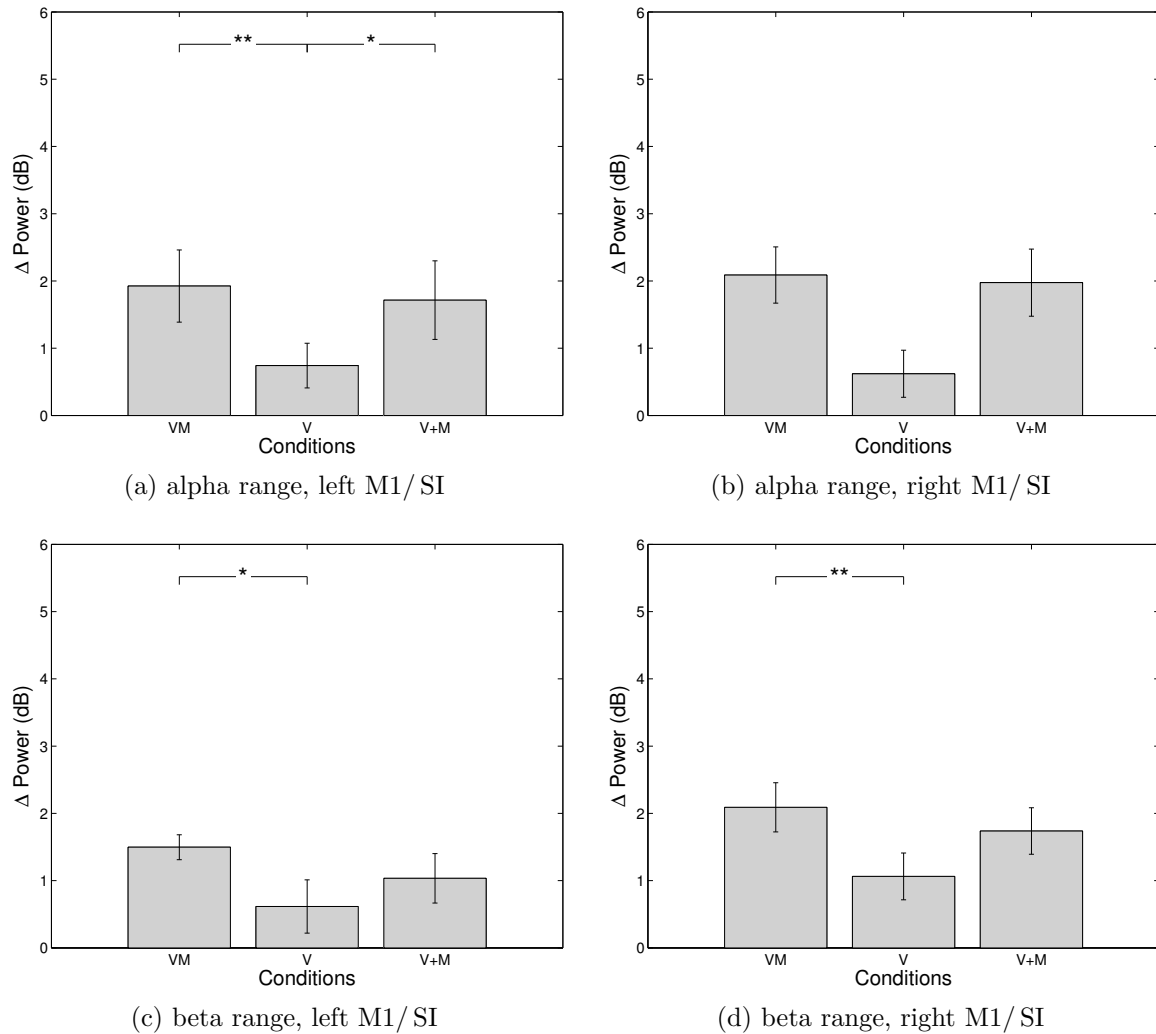


Figure 2.10: The comparison of the mean Δ Power in the alpha range (8-13 Hz, top row) and the beta range (13.7-24 Hz, bottom row) in the conditions VM *vs.* V and V + M *vs.* V for Group I (25 years) at the left (left column) and right M1 SI (right column) is shown. The two-tailed paired *t* tests revealed significant differences in the alpha range between the left M1/ SI in the conditions VM *vs.* V and V + M *vs.* V, and in the beta range for the conditions VM *vs.* V (** $P < 0.01$, * $P \leq 0.05$). Errorbars indicate standard error of the mean.

The two-tailed paired *t* tests between the conditions VM *vs.* V and V + M *vs.* V for the first age group (Group I: 25 years) in the alpha range (8-13 Hz) for the virtual channel placed over the left parietal cortex revealed a significant difference between conditions VM and V ($P = 0.0234$) as well as between V + M and V ($P = 0.0267$). The two-tailed paired *t* test between the conditions VM *vs.* V for the virtual channels placed over the right parietal cortex showed a trend ($P = 0.0509$) for a significant difference in

the alpha range (8-13 Hz). In Figure 2.11 can be seen that the mean Δ Power for both the unimodal condition V is lower than for the complex conditions VM and V + M.

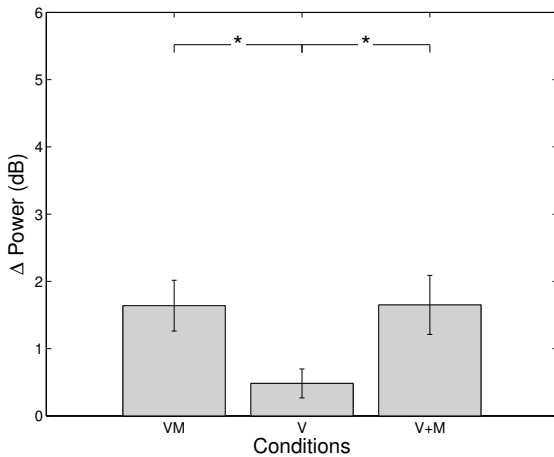


Figure 2.11: The comparison of the mean Δ Power in the alpha range (8-13 Hz) for the conditions VM *vs.* V and V + M *vs.* V for Group I (25 years) at the left parietal cortex is shown. The two-tailed paired *t* tests revealed significant differences between the conditions V + M *vs.* V as well as V + M *vs.* V ($*P \leq 0.05$). Errorbars indicate standard error of the mean.

The two-tailed paired *t* tests between the conditions VM *vs.* V and V + M *vs.* V for the first age group (Group I: 25 years) in the beta range (13.7-24 Hz) for the virtual channel placed over the right parietal cortex revealed a significant difference between conditions VM and V ($P = 0.0187$). For the virtual channel placed over the left parietal cortex, the two-tailed paired *t* tests for Group I showed a tendency for a significant difference between the conditions VM *vs.* V ($P = 0.055$) and V + M *vs.* V ($P = 0.0421$). Figure 2.12 displays the mean Δ Power in the beta range for the right parietal cortex in Group I. The mean Δ Power is higher for the complex conditions VM and V + M compared to the visual condition.

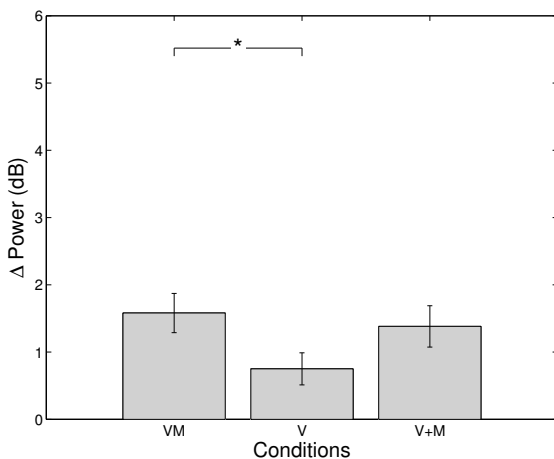


Figure 2.12: The comparison of the mean Δ Power in the beta range (13.7-24 Hz) for the conditions VM *vs.* V and V + M *vs.* V for Group I (25 years) at the right parietal cortex is shown. The two-tailed paired *t* tests revealed a significant difference between the conditions V + M *vs.* V ($*P \leq 0.05$). Errorbars indicate standard error of the mean.

The two-tailed paired *t* tests between the conditions VM *vs.* V and V + M *vs.* V for the fourth age group (Group IV: 80 years) in the alpha range (8-13 Hz) for the virtual channel placed over the left M1/SI revealed a significant difference between the conditions VM and V ($P = 0.0037$). For the virtual channel placed over the right M1/SI a significant

difference was found also between the conditions VM and V ($P = 0.007$). In the beta range (13.7-24 Hz), the two-tailed paired t tests showed significant differences between the conditions VM and V for the left M1/SI ($P = 0.0044$) and the right M1/SI ($P = 0.0094$) as well as between the conditions $V+M$ and V for the left M1/SI ($P = 0.012$) and the right M1/SI ($P = 0.016$). In Figure 2.13 the mean Δ Power for Group IV in the alpha (top row) and beta range (bottom row) for the left (left column) and right M1/SI (right column) is displayed. The mean Δ Power is lowest for the visual condition compared to the complex conditions VM and $V+M$.

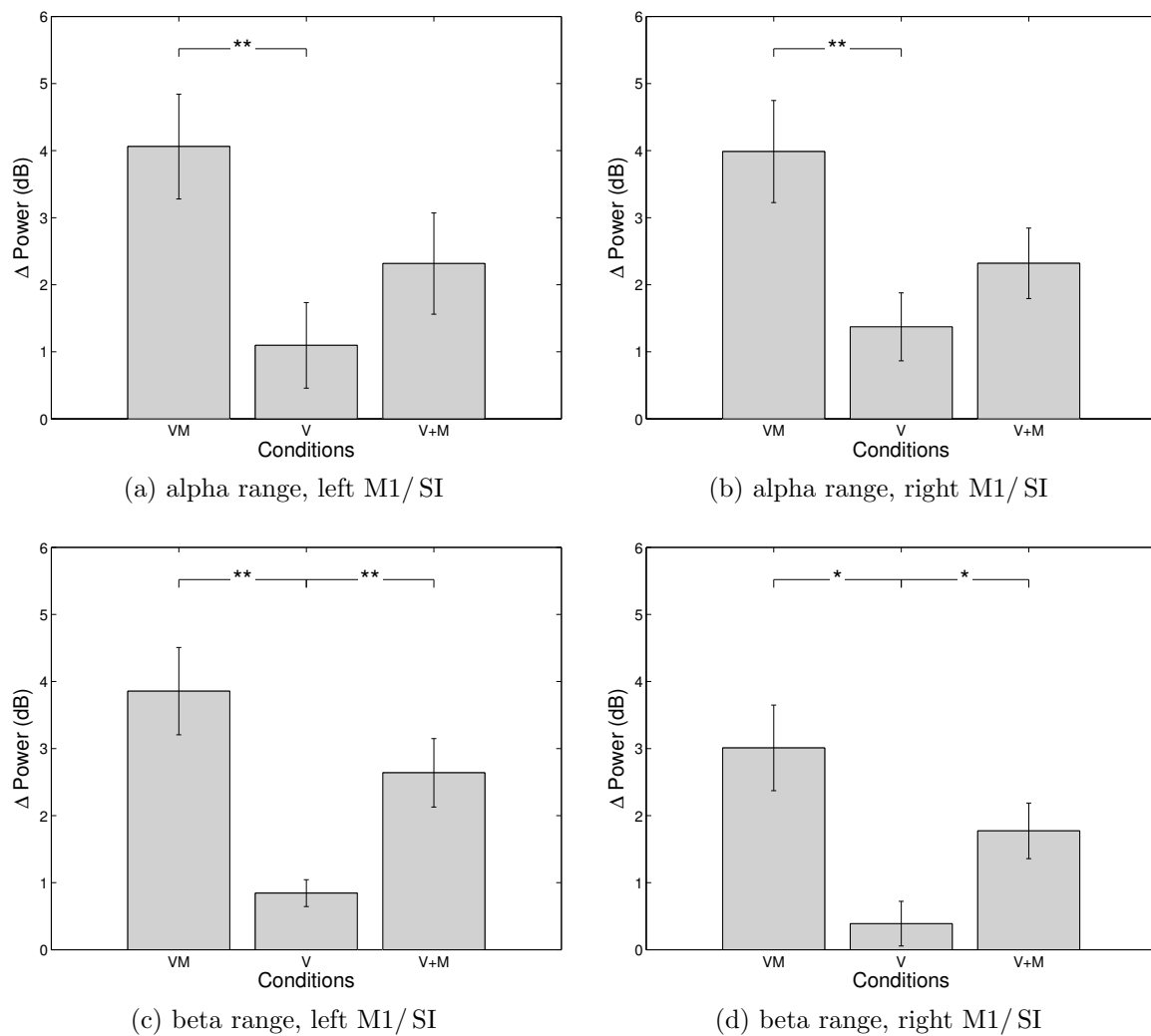


Figure 2.13: The comparison of the mean Δ Power in the alpha range (8-13 Hz, top row) and the beta range (13.7-24 Hz, bottom row) in the conditions VM vs. V and $V+M$ vs. V for Group IV (80 years) at the left (left column) and right M1/SI (right column) is shown. The two-tailed paired t tests revealed significant differences in the alpha range between the conditions VM vs. V , and in the beta range for the conditions VM vs. V as well as $V+M$ vs. V (** $P < 0.01$, * $P \leq 0.05$). Errorbars indicate standard error of the means.

The two-tailed paired t tests comparing the activity in the condition VM for the fourth age group (Group IV: 80 years) in the beta range (13.7-24 Hz) for the virtual channel placed over the left *vs.* the right prefrontal cortex revealed a significant difference between the two cortical sides ($P = 0.048$). The same test was performed for Group I, but did not yield any statistically significant differences. Figure 2.14 displays the mean Δ Power for the condition VM in the beta range for the left *vs.* the right prefrontal cortex in Group IV. The mean Δ Power is higher for the condition VM at the right prefrontal cortex compared to the left prefrontal cortex.

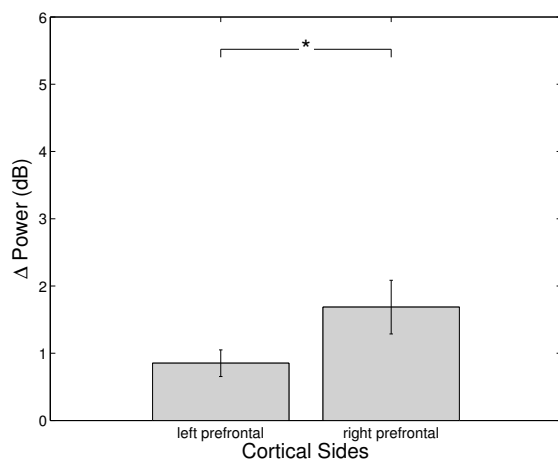


Figure 2.14: The comparison of the mean Δ Power in the beta range (13.7-24 Hz) in the condition VM for Group IV (80 years) at the left and right prefrontal cortex is displayed. The two-tailed paired t test revealed a significant difference between the two cortical sides with respect to the condition VM ($*P \leq 0.05$). In Group I this comparison did not yield any statistically significant differences. Error bars indicate standard error of the mean.

The two-tailed paired t tests between the conditions VM *vs.* V and V + M *vs.* V for the fourth age group (Group IV: 80 years) in the beta range (13.7-24 Hz) for the virtual channel placed over the right parietal cortex revealed a significant difference between conditions VM and V ($P = 0.022$). For the left side, there was a tendency for a significant difference between VM and V ($P = 0.0486$). In the alpha range (8-13 Hz) there was also a trend towards a significant difference on the parietal cortex on the right hemisphere for the two-tailed paired t test comparing the conditions VM *vs.* V ($P = 0.0653$) in Group IV. In Figure 2.15 on the facing page the mean Δ Power in the beta range for the right parietal cortex in Group IV is shown. The mean Δ Power is higher for the condition VM compared to the visual condition.

There were no statistically significant differences within both age groups regarding the visual area and the IFG.

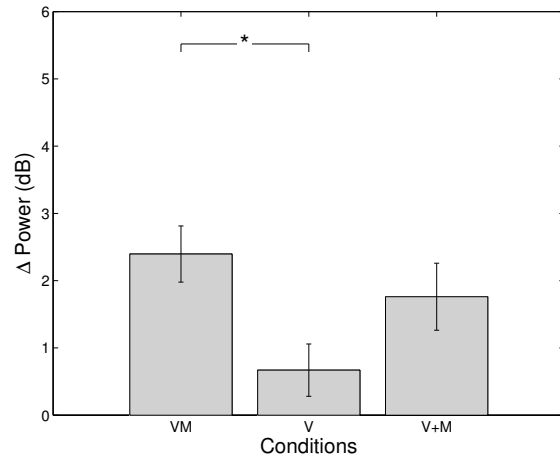


Figure 2.15: The comparison of the mean Δ Power in the beta range (13.7-24 Hz) for the conditions VM *vs.* V and V+M *vs.* V for Group IV (80 years) at the right parietal cortex is shown. The two-tailed paired *t* tests revealed a significant difference between the conditions V+M *vs.* V ($*P \leq 0.05$). Error bars indicate standard error of the mean.

Between Groups Results The independent samples *t* tests comparing the first age group (Group I: 25 years) and the fourth age group (Group IV: 80 years) regarding the condition VM in the alpha range (8-13 Hz) revealed a significant difference between the two age groups for the virtual channel placed over the left M1/ SI ($P = 0.03$) and over the right M1/ SI ($P = 0.0316$). In the beta range (13.7-24 Hz), the independent samples *t* tests showed a significant difference between the two age groups for the left M1/ SI ($P = 0.0009$). In Figure 2.16 on the next page the mean Δ Power for the condition VM comparing Group I and Group IV in the alpha (top row) and beta range (bottom row) for the left (left column) and right M1/ SI (right column) is displayed. The mean Δ Power is lower for the first age group compared to the fourth age group at the M1/ SI area of both hemispheres in the alpha and the beta frequency.

The independent samples *t* tests comparing the first age group (Group I: 25 years) and the fourth age group (Group IV: 80 years) in the condition VM in the beta range (13.7-24 Hz) revealed a significant difference between the two age groups for the virtual channel placed over the left ($P = 0.05$) and over the right ($P = 0.0036$) prefrontal cortex. Figure 2.17 on page 37 shows the mean Δ Power for the condition VM comparing Group I and Group IV in the beta range for the left (left) and right prefrontal cortex (right). The mean Δ Power is higher for the fourth age group compared to the first age group at the prefrontal cortex of both hemispheres in the beta frequency.

The 2×2 ANOVA (*Age Groups*: Group I, Group IV; *Conditions*: VM, V+M) for the left SII in the alpha range (8-13 Hz) revealed a main effect for the between factor *Age Groups* ($F_{(1,17)} = 5.104$; $P = 0.037$). Figure 2.18 on page 37 shows the mean Δ Power in the alpha range for the left SII in the conditions VM and V+M for the first and the fourth age groups. The activity is higher for Group IV compared to Group I in both conditions.

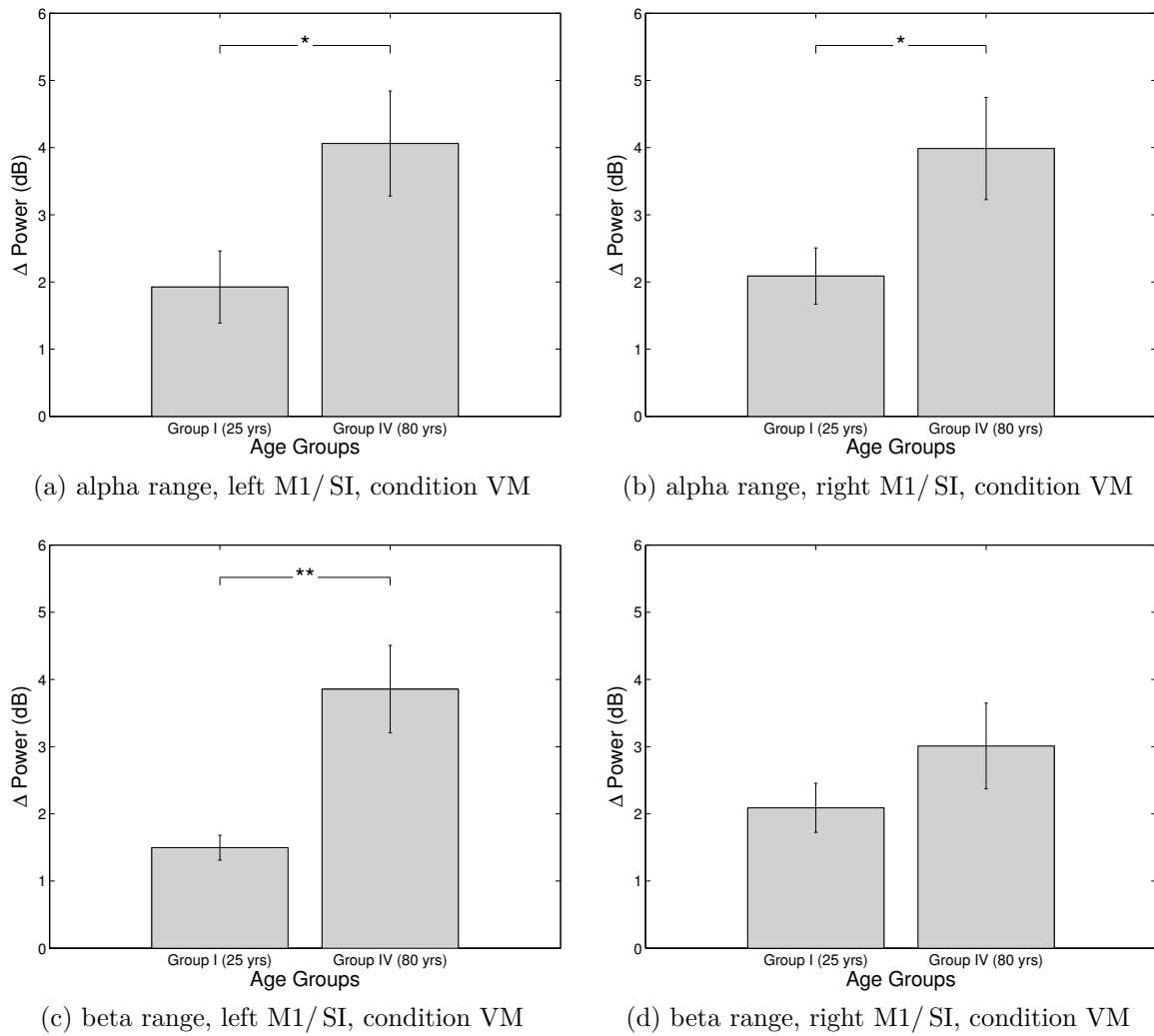


Figure 2.16: The comparison of Group I (25 years) *vs.* Group IV (80 years) regarding the mean Δ Power in the alpha range (8-13 Hz, top row) and the beta range (13.7-24 Hz, bottom row) for the left (left column) and the right M1/SI (right column) in the condition VM is displayed. The independent samples *t* tests revealed significant differences between the two age groups with respect to the condition VM for the left M1/SI in the alpha and beta range, as well as for the right M1/SI in the beta range (** $P < 0.01$, * $P \leq 0.05$). Errorbars indicate standard error of the means.

The independent samples *t* test comparing the first age group (Group I: 25 years) and the fourth age group (Group IV: 80 years) in the condition VM in the beta range (13.7-24 Hz) revealed a significant difference between the two age groups for the virtual channel placed over the left SII ($P = 0.0096$). Figure 2.19 on page 38 displays the mean Δ Power for the condition VM comparing Group I and Group IV in the beta range for the left SII. The mean Δ Power is higher for the fourth age group compared to the first age group at the SII in the beta frequency.

There were no statistically significant differences between the age groups with respect to

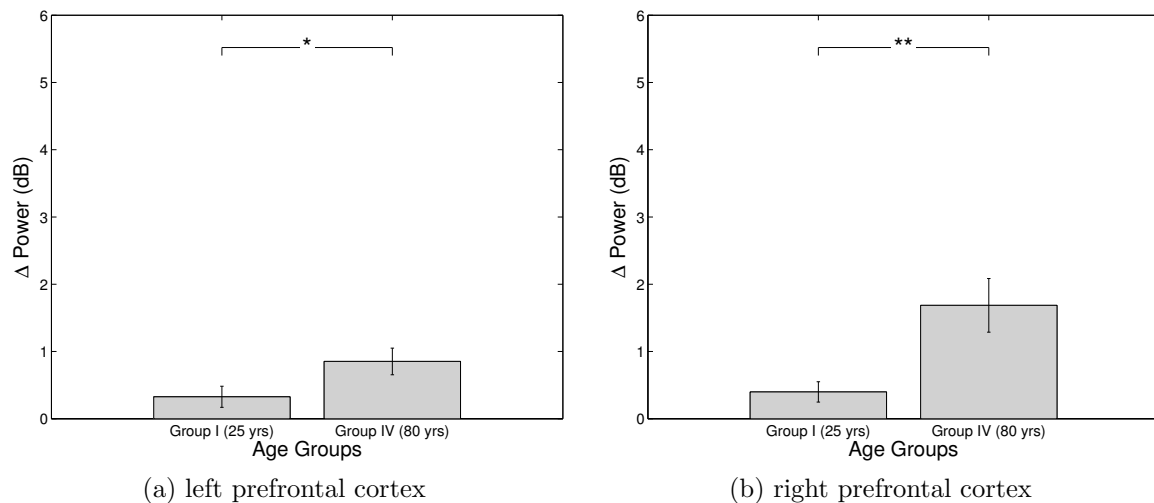


Figure 2.17: The comparison of Group I (25 years) *vs.* Group IV (80 years) regarding the mean Δ Power in the beta range (13.7-24 Hz) for the left and right prefrontal cortex in the condition VM is displayed. An independent samples *t* test revealed significant differences between the two age groups with respect to the condition VM (** $P < 0.01$, * $P \leq 0.05$). Errorbars indicate standard error of the means.

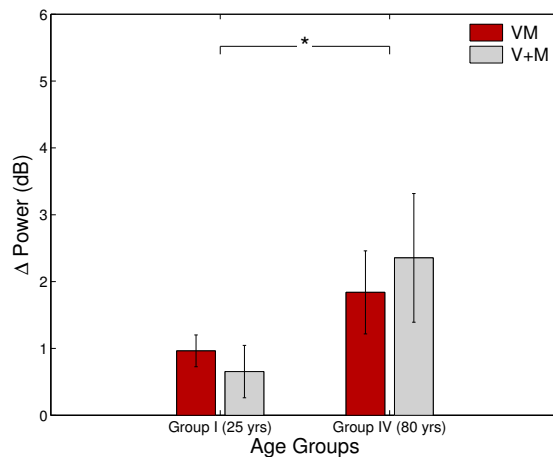


Figure 2.18: A comparison of Group I (25 years) *vs.* Group IV (80 years) regarding the mean Δ Power in the alpha range (8-13 Hz) for the left SII in the conditions VM and V + M is shown. The 2×2 ANOVA (*Age Group* \times *Conditions*) revealed a main effect for the between subject factor *Age Groups* (* $P \leq 0.05$). Error bars indicate standard error of the mean.

the visual area and the IFG. However, there was a tendency for a significant difference between the two groups for the parietal cortex on the right hemisphere in the alpha range (8-17 Hz) in the VM condition ($P = 0.0653$).

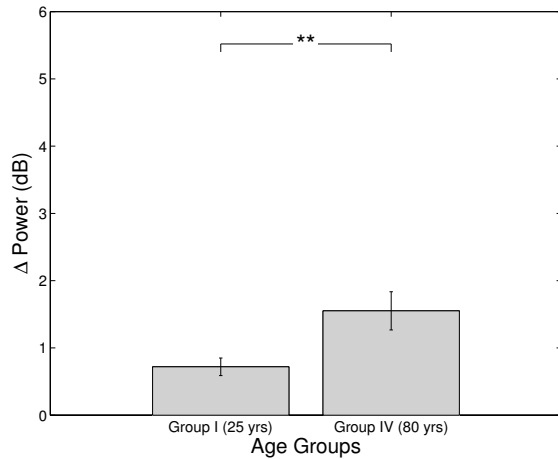


Figure 2.19: The comparison of Group I (25 years) vs. Group IV (80 years) regarding the mean Δ Power in the beta range (13.7-24 Hz) for the left SII in the condition VM is displayed. An independent samples t test revealed significant differences between the two age groups with respect to the condition VM ($*P \leq 0.05$). Error bars indicate standard error of the mean.

Coherence

There were statistically significant differences for the coherence of selected virtual channel combinations in the beta frequency range.

Between Groups Results The independent samples t test comparing the first age group (Group I: 25 years) and the fourth age group (Group IV: 80 years) in the condition VM in the beta range (13.7-24 Hz) revealed a significant difference between the two age groups for the for the virtual channel combination over the left M1/SI – right visual area ($P = 0.018$). Figure 2.20 shows the mean Δ Coherence for the condition VM comparing Group I and Group IV in the beta range for the left M1/SI – right visual area. The mean Δ Coherence is higher for the fourth age group compared to the first age group at the left M1/SI – right visual area in the beta frequency.

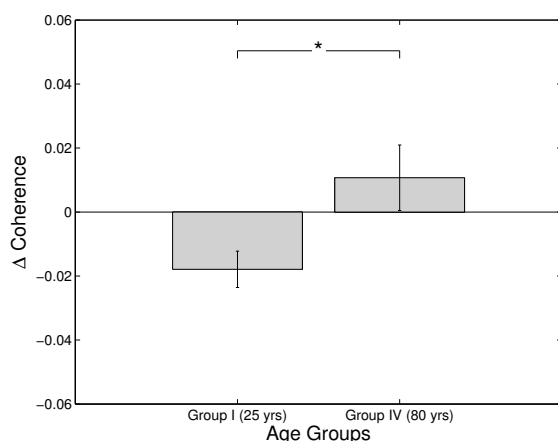


Figure 2.20: The comparison of Group I (25 years) vs. Group IV (80 years) regarding the mean Δ Coherence in the beta range (13.7-24 Hz) for the virtual channel combination left M1/SI – right visual area in the condition VM is displayed. An independent samples t test revealed significant differences between the two age groups with respect to the condition VM ($*P \leq 0.05$). Error bars indicate standard error of the mean.

The independent samples t test comparing the first age group (Group I: 25 years) and the fourth age group (Group IV: 80 years) in the condition V + M in the beta range (13.7-24 Hz) revealed a significant difference between the two age groups for the for the

virtual channel combination over the left prefrontal cortex – left visual area ($P = 0.0239$). Figure 2.21 shows the mean Δ Coherence for the condition VM comparing Group I and Group IV in the beta range for the left M1/SI – right visual area. The mean Δ Coherence is higher for the fourth age group compared to the first age group at the left prefrontal cortex – left visual area in the beta frequency.

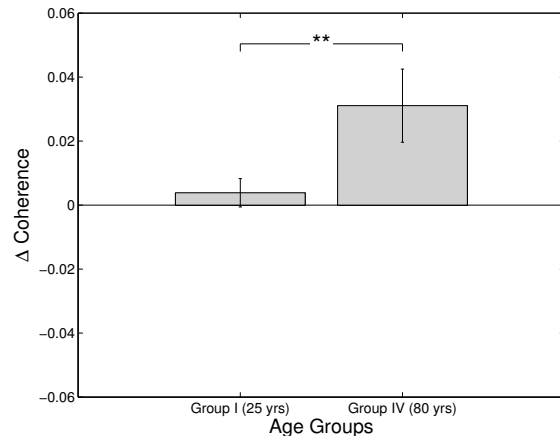


Figure 2.21: The comparison of Group I (25 years) *vs.* Group IV (80 years) regarding the mean Δ Coherence in the beta range (13.7-24 Hz) for the virtual channel combination left prefrontal cortex – left visual area in the condition VM is displayed. An independent samples *t* test revealed significant differences between the two age groups with respect to the condition VM ($*P \leq 0.05$). Error bars indicate standard error of the mean.

2.3.4 EEG Data

In the following section the results of the statistical analysis of the EEG data will be described.

Power Spectra

Within Group Results The two-tailed paired *t* tests between the conditions VM *vs.* V and V + M *vs.* V for the first age group (Group I: 25 years) in the alpha range (8-13 Hz) revealed a significant difference between the conditions V + M and V for the bipolarized EEG channel FC3-CP3 over the left hemisphere ($P = 0.0184$) and for the bipolarized EEG channel FC4-CP4 over the right hemisphere ($P = 0.0133$). In Figure 2.22 on the next page the mean Δ Power for Group I in the alpha range for the bipolar channels FC3-CP3 (left side) and FC4-CP4 (right side) is displayed. The mean Δ Power is lowest for the visual condition compared to the complex conditions VM and V + M.

The two-tailed paired *t* tests between the conditions VM *vs.* V and V + M *vs.* V for the first age group (Group I: 25 years) in the beta range (13.7-24 Hz) for bipolar channel P7-P3 revealed a significant difference between conditions V + M and V ($P = 0.0038$). Figure 2.23 on the following page shows the mean Δ Power in the beta range for the

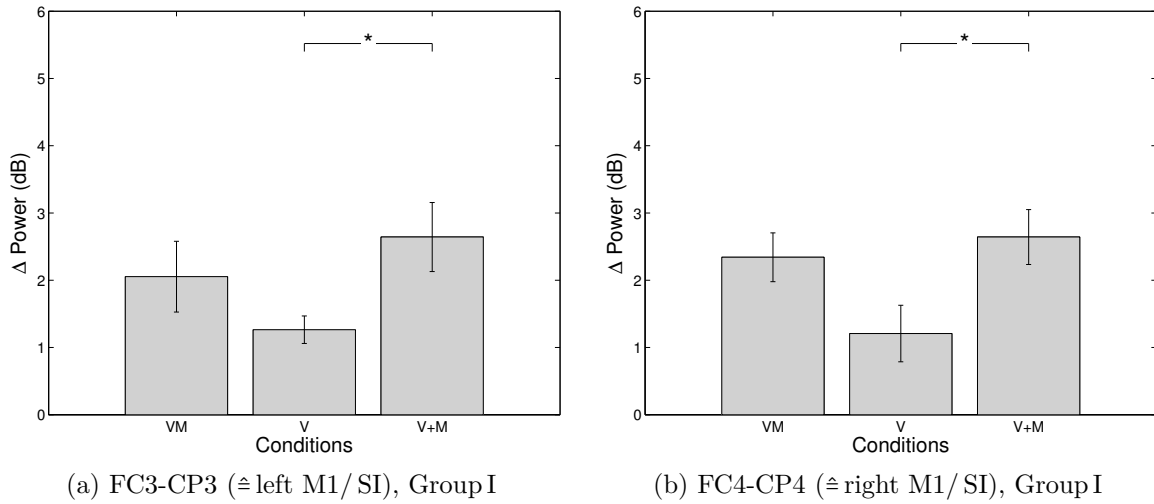


Figure 2.22: The comparison of the mean Δ Power in the alpha range (8-13 Hz) for the conditions VM *vs.* V and V + M *vs.* V for Group I (25 years) at FC3-CP3 (left side) and FC4-CP4 (right side) is shown. The two-tailed paired *t* tests revealed a significant difference between the conditions V + M *vs.* V ($*P \leq 0.05$). Errorbars indicate standard error of the mean.

right parietal cortex in Group IV. The mean Δ Power is higher for the condition V + M compared to the visual condition.

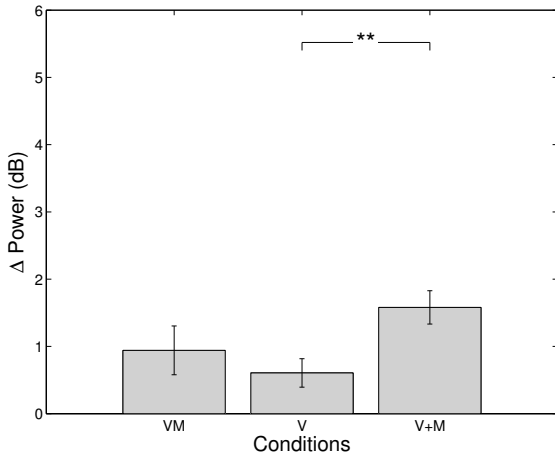


Figure 2.23: The comparison of the mean Δ Power in the beta range (13.7-24 Hz) for the conditions VM *vs.* V and V + M *vs.* V for Group I (25 years) at P7-P3 (≅ left parietal cortex) is shown. The two-tailed paired *t* tests revealed a significant difference between the conditions V + M *vs.* V ($**P \leq 0.01$). Error bars indicate standard error of the mean.

The two-tailed paired *t* tests between the conditions VM *vs.* V and V + M *vs.* V for the fourth age group (Group IV: 80 years) in the alpha range (8-13 Hz) revealed a significant difference between the conditions VM and V for the bipolarized EEG channel FC3-CP3 over the left hemisphere ($P = 0.0104$) and for the bipolarized EEG channel FC4-CP4 over the right hemisphere ($P = 0.038$). Additionally, for the bipolarized EEG channel FC4-CP4 (right hemisphere) there was a significant difference between the conditions V + M and V ($P = 0.0224$). In Figure 2.24 on the next page the mean Δ Power for

Group IV in the alpha range for the bipolar channels FC3-CP3 (left side) and FC4-CP4 (right side) is displayed. The mean Δ Power is lowest for the visual condition compared to the complex conditions VM and V + M.

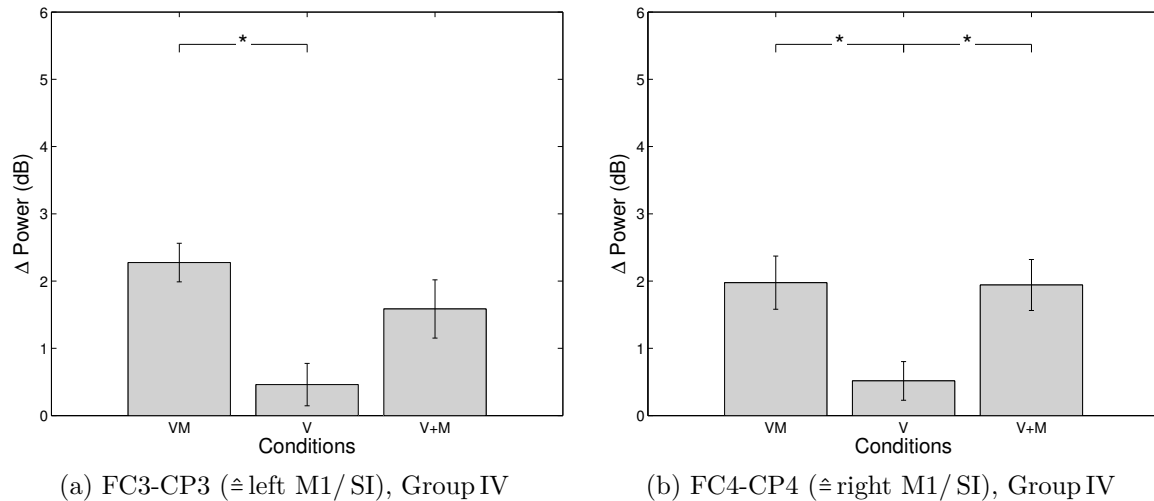


Figure 2.24: The comparison of the mean Δ Power in the alpha range (8-13 Hz) for the conditions VM *vs.* V and V + M *vs.* V for Group IV (80 years) at FC3-CP3 (left side) and FC4-CP4 (right side) is shown. The two-tailed paired *t* tests revealed a significant difference between the conditions V + M *vs.* V ($*P \leq 0.05$). Errorbars indicate standard error of the mean.

Between Groups Results The independent samples *t* tests revealed no statistically significant differences between the Group I and Group IV in the condition VM in both frequency ranges.

Coherence

There were no statistically significant differences within group comparisons (two-tailed paired *t* tests) or between group comparisons (independent samples *t* tests) with respect to the coherence in the alpha and beta frequency range.

2.3.5 Summary of Results

In Table 2.3 on the following page and Table 2.4 on page 43 the results of the current study, *Visuo-motor Integration and Age Dependent Alterations*, are summarized.

Table 2.3: Summary of the Results of the First Study: Visuo-motor Integration and Age Dependent Alterations. Comparisons of Conditions for Single Groups. MEG and EEG Data.

Comparisons between Groups: independent samples <i>t</i> tests					
Age Group	Frequency	Side	Cortical Area	Conditions	
				VM <i>vs.</i> V	V + M <i>vs.</i> V
MEG Data Power Spectra					
<i>Group I</i>	alpha	left	M1SI	$P = 0.0013$	$P = 0.0181$
		left	parietal	$P = 0.0234$	$P = 0.0267$
	beta	left	M1SI	$P = 0.0187$	n.s.
		right	M1SI	$P = 0.007$	n.s.
<i>Group IV</i>	alpha	left vs. right	prefrontal	$P = 0.048$	
		beta	left	M1SI	$P = 0.0044$
	right	M1SI	$P = 0.0120$	$P = 0.0160$	
	right	parietal	$P = 0.022$	n.s.	
MEG Data Coherence					
<i>Group IV</i>	beta	left prefrontal – left visual			$P = 0.0037$
		right prefrontal – right visual			$P = 0.0242$
EEG Data Power Spectra					
<i>Group I</i>	alpha		FC3CP3	n.s.	$P = 0.0184$
			FC4CP4	n.s.	$P = 0.0133$
	beta		P7P3	n.s.	$P = 0.0038$
<i>Group IV</i>	beta		FC3CP3	$P = 0.0104$	n.s.
			FC4CP4	$P = 0.038$	$P = 0.0224$

Table 2.4: Summary of the Results of the First Study: Visuo-motor Integration and Age Dependent Alterations. Comparisons between the two extreme Groups. MEG Data.

Comparisons between Groups: independent samples <i>t</i> tests					
Age Group	Frequency	Side	Cortical Area	Conditions	
				VM	V + M
MEG Data Power Spectra					
<i>Group I</i> vs. <i>Group IV</i>	alpha	left	M1SI	$P = 0.03$	
		right	M1SI	$P = 0.0316$	
		left	SII	$P = 0.037$	$P = 0.037$
	beta	left	prefrontal	$P = 0.05$	
		right	prefrontal	$P = 0.0036$	
		left	M1SI	$P = 0.0009$	
		left	SII	$P = 0.0096$	
	MEG Data Coherence				
<i>Group I</i> vs. <i>Group IV</i>	beta	left M1/SI – right visual			$P = 0.018$
		left prefrontal cortex – left visual			$P = 0.0239$

2.4 Discussion

So far, the present study is the first examining oscillatory activity by comparing healthy young and elderly people using combined MEG and EEG recordings during the performance of a continuous visuo-motor task. Previous findings showed that occipitoparietal and precentral brain regions constitute the network accomplishing visuo-motor integration (Andersen and Buneo 2002, Battaglia-Mayer and Caminiti 2002, Caminiti et al. 1998, Kalaska et al. 1997, Medendorp et al. 2008, Thoenissen et al. 2002, Wise et al. 1997). Our results with respect to the power suppression in the alpha and beta frequency ranges comparing the complex visuo-motor task with the pure visual condition are in line with these findings. Another key finding of the present study is the confirmation of the increased activity in prefrontal areas in elderly subjects compared to young adults. This is in excellent agreement with the report of the shift of activity from posterior to more frontal areas (Kolev et al. 2002, Davis et al. 2009, for review see Niedermeyer 1997, Palva and Palva 2007, Rossini et al. 2007). The activity of the elderly being more pronounced in general, in the beta range in particular, corresponds also to previous findings (e.g. Labyt et al. 2006, Vallesi et al. 2010). Furthermore, several studies delineated age related increases in parietal activity (Anderson et al. 2000, Grady et al. 2002, 2003, Madden et al. 2007). The results found in the present study are pointing towards this finding. Physiologically, with increasing age, a behavioural slowing in sensorimotor tasks and impaired motor performance is observed (Inuggi et al. 2009, Mattay et al. 2002, Labyt et al. 2006, Smith et al. 1999, Vallesi et al. 2009, Welford 1988). Our result that there is a gradual decrease in task performance across the four age groups, is perfectly in line with these former reports. However, according to our hypothesis', we expected to find a task specific increase of coherence in the VM task in the youngest group, and a decrease of coherence when comparing the younger group with the elderly group. Both hypothesis' could not be confirmed.

A power decrease of oscillatory brain signals induced by a voluntary movement corresponds to the activation of sensorimotor cortex in the alpha range (Pfurtscheller and Aranibar 1977) and has been associated with increased *blood oxygen level dependent (BOLD)* measures (Brookes et al. 2005). The Δ Power measure of the current study, i.e. subtracting the amplitudes of the *task* periods from the *rest* time windows, represents the suppression of the μ Rhythm: the higher the difference between rest and task, the higher the power suppression and the higher the activation. We therefore adopt the general view that event-related source power decrease in relatively low frequencies (i.e. alpha and lower beta band as used here) is related to increased neural activation

(Pfurtscheller 1992, Singh et al. 2002, 2003).

Motor related activity has been shown to undergo age dependent alterations due to functional reorganization of the central motor networks (Minati et al. 2007, Kido et al. 2004, Ward and Frackowiak 2003). This can be explained with a more extensive, and less selective, recruitment of neural populations (Inuggi et al. 2009) which is most probably due to increased local connectivity within and between the primary motor cortices of both hemispheres. Another reason might be the dysfunction of inhibitory circuits that accompanies aging (Peinemann et al. 2001, Talelli et al. 2008). In the healthy adolescents, activity in the motor cortex is usually associated with contralateral effector movement (Kolb and Wishaw 1996, Graziadio et al. 2010, Vallesi et al. 2010), while in childhood as well as in elderly there is no such lateralization (Graziadio et al. 2010, Labyt et al. 2004, Naccarato et al. 2006, Talelli et al. 2008, Vallesi et al. 2010, Ward and Frackowiak 2003). TMS experiments demonstrated the inhibition of ipsilateral activation of M1 during unimanual movements (Ghacibeh et al. 2007, Leocani et al. 2000) in healthy young subjects. Even though our VM task was performed using only one hand, we observed bilateral activation in M1/SI regions not only in the elderly, but also in the youngest age group. The occurrence of bilateral activation in one-handed tasks is a frequent finding, especially in more complex unimanual motor actions (Kawashima et al. 1998, Rao et al. 1993, Roland and Zilles 1996). Opposed to our complex continuous visuo-motor task, the studies of Graziadio et al. (2010), Labyt et al. (2004), and Vallesi et al. (2010) used simple motor tasks, such as *go/nogo* (Vallesi et al. 2010), isometric contraction exerted with the right thumb and index finger against a resistance of a compliant object (Graziadio et al. 2010) or contraction (extension and elevation) and relaxation of finger, arm, and hand (Labyt 2003, Labyt et al. 2004, 2006). This is one reason that in the present study the formerly expected age dependent alteration regarding the loss of hemispheric lateralization in the motor area could not be detected. Another reason might be the difficulty to distinguish between excitatory and inhibitory activity.

Another important point to discuss is the choice of the task and the experimental setup. In the present study, we can rule out any effects arising from movement during recordings. The studies serving as references for our present experiment (Classen et al. 1998, Labyt 2003, Labyt et al. 2004, 2006), used EEG for recording the brain activity. First of all, our task is designed as such that it requires and allows only the movement of the thumb and the index finger. Furthermore, recording MEG, whereby subjects' head were placed in a dewar and additionally padded in order to avoid any head movement, it was ensured that we did not introduce any movement-related effects.

The less pronounced differences that we found between the elderly and the younger

subjects, could be due to the inhomogeneity of the elderly group. Across their lives, they developed numerous strategies to cope with age dependent physiological changes. To date, aging is widely reported as being accompanied by morphological and functional changes in various cerebral structures (Andersen and Buneo 2002, Jernigan et al. 1991, Dujardin et al. 1994, 1995, Hubble 1998). Nevertheless, the differences in the degree of behavioural success in our visuo-motor task did not become statistically significant. The performance was gradually declining from the youngest to the middle aged, the third group and finally to the oldest group. Additionally, the subjects from the eldest group represent a selection of the population, not the average. Considering the mean age of this group of ~ 80 years, and injuries during their lifetime, and taking into account the eligibility to participate in a study essentially requiring that they are absolutely metalfree and meeting our criteria being healthy, these subjects can be assumed to have developed very successful strategies in coping for example with normal occurrence of age dependent changes. Also the above-average educational background in these subjects should not be disregarded. Taken together, the beforehand mentioned physiological and anatomical changes might be less or differently formed compared to other elderly representing a presentable cross section of the population.

Previous animal (Roelfsema et al. 1997) and human studies (Classen et al. 1998) reported synchronization among different brain regions during visuomotor tasks in the alpha or beta range. Surprisingly, with the analysis strategy used in the present study we did not unmask the cortico-cortical coupling of the regions involved in the network of visuo-motor integration, neither in the MEG nor in the EEG data. According to the hypothesis' of the present study, we expected to find the same pattern of oscillatory activity as in the EEG, i. e. cortico-cortical coupling between the areas involved in visuo-motor integration, also in the MEG data. For the analysis of the EEG recordings, we used bipolar EEG channels in contrast to Classen et al. (1998) who focused on single EEG channels. Due to the nature of the EEG to constitute a potential, i. e. a difference between two sides, there is always the problem of a reference. In order to circumvent this and to minimize volume conduction effects and increase the signal to noise ratio, in the current study we did not use single EEG electrodes for analysis. There are several methods for reducing effects caused by the reference, such as current source density (Mima and Hallett 1999), but the Laplacian estimation depends critically on the number of recording electrodes (Nunez and Srinivasan 2006) and is recommended for EEG montages with > 64 channels. If less than 64 electrodes are used, like in our case, bipolar channels have been proven to be the best choice for a decent spatial resolution of the EEG (Andrew and Pfurtscheller 1996, Nunez and Srinivasan 2006). This difference in

the analysis accounts for the fact that we could not confirm the findings of Classen et al. (1998) in the EEG data.

To date, there is no general agreement on the definition of cortico-cortical coupling. Some authors name this concept *coherence*, others call it *synchronization* (Winterer et al. 2003). Accordingly, numerous mathematical approaches were developed in recent years in order to describe this concept (for an overview see Jirsa and McIntosh 2007). For example, Lachaux et al. (1999) refers to the frequency-specific cortico-cortical coupling as *synchronization* or *transient phase-locking* and quantifies it using the so called *phase locking value (PLV)*. Another approach is the calculation of the *spatial analytic phase difference* (Pockett et al. 2009). The classical approach to characterize cross-spectra realtion is to calculate the *coherence* (Schnitzler and Gross 2005a), as it was done in the present study, after applying a *Fast Fourier Transformation (FFT)* to the data.

In general, there are two ways to extract the spectrum. *One* way is the FFT. Thereby, it is assumed that the signal is infinite and stationary over time. This assumption poses a handicap, because signals that we record using MEG or EEG are not infinite. The *Welch Method* is one way to cope with this ill poseness by treating the signal as being composed of different segments of the same length: the more segments that can be extracted from the signal, the better is the estimation of the spectrum. But there are limitations. Variance decreases with increasing number of segments. But this requires many segments. In turn, if there are too many segments, the hypothesis that the signal is relatively stable over time cannot be fulfilled. The challenge by using the FFT is to balance the distortion, i. e. the estimation of the signal in one segment does not necessarily equals the estimation of the signal in the next segment. If the segments are too short, or the number of segments is too small, the frequency resolution will be reduced. Therefore, it is essential to provide the right number of segments to ensure stationarity of the signal without risking the loss of frequency resolution.

A *second* way are parametric methods. Thereby, it is discriminated between a *monovariate* approach (assuming that there is one signal), and a *multivariate* approach (assuming that there is more than one signal). The multivariate approach is based on the monovariate approach. Both are methods modeling signals using *autoregressive modeling (AR)*: Thereby, the segment is modeled as it is, i. e. it allows to extract the information about the dynamics generating the signal on the basis of the samples that constitute the signal. The idea behind this is to explain the signal as consequence of an unpredictable process.

$$Y(n) = \sum_{k=1}^p A(k)Y(n-k) + U(n) \quad (2.3)$$

The spectrum is estimated as an outcome of a linear system whose input is the white noise (U) given the assumption that all the dynamics could be described by a linear system. Every sample (n) of the signal (X) is described as a linear function of the previous samples, i. e. what happened in the past predicts what happens in the future. The model order p represents the number of samples that are considered for the prediction of the next sample. Every present sample is described as the sum of samples in the past weighted by a model coefficient to improve the estimation.

Therefore, a coefficient should be found that provides the best prediction for the estimation of the present sample. If there is more than one signal, i. e. channel in our case, the multivariate approach is used whereby the present value is predicted as a linear function of the past samples of the same signal and by the past of the other signals (Kay 1988).

Taken together, the synchronized brain activities are masked by the spontaneous brain activity. Therefore, fine tuned analysis strategies are necessary to extract the synchronized activities. It might be insufficiently to estimate the frequency spectrum without apriori assumptions, but convenient requirements should be provided to detect oscillatory activities. Using autoregressive modeling, oscillatory activities are modeled within a narrow frequency spectrum and additional activities are suppressed. This approach assumes apriori that oscillations are autoregressive processes. Also, very preliminary results of a currently ongoing second analysis of the younger age group done in collaboration with the Biophysics and Biosignal Laboratory (Department of Physics, University of Trento) using the multivariate approach suggest that the AR method might be better suited for the analysis of oscillatory activities in our visuo-motor integration task. But this methodological approach is beyond the scope of the present thesis.

In conclusion, the present study is so far the very first to investigate oscillatory activity by comparing healthy young and elderly people using combined MEG and EEG recordings during the performance of a continuous visuo-motor task. There were six main findings in the present study. *Firstly*, the network accomplishing visuo-motor consists of occipito-parietal and precentral brain regions. *Secondly*, there is a shift of brain activity to more prefrontal areas, specifically to right prefrontal regions, in the elderly subjects. *Third*, the elderly showed an overall higher neuronal activity, yet more pronounced in the beta frequency, compared to young adults. *Fourth*, there is a tendency for an increased activity of the parietal cortex in the elderly. *Fifth*, we found a gradual decrease of motor performance. And *sixth*, we could not replicate previously reported results on cortico-cortical coupling between the areas involved in visuo-motor integration, nor

could we confirm the decrease of coherence in the VM task when comparing young and elderly subjects.

3 Second Study: Asynchronous Bifocal Stimulation

While the study described in the previous chapter was designed to further elucidate the mechanisms contributing to the coupling of oscillatory activity in the visuo-motor system, the present study investigated the possibilities of modulating cortico-cortical coherence.

3.1 Introduction: Aims and Hypotheses

Recently, it has been shown that coupling of oscillatory activity can be selectively enhanced by synchronous rTMS given to distinct brain areas (Plewnia et al. 2008). In order to extend the findings of modulatory effects of rTMS on oscillatory activities, the present study aimed to *firstly*, replicate the finding of the previous study that synchronous rTMS applied to M1 and V1 increases cortico-cortical coherence between these areas and *secondly*, to compare the effects of three different asynchronous bifocal rTMS stimulations *vs.* the synchronous bifocal stimulation. *Asynchronous* refers to the temporal delay between the two pulses given to M1 and V1. We suggest that an asynchronous bifocal stimulation is more effective with respect to the modulation, i. e. increase, of coherence compared to the synchronous bifocal stimulation, based on the given temporal delay in signal transfer between the V1 and M1 due to the spatial distance between both cortical areas.

3.2 Methods

In the current section, the methodological details of the study and the data analysis will be described. The experiment was conducted at the Department for Psychiatry and Psychotherapy of the University of Tübingen.

3.2.1 Subjects

Ten healthy volunteers (mean age: 28.47 ± 7.77 years, 5 females) were recruited within the student population of the University of Tübingen. All participants were right handed according to the Edinburgh handedness inventory (Oldfield 1971). They perceived phosphenes as evaluated in a preceding screening. The study was approved by the local medical ethics committee, and written informed consent according to the Declaration of Helsinki was obtained from all participants prior to the experiment. All subjects were free of known past or present mental health or neurological problems and received monetary compensation for their participation.

3.2.2 Stimuli and Procedure

During the experiment, subjects were seated comfortably approximately 1 m in front of a screen. They were asked to fixate on a stationary cross displayed on the monitor, and to avoid blinking.

TMS was applied using a Magstim Super Rapid and a Magstim 200 (The Magstim Company Ltd, Whitland, UK) with figure-eight coils (diameter of each winding: 70 mm, biphasic stimulus of $250 \mu\text{s}$, peak magnetic field: 2 T). The coils were placed at the position of the lowest *Motor Threshold (MT)* for stimulating the right APB and approximately 1 cm to the left of the occipital pole (V1) where the lowest *Phosphene Threshold (PT)* was found (see Figure 3.1 on the facing page).

The individual MT and PT were assessed at the beginning of the experiment. The optimal stimulation position, i. e. the position of the lowest MT, was determined by placing the center of the coil touching the skull angled at approximately 45° (handle pointing posteriorly) to the head's midline above the left motor cortex and moving the coil in 1 cm steps across the scalp. Stimulation intensity was varied in steps of 2% of the maximum intensity output. MT was defined as the lowest stimulus intensity evoking a MEP amplitude $> 50 \mu\text{V}$ in 5 out of 10 consecutive trials in the relaxed contralateral APB. MEPs were recorded using surface electrodes in a belly-tendon montage. The analog signals were amplified (CED 1902 CED, Cambridge, England), and digitally converted (CED micro 1401, CED, Cambridge, England). To determine the PT, the coil was placed tangentially over the occipital pole, angled at 90° relative to the midline (handle pointing caudally) and then moved approximately 1 cm to the left. The PT was defined as the minimal intensity required to induce phosphenes in 5 of 10 consecutive trials starting with 60% of the maximum stimulator output which was increased by

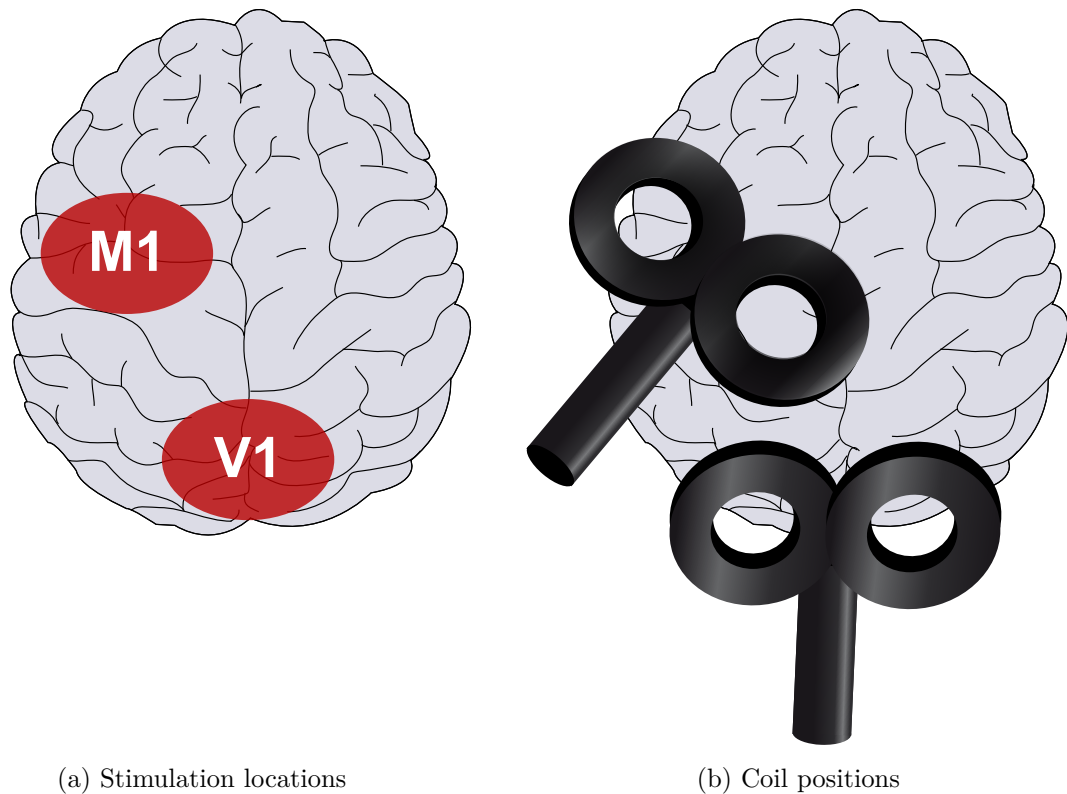


Figure 3.1: Stimulation locations and coil positions for bifocal stimulation: over left M1 and approximately 1 cm to the left of the occipital pole (V1)

5 % steps until phosphenes were reported. Stimulation intensity was then reduced by 2 % until subthreshold intensity. For both coil locations, the stimulation intensity was set to 120 % of the individual threshold.

Before the assessment of MT and PT as described above, a pre-threshold baseline of 3 min resting EEG was recorded. The experiment consisted of 4 blocks each representing a different condition, depending on the time delay between the pulses of the two coils. The delays were chosen according to the cortico-cortical signal conduction velocity (Stefan et al. 2000) and were as follows:

- synchronous stimulation: 0 ms
- asynchronous stimulation: i. e. the pulse from the coil placed over V1 preceded the pulse of the other coil (over M1) by:
 - ▶ 3 ms
 - ▶ 7 ms
 - ▶ randomly between 0 ms and 7 ms (random numbers where generated using MATLAB[®] R2007a)

Figure 3.2 displays the procedure of the experiment. Each block (i. e. each condition) started with a baseline of 3 min EEG recording. Subsequently, the amplifier was blocked and three trains of rTMS were applied simultaneously over the left M1 and V1. The trains of rTMS were each separated by a pause of 30 seconds. Each train lasted 2.5 seconds and consisted of 25 pulses (10 Hz, 120 % MT/ PT).

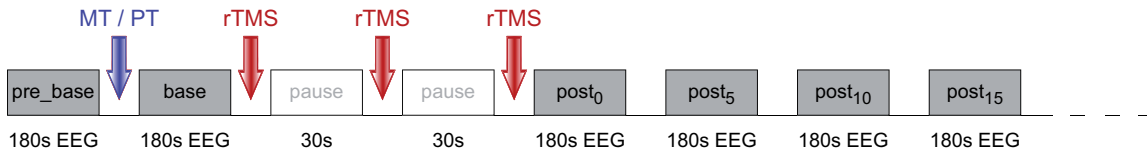


Figure 3.2: Schematic representation of the experimental procedure of the study. A baseline EEG of three minutes *pre_base* was recorded before MT and PT were assessed. A total of four conditions (= blocks) was run. Each block consisted of a baseline EEG recording, a stimulation train (= 3×2.5 s rTMS at 10 Hz), and five post stimulation EEG recordings: immediately (*Post₀*), 5 min (*Post₅*), 10 min (*Post₁₀*), and 15 min (*Post₁₅*) after stimulation.

The frequency of 10 Hz was chosen to affect coherence particularly in the alpha frequency range (8-13 Hz), since coherence of alpha and low beta oscillations have been shown to play a dominant functional role in information processing in large-scale networks underlying visuo-motor (Classen et al. 1998) and visuo-tactile (Hummel and Gerloff 2005) integration. One second after the last TMS pulse of the third rTMS train, the amplifier was deblocked automatically and EEG at rest was recorded for 3 min (*Post₀*). On behalf of evaluating the effect duration, resting EEG was recorded for 3 minutes at 5 (*Post₅*), 10 (*Post₁₀*), and 15 (*Post₁₅*) minutes after the last train of stimulation. Before each baseline and after the last EEG recording *Alertness* and *Tiredness* were assessed by means of a VRS. Subjects were asked to rate their current status of alertness (*extremely bad* \leftrightarrow *extremely good*) and tiredness (*none* \leftrightarrow *extremely tired*) on a scale ranging from 0 to 10.

3.2.3 EEG Recording

EEG (online band pass 0.5 to 100 Hz, sampling rate 500 Hz (NeuroScan, Herndon, VA, USA)) was recorded from 33 (Ag-AgCl) surface electrodes, mounted in a cap (EASYCAP GmbH, Herrsching-Breitbrunn, Germany). Scalp positions were according to the standard 10-20 system, referenced to left and right mastoids, and grounded to FPz (see Figure 3.3 on the facing page). Electrode impedances were kept below 5 k Ω . The EOG (same band pass and sampling rate as for EEG) was recorded at FP1 and FP2.

3.2.4 Offline Analysis

EEG data were analyzed using MATLAB[®] R2009b (The MathWorks[™], Natick, MA, USA) and EEGLab (<http://sccn.ucsd.edu/eeglab/>). Data were re-referenced to an average reference, whereby the average of the voltages recorded at all electrodes on the head at that time point is subtracted from each electrode. Re-referencing to an average reference circumvents the problem of inducing artificial synchrony as it can happen when re-referencing to a common reference (Pockett et al. 2009). Ocular correction was done using an *Independent Component Analysis (ICA)* (Mognon et al. 2010), in order to avoid introducing artificial coherence. Thereby, ICA is data driven, and suffers not from non-physiological constraints requiring the components to be orthogonal.

Further analysis was performed using the following approach. ROIs for the sensorimotor and the visual cortex each were defined according to the study of Plewnia et al. (2008). Therefore, for the left stimulated side channels FP3 and CP3 as well as O1 and Oz were bipolarized by subtraction. The same was done for the right non-stimulated side using FP4 and CP4, and O2 and Oz, respectively (see Figure 3.3).

The time windows were defined according to the study of Plewnia et al. (2008). That are sliding windows of 60 s length each: 0 to 60, 30 to 90, 60 to 120, 90 to 150 s, and 0 to 150 s (see Figure 3.4 on the following page).

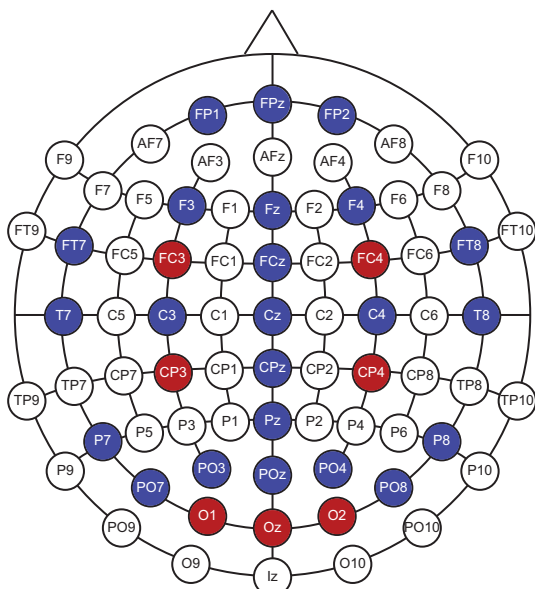


Figure 3.3: The scalp positions were chosen according to the standard 10-20 system. Channels were referenced to left and right mastoids, and grounded to FPz. The red marked channels are the ROIs also used in the study by Plewnia et al. (2008). Two channels were bipolarized by subtraction. For the left stimulated side: FC3-CP3 and O1-Oz. Accordingly, FC4-CP4 and O2-Oz for the right non-stimulated side.

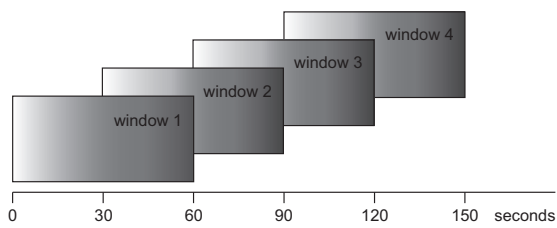
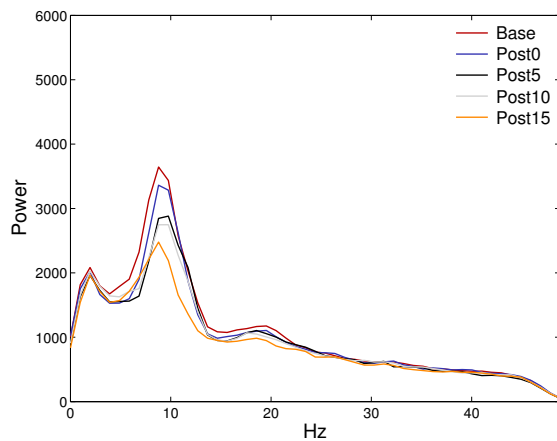


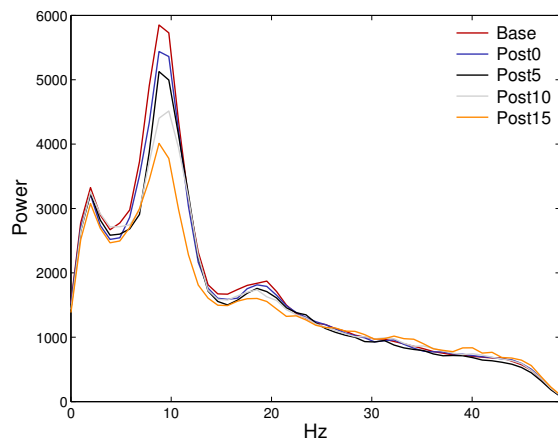
Figure 3.4: The time windows. For the bipolar channels were four sliding windows computed. Each with a length of 60 s and an overlap of 30 s plus one window (not indicated in the scheme) spanning 150 s.

Power Spectra

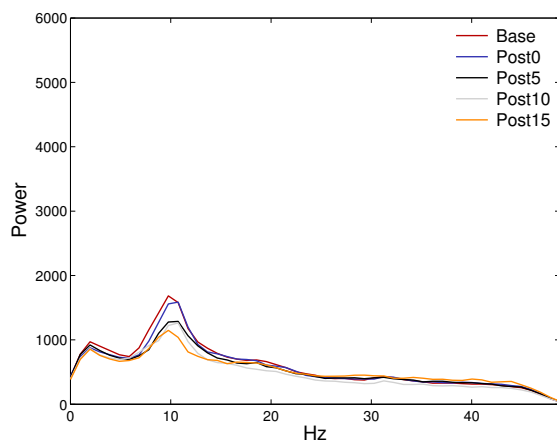
The signal was transferred into the frequency domain by applying a FFT using non overlapping segments of 1024 data points and then the power spectra were computed.



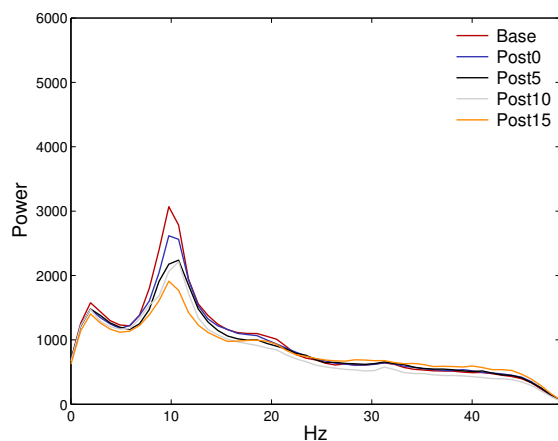
(a) Power spectra at FC3CP3, first sliding window (0 - 60 s) for condition 0 ms



(b) Power spectra at FC3CP3 averaged across 150 s for condition 0 ms



(c) Power spectra at O1Oz, first sliding window (0 - 60 s) for condition 0 ms



(d) Power spectra at O1Oz averaged across 150 s for condition 0 ms

Figure 3.5: Power spectra at FC3CP3 and O1Oz for the first sliding window ranging from 0 - 60 s (left column) vs. an average across 150 s (right column) for condition 0 ms is shown. A typical power spectra can be seen, i. e. an alpha peak at about 7 to 13 Hz.

According to previous findings (for review see, e. g. Schnitzler and Gross 2005b), and what can be seen in Figure 3.5 on the preceding page, the alpha range (roughly 8- 12 Hz) shows strongest differences. Subsequently, further analysis was limited to the alpha band.

The power spectra were computed for the four bipolarized channels (FC3CP3, O1Oz, FC4CP4, O2Oz). In order to assess the pure stimulation related effect, the power values of the baseline (*base*) were subtracted from the power values of all post (*post*) measurements, i. e. for further analysis the *Stimulation Related Power (SRPower)* values were used.

$$SRPower_{xx} = Power_{[post]} - Power_{[base]} \quad (3.1)$$

Coherence

Coherence (Coh) was obtained by dividing the magnitude squared cross spectrum (P) of the frequency range of interest (f , in our case: alpha range from 7.8- 13.7 Hz) by the power spectra (P) of both time series (Schnitzler and Gross 2005a).

$$Coh_{xy}(f) = \frac{|P_{xy}(f)|^2}{P_{xx}(f)P_{yy}(f)} \quad (3.2)$$

Coherence was computed for the following bipolar channel combinations: *left stimulated side*: FC3CP3-O1Oz and *right non-stimulated side*: FC4CP4-O2Oz.

Subsequent analysis was done using the *Stimulation Related Coherence (SRCoh)* of all post measurements, i. e. the baseline was subtracted from each post measurement. Additionally, coherence estimates were normalized by the inverse hyperbolic tangent (Halliday et al. 1995), i. e. *atanh* in order to achieve constant variance for statistical analysis.

$$SRCoh_{xy} = atanh(Coh_{xy[post]}) - atanh(Coh_{xy[base]}) \quad (3.3)$$

Incrementing SRCoh magnitudes are expressed as positive values, while decrements are expressed as negative values.

3.2.5 Statistical Analysis

For all statistical comparisons, ANOVAs were computed using SPSS 16.0 (SPSS Inc., Chicago, Illinois, USA). Except as noted otherwise two-tailed paired t tests were calculated for posthoc analysis.

Alertness and Tiredness

For both variables one factorial ANOVAs with repeated measurements were computed. The factor *Time Course* had five levels (baseline, after first block, after second block, after third block, after fourth block).

Power Spectra

In order to compare the four conditions, an ANOVA with repeated measurements (subjects) was computed in an $4 \times 4 \times 4$ design (four bipolar channels: FC3CP3, O1Oz, FC4CP4, O2Oz; four conditions: 0 ms, 3 ms, 7 ms, random; and four post recordings: $Post_0$, $Post_5$, $Post_{10}$, $Post_{15}$). The baseline was subtracted from each post recording. To explore the short term effects, for each of the four conditions an ANOVA (4×4 design, i. e. four bipolar channels: FC3CP3, O1Oz, FC4CP4, O2Oz; four time windows: 0-60 s, 30-90 s, 60-120 s, 90-150 s) was calculated.

Coherence

To compare all four conditions an ANOVA with repeated measurements and an $2 \times 4 \times 4$ design (two bipolar channel combinations: FC3CP3-O1Oz, FC4CP4-O2Oz; four conditions: 0 ms, 3 ms, 7 ms, random; and four post measurements, i. e. recordings: $Post_0$, $Post_5$, $Post_{10}$, $Post_{15}$) was run. Additionally, a 4×4 ANOVA with repeated measurements (*Conditions*: 0 ms, 3 ms, 7 ms, random; *Recordings*: $Post_0$, $Post_5$, $Post_{10}$, $Post_{15}$) for the first sliding window (0-60 s) only at the left stimulated side (bipolar channel combination FC3CP3-O1Oz) was calculated. In order to explore the short term effects for each of the four conditions an ANOVA with repeated measurements was computed using a design of 2×4 (two channel combinations: FC3CP3-O1Oz, FC4CP4-O2Oz and four sliding time windows: 0-60 s, 30-90 s, 60-120 s, 90-150 s).

3.3 Results

In this section the results of the behavioural assessments, i. e. Alertness and Tiredness, and of the Power Spectra and the Coherence Analysis will be described.

3.3.1 Alertness and Tiredness

There were no significant results in the ANOVAs with respect to Alertness and Tiredness.

3.3.2 Power Spectra

The $4 \times 4 \times 4$ ANOVA (*Channels*: FC3CP3, O1Oz, FC4CP4, O2Oz; *Conditions*: 0 ms, 3 ms, 7 ms, random; *Recordings*: $Post_0, Post_5, Post_{10}, Post_{15}$) revealed a main effect *Conditions* ($F_{(3,27)} = 4.196$; $P = 0.015$; $\varepsilon(\text{GG}) = 0.477$), and a main effect *Recordings* ($F_{(3,27)} = 3.935$; $P = 0.019$; $\varepsilon(\text{GG}) = 0.677$), as well as a significant interaction *Channels* \times *Recordings* ($F_{(9,81)} = 2.666$; $P = 0.009$; $\varepsilon(\text{GG}) = 0.409$). For the main effect *Conditions* pairwise comparisons showed significant differences between conditions *7ms vs. 0ms* ($P = 0.011$) and *7ms vs. random* ($P = 0.008$). Figure 3.6 displays the SRPower for each condition, averaged across the four recordings ($Post_0, Post_5, Post_{10}, Post_{15}$) and the four bipolar channels (FP3CP3, O1Oz, FP4CP4, and O2Oz). Condition *7ms* reached the highest stimulation related amplitudes.

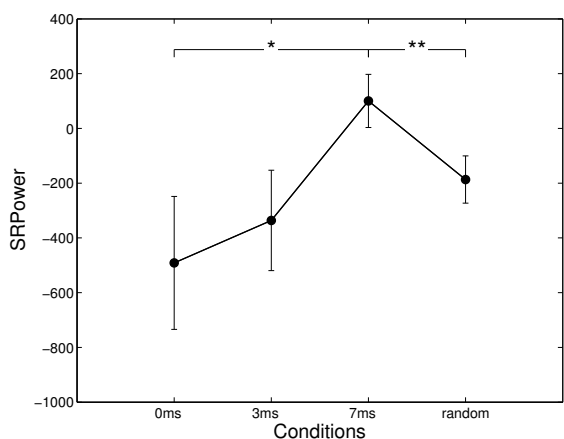


Figure 3.6: The mean SRPower across all subjects and the four bipolarized channels (FP3CP3, O1Oz, FC4CP4, and O2Oz) and the four post measurement recordings ($Post_0, Post_5, Post_{10}, Post_{15}$) are displayed at each of the four conditions in the alpha range (7.8-13.7 Hz). The $4 \times 4 \times 4$ ANOVA (*Channels* \times *Conditions* \times *Recordings*) yielded a main effect for factor *Conditions*. Posthoc analysis revealed significant differences between conditions *7ms vs. 0ms* and *7ms vs. random* ($**P < 0.01$, $*P < 0.05$). Error bars indicate standard error of the mean.

Pairwise comparisons for the main effect *Recordings* revealed significant differences between $Post_0$ vs. $Post_5$ ($P = 0.019$), as well as for $Post_0$ vs. $Post_{15}$ ($P = 0.038$). Accordingly, Figure 3.7 on the next page depicts the means of SRPower across the four conditions (0 ms, 3 ms, 7 ms, random) and the four bipolarized channels (FP3CP3, O1Oz, FP4CP4, O2Oz) at each of the four stimulation related post measurements ($Post_0, Post_5, Post_{10}, Post_{15}$). Immediately after stimulation the SRPower values were highest compared to the other recordings. There is a decrease of the SRPower within the next five minutes, and a slight increase after 10 minutes, before the SRPower decreases at 15 minutes after stimulation.

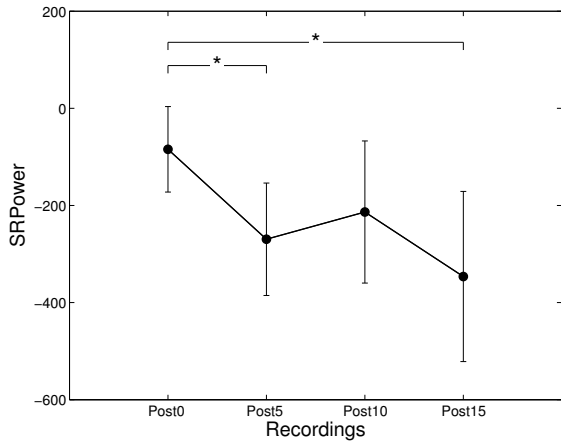


Figure 3.7: The SRPower mean values of the four conditions (0 ms, 3 ms, 7 ms, random) and the four bipolar channels (FP3CP3, O1Oz, FP4CP4, O2Oz) are displayed at each of the four stimulation related post recordings in the alpha range (7.8 - 13.7 Hz). The main effect for factor *Recordings* of the $4 \times 4 \times 4$ ANOVA (*Channels* \times *Conditions* \times *Recordings*). Posthoc analysis showed significant differences between *Post*₀ vs. *Post*₅, as well as for *Post*₀ vs. *Post*₁₅ ($*P < 0.05$). Error bars indicate standard error of the mean.

Posthoc analysis for the significant interaction *Channels* \times *Recordings* showed significant differences for *Post*₀ vs. *Post*₅ ($P = 0.05$ at channel FC3CP3; $P = 0.018$ at channel FC4CP4) and *Post*₀ vs. *Post*₁₅ ($P = 0.03$ at channel FC3CP3; $P = 0.048$ at channel FC4CP4). Figure 3.8 shows the mean values of the SRPower across the four post recordings (*Post*₀, *Post*₅, *Post*₁₀, *Post*₁₅) at each of the bipolarized channels (FC3CP3, O1Oz, FC4CP4, O2Oz). The most prominent differences of the SRPower are at the electrode sides covering the motor cortices (left stimulated side: FC3CP3, right non-stimulated side: FC4CP4) between the red bar (i.e. *Post*₀) and the gray bar (i.e. *Post*₁₅).

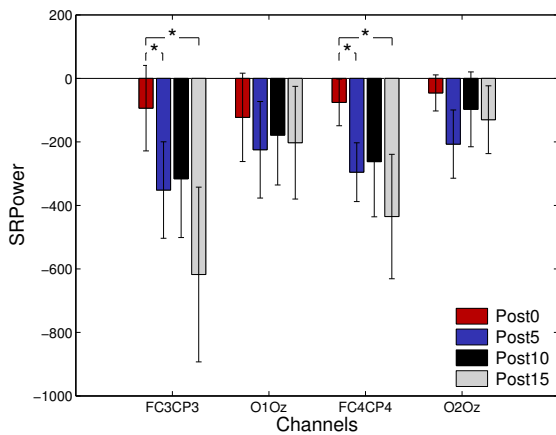


Figure 3.8: The mean SRPower of the four post stimulation recordings, is displayed at each of the four bipolar channels in the alpha range (7.8 - 13.7 Hz). The $4 \times 4 \times 4$ ANOVA (*Channels* \times *Conditions* \times *Recordings*) yielded a significant interaction for the factors *Channels* \times *Recordings*. Posthoc analysis revealed significant differences between *Post*₀ vs. *Post*₅ and *Post*₀ vs. *Post*₁₅ at channels FC3CP3 and FC4CP4 ($*P < 0.05$). Error bars indicate standard error of the mean.

None of the four 4×4 ANOVAs (*Channels*: FC3CP3, O1Oz, FC4CP4, O2Oz; *Time Windows*: 0 - 60 s, 30 - 90 s, 60 - 120 s, 90 - 150 s) with respect to the short term effects within each of the four conditions (0 ms, 3 ms, 7 ms, and random) yielded any significant results.

3.3.3 Coherence

Figure 3.9 on the next page displays both bipolar channel combinations: the left column of the figure shows the *Stimulation Related Coherence (SRCoh)* for the channel combination FC3CP3-O1Oz, i. e. the left stimulated side, and the right column depicts the SRCoh for the channel combination FC4CP4-O2Oz, i. e. the right non-stimulated side. The SRCoh values at each post recording ($Post_0$, $Post_5$, $Post_{10}$, $Post_{15}$) for each condition (0 ms, 3 ms, 7 ms, random) are shown in separate plots for the average time window across 150 seconds in the alpha range (7.8-13.7 Hz).

The respective $2 \times 4 \times 4$ ANOVA (*Channels*: FC3CP3-O1Oz, FC4CP4-O2Oz; *Conditions*: 0 ms, 3 ms, 7 ms, random; *Recordings*: $Post_0$, $Post_5$, $Post_{10}$, $Post_{15}$) did not yield any significant differences as shown in Figure 3.9 on the following page that displays the mean *Stimulation Related Coherence (SRCoh)* values across all subjects at each condition (0 ms, 3 ms, 7 ms, and random) for the left stimulated side (channel combination FC3CP3-O1Oz, see left column) *vs.* the right non-stimulated side (channel combination FC4CP4-O2Oz, see right column). However, there is a weak tendency for a main effect *Conditions* ($F_{(3,27)} = 2.359$; $P = 0.094$). Condition *0 ms* at the left stimulated side (see the plot in the upper left corner) revealed a decrease of the SRCoh from $Post_0$ to $Post_{15}$, similar to the effect described and depicted by Plewnia et al. (2008) in the same frequency band (i. e. alpha). The similarity of the effect in the alpha range of Plewnia et al. (2008) also holds true for the right non-stimulated side, that can be seen in Figure 3.9 on the next page in the upper right corner: an increase of SRCoh from $Post_0$ to $Post_5$ and thereafter a decrease. Likewise, a gradual decrease on the left stimulated side and an analogue increase from $Post_0$ to $Post_{15}$ occurred in condition *3 ms*, displayed in the second row. A rather random pattern of decrease and increase of SRCoh can be seen in rows 3 and 4, i. e. conditions *7 ms* and *random*.

However, Figure 3.10 on page 63 shows the SRCho for the first sliding window at each post recording for each condition. Again, the left column displays the SRCoh values of the left stimulated side (channel combination FC3CP3-O1Oz) and the right column the analogue right non-stimulated side (channel combination FC4CP4-O2Oz). The 4×4 ANOVA (*Conditions*: 0 ms, 3 ms, 7 ms, random; *Recordings*: $Post_0$, $Post_5$, $Post_{10}$, $Post_{15}$) for the first sliding window (0-60 seconds) at the left stimulated side (bipolar channel combination FC3CP3-O1Oz) revealed a main effect for the factor *Recordings* ($F_{(3,27)} = 4.514$; $P = 0.011$; $\varepsilon(\text{GG}) = 0.548$).

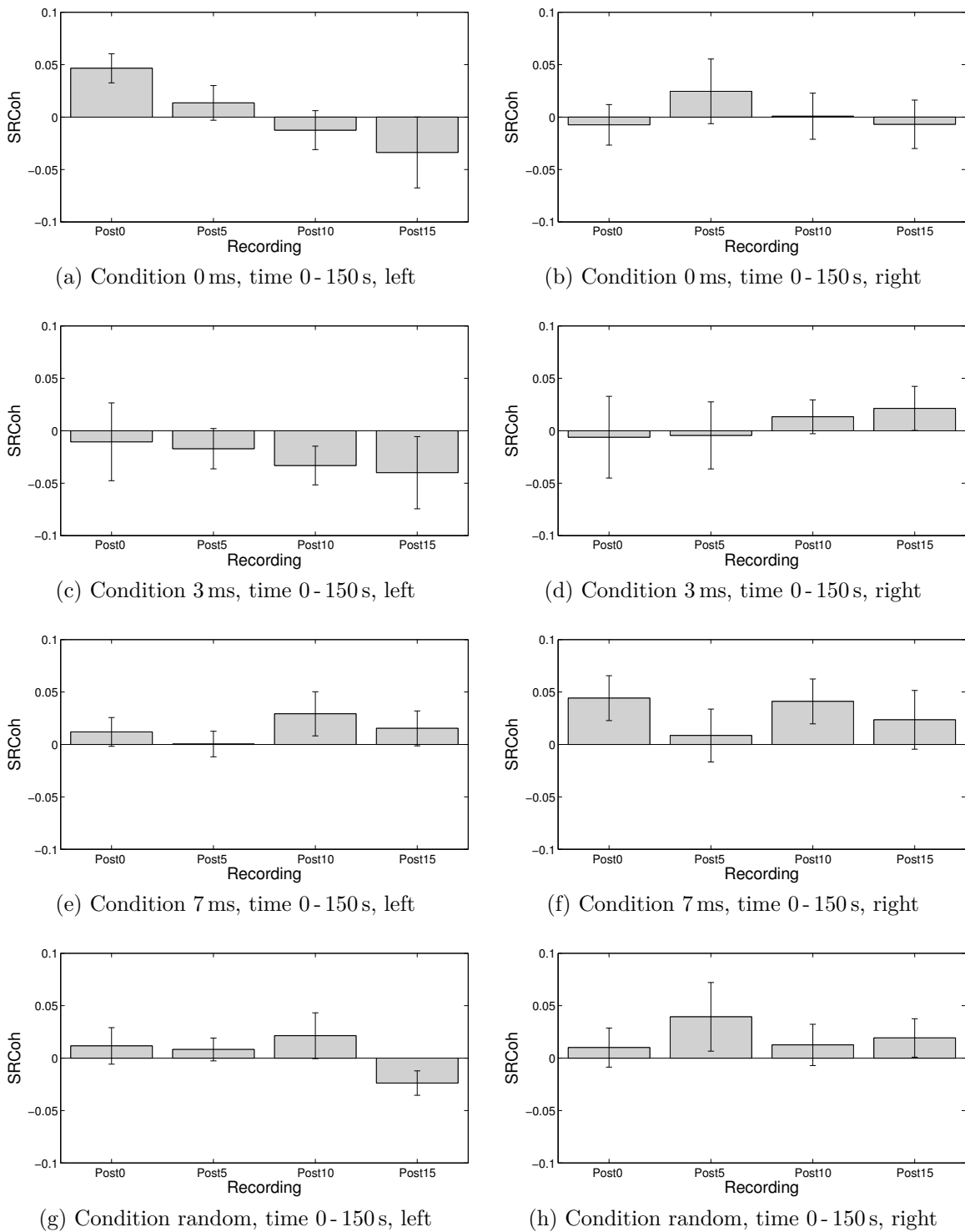


Figure 3.9: Mean SRCoh values are displayed for the bipolarized channels (left column: left stimulated side, i.e. FC3CP3-O1Oz; right column: right non-stimulated side, i.e. FC4CP4-O2Oz), averaged across subjects for all conditions in separate plots at each post recording for the averaged time range of 0 to 150s in the alpha range (7.8-13.7 Hz). Error bars indicate standard error of the mean. There were no statistically significant differences.

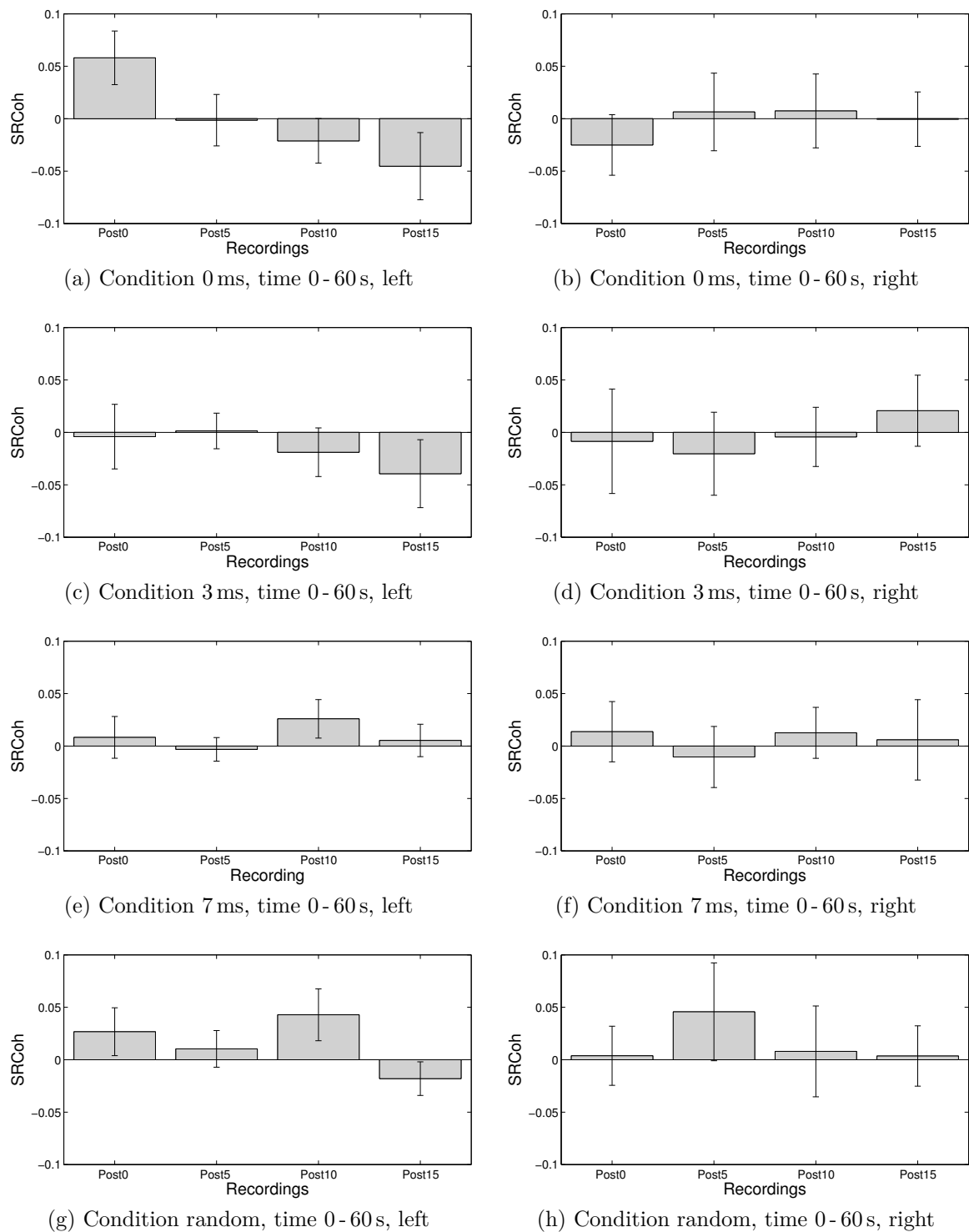


Figure 3.10: Mean SRCoh values are shown for the bipolarized channels (left column: left stimulated side, i. e. FC3CP3-O1Oz; right column: right non-stimulated side, i. e. FC4CP4-O2Oz), averaged across subjects for all conditions in separate plots for the first sliding window (time range 0 to 60 s) at each post recording minus the baseline in the alpha band (7.8-13.7 Hz). Error bars indicate standard error of the mean. The 4×4 ANOVA (*Conditions* \times *Recordings*) for the left stimulated side (FC3CP3-O1Oz) yielded a main effect for the factor *Recordings* ($*P \leq 0.05$).

The increase of SRCoh immediately after stimulation and the decrease until $Post_{15}$ is most prominent in condition $0ms$ that reached statistical significance in the first sliding window (0 to 60 s) at the left stimulated side. The pattern of coherence increase and decrease in the alpha range for the condition $0ms$ at both sides is in line with the effect reported by Plewnia et al. (2008). The coherence patterns observed in the other three conditions are rather not systematic (see Figure 3.10 on the previous page).

The two-tailed paired t tests for posthoc analysis of the 4×4 ANOVA for the first sliding window at the left stimulated side showed a significant difference between $Post_0$ vs. $Post_5$ ($P=0.05$), $Post_0$ vs. $Post_{15}$ ($P=0.028$), and $Post_{10}$ vs. $Post_{15}$ ($P=0.006$). In Figure 3.11 the mean SRCoh across all subjects and all conditions (0 ms, 3 ms, 7 ms, random) at each post measurement ($Post_0$, $Post_5$, $Post_{10}$, $Post_{15}$) at the bipolar channel combination FC3CP3-O1Oz, i. e. left stimulated side, is depicted. There is a decrease in SRCoh from $Post_0$ to $Post_5$ followed by a slight increase of coherence until $Post_{10}$ and thereafter the coherence decreases reaching its minimum value at $Post_{15}$.

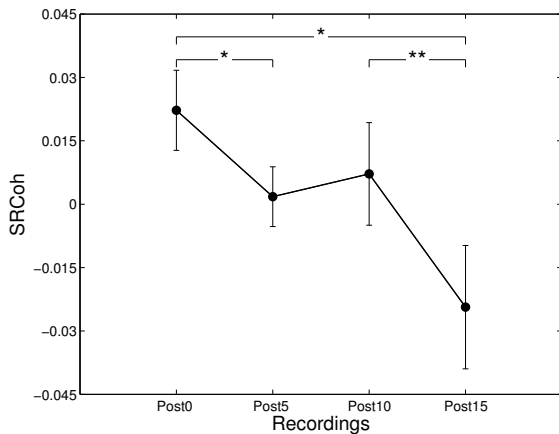


Figure 3.11: SRCoh averaged across subjects and all conditions (0 ms, 3 ms, 7 ms, random) for all post measurements, in the first time window (0 to 60 s), the left stimulated side (bipolar channel combination FC3CP3-O1Oz) in the alpha range (7.8-13.7 Hz). The 4×4 ANOVA ($Conditions \times Recordings$) revealed a main effect for factor $Recordings$ for the left stimulated side. Posthoc tests showed significant differences between $Post_0$ vs. $Post_5$, $Post_0$ vs. $Post_{15}$, and $Post_{10}$ vs. $Post_{15}$ (** $P \leq 0.01$, * $P \leq 0.05$). Error bars indicate standard error of the mean.

In Figure 3.12 on the next page the short term effects are displayed, i. e. the time course of the average SRCoh values across all subjects for each of the four sliding time windows (0 to 60 s, 30 to 90 s, 60 to 120 s, 90 to 150 s) for the left stimulated side (bipolarized channel FC3CP3-O1Oz) vs. the right non-stimulated side (bipolar channel FC4CP4-O2Oz) within each condition (0 ms, 3 ms, 7 ms, and random). The differences between both sides (left stimulated vs. right non-stimulated side) are most prominent in conditions $0ms$ and $7ms$: in condition $0ms$ the left stimulated side shows the highest SRCoh values and a slow decrease of coherence from the first to the last sliding time window and the opposite for the right non-stimulated side. In contrast, in condition $7ms$ the right non-stimulated side shows an increase of SRCoh from $Post_0$ to $Post_{10}$.

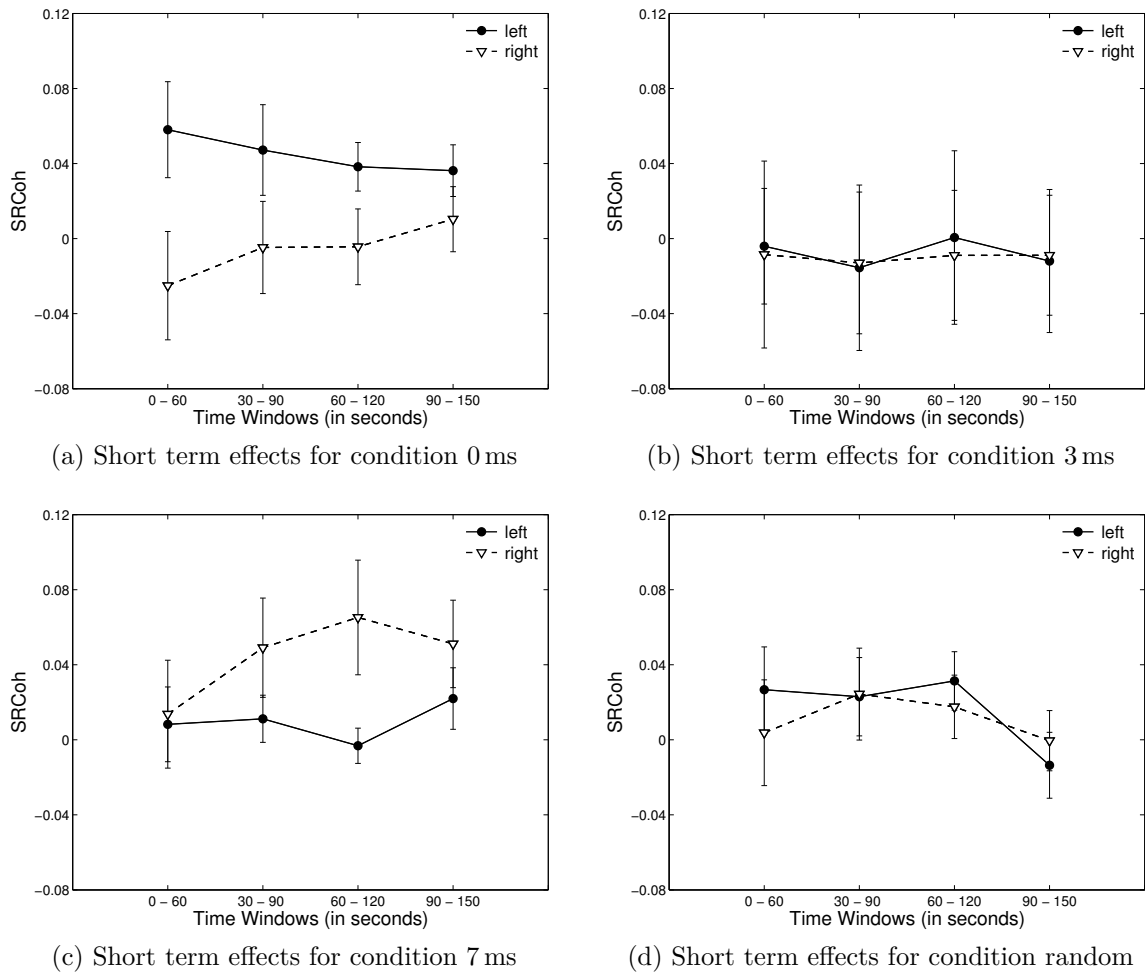


Figure 3.12: Short term effects in the alpha range (7.8-13.7 Hz) with respect to SRCoh within each condition (0 ms, 3 ms, 7 ms, and random, see plots (a)-(d)), averaged across subjects at each of the 4 sliding time windows for both sides: left stimulated side (bipolar channel FC3CP3-O1Oz) vs. right non-stimulated side (bipolar channel FC4CP4-O2Oz) are shown. The 2×4 ANOVA (*Channels* \times *Time Windows*) revealed a main effect for the factor *Channels* ($**P \leq 0.01$) in the condition 0 ms and a main effect *Time Windows* ($*P \leq 0.05$) in the condition random. Error bars indicate standard error of the mean.

The 2×4 ANOVAs (*Channels*: FC3CP3-O1Oz, FC4CP4-O2Oz; *Time Windows*: 0-60 s, 30-90 s, 60-120 s, 90-150 s) with respect to the short term effects revealed two main effects.

One main effect was found in the condition 0 ms for the two levels factor *Channels*, i. e. left stimulated vs. right non-stimulated side ($F_{(1,9)} = 10.921$; $P = 0.009$; $\varepsilon(\text{GG}) = 1$). Compared to the right non-stimulated side the SRCoh value on the left stimulated side is much higher.

In the condition *random* was the other main effect for the factor *Time Windows* ($F_{(3,27)} = 3.626$; $P = 0.026$; $\varepsilon(\text{GG}) = 0.616$) for time windows 30-90 s vs. 90-150 seconds

($P = 0.005$) and $60 - 120\text{ s}$ vs. $90 - 150\text{ s}$ ($P = 0.011$) which is shown in Figure 3.13, i. e. the mean SRCoh across all subjects and both channel combinations (left stimulated side: FC3CP3-O1Oz and right non-stimulated side: FC4CP4-O2Oz) at each of the four sliding windows (0-60 s, 30-90 s, 60-120 s, 90-150 s). There is a slight increase of the SRCoh from the first to the second sliding time window, but almost no difference between the second and the third time window, but a sharp decrease in coherence from the third to the fourth sliding time window.

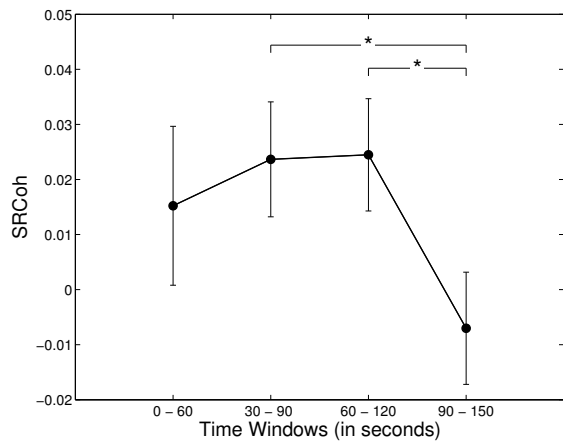


Figure 3.13: The average SRCoh values across all subjects and the two bipolar channel combinations (left stimulated side: FC3CP3-O1Oz and right non-stimulated side: FC4CP4-O2Oz) at each of the four sliding windows in the alpha range (7.8-13.7 Hz) are displayed. The 2×4 ANOVA (*Channels* \times *Time Windows*) revealed a main effect for factor *Time Windows* only in the condition random. Posthoc analysis showed a significant difference for time windows $30 - 90\text{ s}$ vs. $90 - 150\text{ s}$ and $60 - 120\text{ s}$ vs. $90 - 150\text{ s}$ ($*P \leq 0.05$). Error bars indicate standard error of the mean.

3.3.4 Summary of Results

In Table 3.1 on the next page the results of the current study, *Asynchronous Bifocal Stimulation*, are summarized.

Table 3.1: Summary of the Results of the Second Study: Asynchronous Bifocal Stimulation

Power Spectra	
Comparison of Conditions: $4 \times 4 \times 4$ ANOVA (<i>Channels</i> \times <i>Conditions</i> \times <i>Recordings</i>), Time Window: 0 - 150 sec	
Main Effects	<p>Conditions 7 ms vs. 0 ms $P = 0.011$</p> <p>Recordings 7 ms vs. random $P = 0.008$ $Post_0$ vs. $Post_5$ $P = 0.019$ $Post_0$ vs. $Post_{15}$ $P = 0.038$ $Post_0$ vs. $Post_5$ FC3CP3: $P = 0.05$ FC4CP4: $P = 0.018$</p>
Significant Interaction	Channels \times Recordings
Short Term Effects: 4×4 ANOVA (<i>Channels</i> \times <i>Time Windows</i>) no significant effects	
Coherence Analysis	
Comparison of Conditions: $2 \times 4 \times 4$ ANOVA (<i>Channels</i> \times <i>Conditions</i> \times <i>Recordings</i>), Time Window: 0 - 150 sec no significant effects	
Comparison of Conditions: 4×4 ANOVA (<i>Conditions</i> \times <i>Recordings</i> for only FC3CP3-O1Oz), Time Window: 0 - 60 sec	
Main Effects	<p>Recordings $Post_0$ vs. $Post_5$ $P = 0.05$ $Post_0$ vs. $Post_{15}$ $P = 0.028$ $Post_{10}$ vs. $Post_{15}$ $P = 0.006$</p>
Short Term Effects: 2×4 ANOVA (<i>Channels</i> \times <i>Time Windows</i>)	
Main Effects	<p>Condition: 0 ms: Channels FC3CP3-O1Oz vs. FC4CP4-O2Oz $P = 0.009$</p> <p>Condition: random: Time Windows 30 - 90 sec vs. 90 - 150 sec $P = 0.005$ 60 - 120 sec vs. 90 - 150 sec $P = 0.005$</p>

3.4 Discussion

So far, a few groups used ppTMS, i. e. two consecutive single pulses, on different cortical sites, e. g. on PMv and M1 (Koch et al. 2006, O’Shea et al. 2007, Davare et al. 2009, Mars et al. 2009, Buch et al. 2010) in order to investigate the functional role of these areas during execution of specific tasks, e. g. grasping. Recently, it has been shown that coupling of oscillatory activity can be selectively increased by synchronous rTMS given to two distinct brain areas (Plewnia et al. 2008). This is so far the only study in which rTMS was applied simultaneously to two cortical sides. The question remained whether a short temporal delay between the pulses given to M1 and V1, i. e. an asynchronous bifocal stimulation, would be more or less effective compared to the simultaneous stimulation. The present study was designed to *firstly*, replicate the finding of the previous study that synchronous rTMS applied to M1 and V1 increases cortico-cortical coherence between these areas, and *secondly*, to compare the effects of three different asynchronous bifocal rTMS stimulations *vs.* the synchronous bifocal stimulation.

We confirmed the key finding of the reference study by Plewnia et al. (2008). The increase of coherence after synchronous bifocal stimulation applied to the primary visual and motor cortices developing within two minutes and vanishing roughly after 15 minutes.

Our results show that the synchronous bifocal stimulation (condition: 0 ms) increases the coherence immediately after stimulation exclusively in a time range from 0 to 60 seconds at the left stimulated side.

However, there is a weak tendency for a main effect *Conditions* when averaged across 150 seconds and both sides, i. e. left stimulated side and right non-stimulated side are considered. Plewnia et al. (2008) found this effect slightly delayed in the fourth sliding time window, i. e. from 90 to 150 seconds at the left stimulated side. According to Plewnia et al. (2008) this increase returned to baseline after 20 minutes.

For the power spectra, a main effect of conditions was found, showing a significant difference between the conditions 7 ms and 0 ms as well the random delay. The conditions 7 ms shows the strongest increase in power and therefore a delay of 7 ms between stimulation of V1 and stimulation of M1 seems to be most effective.

A main effect *Recordings* in the power spectra was found as well as an interaction *Channels* \times *Recordings*. The left (FC3CP3) and the right (FC4CP4) bipolarized channels showed the highest power value immediately after stimulation $Post_0$. This value differed

significantly from the power value after $Post_5$ and $Post_{15}$. The effect of rTMS on power is highest directly after stimulation and decreases with time.

For the coherence analysis, the $2 \times 4 \times 4$ ANOVA (*Channels* \times *Conditions* \times *Recordings*) across the whole length of the recording time did not reveal significant differences. While in the 4×4 ANOVA (*Conditions* \times *Recordings*) of the first time window for the left hemisphere, a main effect of *Recordings* was found. Post hoc tests revealed a similar pattern for the effect found in the power analysis.

When looking in more detail at the different sliding windows separately for the four conditions with the 2×4 ANOVA (*Channels* \times *Time Windows*), a main effect of *Channels* was found for the synchronous condition (delay: 0 ms). The coherence of the left hemisphere was stronger than of the right hemisphere. As the left hemisphere was the stimulated site, these effects are not surprising. Additionally, a main effect of *Time Windows* in the condition *random* was found in the 2×4 ANOVA (*Channels* \times *Time Windows*). The second and third time windows were significantly different from the fourth time window. The second and the third time windows show the highest coherence values, in the fourth window coherence decreased.

Comparing the plots in Figure 3.9 on page 62 with the plots in Plewnia et al. (2008) the same pattern at the left stimulated side and the right non-stimulated side in the alpha frequency can be described. In the current study the differences did not reach statistical significance. This may be explained by differences in the study designs:

In the current study, we focused on the effect of asynchronous stimulation, while Plewnia et al. (2008) demonstrated the superiority of the bifocal stimulation over the monofocal stimulation. Plewnia et al. (2008) did not only calculate SRPower and SRCoh, but computed $SR_{\Delta}Power$ and $SR_{\Delta}Coh$ by subtracting the values of the monofocal condition from the bifocal condition.

Therefore, the experimental procedure used in the present study was slightly modified.

Plewnia et al. (2008) recorded EEG blocks between the three trains of rTMS (each 2.5 s at 10 Hz) and finally averaged these three blocks, while we intended to accumulate the effect of all three rTMS trains by applying them immediately after each other according to the safety guidelines by Wassermann (1998). In our study, EEG recording started after all rTMS trains had been applied.

Another modification of the experimental setup concerned the assessment of EEG after the stimulation. While Plewnia et al. (2008) recorded the EEG immediately after stimulation, after 10 minutes, 20 minutes, and after 30 minutes, in the present study

we assessed the effects of the stimulation immediately after, after 5, after 10 and after 15 minutes. Since Plewnia et al. (2008) reported a return to baseline of the coherence increase after 20 minutes of stimulation, we waited for another 15 minutes after the last EEG recording before proceeding with the next condition, so that there was a total of 30 minutes between the last stimulation and the baseline of the following condition.

For the future it remains to be investigated whether reversing the order of the pulses (chosen here: pulse applied to V1 precedes the pulse over M1) would cause different results.

In a visuo-tactile task (Hummel and Gerloff 2005) and during memory encoding (Weiss and Rappelsberger 2000) the magnitude of task specific EEG coherence and the degree of behavioural success could be directly linked. Continuative investigations are necessary to strengthen the concept of interregional coherence being a neuronal mechanism underlying cognitive effort and performance in sensorimotor tasks (Hummel and Gerloff 2005, Kay 2005). Respective results would be particularly important for therapeutical interventions in motor impaired patients.

In conclusion, the current study is so far the second study applying bifocal rTMS to two distinct brain areas. The key finding is the confirmation of an increased coherence specifically at the stimulated side after applying bifocal synchronuous rTMS developing immediately after stimulation and gradually vanishing after 15 minutes.

4 Conclusion

The present thesis aimed (1.) to further elucidate the neuronal mechanisms underlying visuo-motor integration, (2.) to investigate which alterations occur depending on aging and (3.) to explore whether it is possible to modulate cortico-cortical coupling using rTMS applied simultaneously to two cortical sides.

The first study of this thesis was designed to investigate mechanisms contributing to visuo-motor integration and changes occurring during healthy aging. Therefore, four different age groups (25 years, 40 years, 60 years, and 80 years) were recruited and combined MEG/EEG was recorded while subjects performed a *continuous visuo-motor (VM)*, *visual (V)*, *motor (M)*, or *visual plus motor (V+M)* (without feedback) task. Using *Synthetic Aperture Magnetometry (SAM)*, a beamformer technique for MEG source localization, and performing a group level analysis of the localized sources, the regions contributing to the network for visuo-motor integration were identified. In a second step, the power spectra and coherence, a measure for cortico-cortical coupling (Schnitzler and Gross 2005a), were computed for MEG and EEG data. The following results were found:

Firstly, we could replicate former results stating that the network for visuo-motor integration comprises occipito-parietal and precentral cortices. *Secondly*, we found the formerly described shift of brain activity to more prefrontal areas in the elderly subjects. *Third*, the elderly showed an overall higher neuronal activity, yet more pronounced in the beta frequency, compared to young adults. *Fourth*, we found a tendency in an increased activity of the parietal cortex in the elderly. *Fifth*, we found a tendency towards previous reports that aging is accompanied by progressing impairment of motor performance which also corresponds to previous findings (Inuggi et al. 2009, Mattay et al. 2002, Labyt et al. 2006, Smith et al. 1999, Vallesi et al. 2009, Welford 1988). And *sixth*, we could not replicate previously reported results on cortico-cortical coupling between the areas involved in visuo-motor integration (Classen et al. 1998), nor could we confirm the decrease of coherence in the VM task when comparing young and elderly subjects.

The SAM beamformer technique is a reliable tool for source localisation of MEG data, since the previous findings (Andersen and Buneo 2002, Battaglia-Mayer and Caminiti

2002, Caminiti et al. 1998, Kalaska et al. 1997, Medendorp et al. 2008, Thoenissen et al. 2002, Wise et al. 1997) on the network of visuo-motor integration could be confirmed. The results of the analysis of the power spectra are in agreement with studies reporting an overall higher neuronal activity in the elderly subjects Labyt et al. (2006), Vallesi et al. (2010) and a shift from posterior to more anterior regions (for review see Niedermeyer 1997, Palva and Palva 2007, Rossini et al. 2007). Furthermore, the results regarding the power spectra point towards a tendency of increased activity in the parietal cortex for the elderly subjects, as it was found in other studies (Anderson et al. 2000, Grady et al. 2002, 2003, Madden et al. 2007). However, the previously reported findings on cortico-cortical coupling in a visuo-motor task (Classen et al. 1998) could not be confirmed. The main reasons therefore are limitations of the analysis strategy used. Within the scope of this thesis, the classical approach for analyzing oscillatory activities – that is applying a FFT – was used for the following reason: Considering the amount of data resulting from more than 40 subjects tested in four conditions and the aim to explore the course of the age dependent alterations occurring in visuo-motor integration, a method is necessary which can be applied using script routines. After this method did not reveal results that could be expected taking findings from previous studies into account, in a next step a more sophisticated analysis using a multivariate *autoregressive modeling (AR)* approach in collaboration with experts in this field will be done. Very preliminary results of this step seem very promising.

In the second study which aimed to extend the findings of (Plewnia et al. 2008) that rTMS applied simultaneously to two distinct brain regions has an ameliorating effect on cortico-cortical coupling by means of increasing EEG coherence, we could confirm the previous results. There were four different stimulation conditions: a synchronous stimulation as it was used in the reference study by Plewnia et al. (2008), and three asynchronous stimulation, i. e. there was a short delay between the two pulses given to *Primary Visual Cortex (V1)* and *Primary Motor Cortex (M1)*: either 3 ms, 7 ms or a random delay between 0 ms and 7 ms. The synchronous stimulation proved to be the one to increase the coherence between M1 and V1 immediately after stimulation. This effect vanished after 15 minutes.

By showing that applying rTMS to two cortical sides simultaneously leads to an increasing cortico-cortical coupling immediately after stimulation strengthens the concept following Hebb's (Hebb 1949) idea of a mechanism whereby an increase in synaptic efficacy arises from the presynaptic cell's repeated and persistent stimulation of the postsynaptic cell. However, since there are no direct anatomical connections between visual and motor areas at least one intermediate synapse is required to connect these

two areas. Recent findings suggest that this intermediate link between perception and action might be located in the *Inferior frontal gyrus (IFG)*. Beyond its role in speech production, the IFG seems to be involved in motor control by interfacing external information about biological motion with internal motor representation of hand and arm actions (for an overview see Binkofski and Buccino 2006). Also, the above mentioned very preliminary results of a more sophisticated analysis of the younger age group in the first study described in this thesis, suggest that the IFG might be also involved in accomplishing a continuous visuo-motor task.

A topic to study for future projects could be the modulation of cortico-cortical coherence when stimulating the visual area and the IFG during the performance of a visuo-motor integration task.

Bibliography

- Aleman A, Sommer I, Kahn R (2007) Efficacy of slow repetitive transcranial magnetic stimulation in the treatment of resistant auditory hallucinations in schizophrenia: a meta-analysis. *J Clin Psychiatry* 68:416–421.
- Andersen RA, Buneo CA (2002) Intentional maps in posterior parietal cortex. *Annu Rev Neurosci* 25:189–220.
- Anderson ND, Iidaka T, Cabeza R, Kapur S, McIntosh AR, Craik FI (2000) The effects of divided attention on encoding- and retrieval-related brain activity: A pet study of younger and older adults. *Journal of cognitive neuroscience* 12:775–92.
- Andrew C, Pfurtscheller G (1996) Dependence of coherence measurements on eeg derivation type. *Med Biol Eng Comput* 34:232–8.
- Arfeller C, Vonthein R, Plontke SK, Plewnia C (2009) Efficacy and safety of bilateral continuous theta burst stimulation (ctbs) for the treatment of chronic tinnitus: design of a three-armed randomized controlled trial. *Trials* 10:74.
- Babiloni C, Babiloni F, Carducci F, Cincotti F, Percio CD, Pino GD, Maestrini S, Priori A, Tisei P, Zanetti O, Rossini PM (2000) Movement-related electroencephalographic reactivity in alzheimer disease. *NeuroImage* 12:139–46.
- Barker AT, Jalinous R, Freeston IL (1985) Non-invasive magnetic stimulation of human motor cortex. *Lancet* 1:1106–7.
- Battaglia-Mayer A, Caminiti R (2002) Optic ataxia as a result of the breakdown of the global tuning fields of parietal neurones. *Brain* 125:225–37.
- Baule G, McFee R (1965) Theory of magnetic detection of heart's electrical activity. *Journal of Applied Physics* 36:2066–2073.
- Belardinelli P, Ciancetta L, Pizzella V, Gratta C, Romani GL (2006) Localizing complex neural circuits with meg data. *Cogn Process* 7:53–59.

- Belardinelli P, Ciancetta L, Staudt M, Pizzella V, Londei A, Birbaumer N, Romani GL, Braun C (2007) Cerebro-muscular and cerebro-cerebral coherence in patients with pre- and perinatally acquired unilateral brain lesions. *NeuroImage* 37:1301–14.
- Berardelli A, Inghilleri M, Rothwell JC, Romeo S, Currà A, Gilio F, Modugno N, Manfredi M (1998) Facilitation of muscle evoked responses after repetitive cortical stimulation in man. *Experimental Brain Research* 122:79–84.
- Binkofski F, Buccino G (2006) The role of ventral premotor cortex in action execution and action understanding. *J Physiol Paris* 99:396–405.
- Braun C, Staudt M, Schmitt C, Preissl H, Birbaumer N, Gerloff C (2007) Crossed cortico-spinal motor control after capsular stroke. *Eur J Neurosci* 25:2935–45.
- Brookes MJ, Gibson AM, Hall SD, Furlong PL, Barnes GR, Hillebrand A, Singh KD, Holliday IE, Francis ST, Morris PG (2005) Glm-beamformer method demonstrates stationary field, alpha erd and gamma ers co-localisation with fmri bold response in visual cortex. *NeuroImage* 26:302–8.
- Brookes MJ, Stevenson CM, Barnes GR, Hillebrand A, Simpson MIG, Francis ST, Morris PG (2007) Beamformer reconstruction of correlated sources using a modified source model. *NeuroImage* 34:1454–65.
- Brookes MJ, Vrba J, Robinson SE, Stevenson CM, Peters AM, Barnes GR, Hillebrand A, Morris PG (2008) Optimising experimental design for meg beamformer imaging. *NeuroImage* 39:1788–802.
- Buch ER, Mars RB, Boorman ED, Rushworth MFS (2010) A network centered on ventral premotor cortex exerts both facilitatory and inhibitory control over primary motor cortex during action reprogramming. *J Neurosci* 30:1395–401.
- Caminiti R, Ferraina S, Mayer AB (1998) Visuomotor transformations: early cortical mechanisms of reaching. *Curr Opin Neurobiol* 8:753–61.
- Chen R, Classen J, Gerloff C, Celnik P, Wassermann EM, Hallett M, Cohen L (1997) Depression of motor cortex excitability by low-frequency transcranial magnetic stimulation. *Neurology* 48:1398–1403.
- Chen WH, Mima T, Siebner HR, Oga T, Hara H, Satow T, Begum T, Nagamine T, Shibasaki H (2003) Low-frequency rtms over lateral premotor cortex induces lasting changes in regional activation and functional coupling of cortical motor areas. *Clin Neurophysiol* 114:1628–37.

- Cheyne D, Bakhtazad L, Gaetz W (2006) Spatiotemporal mapping of cortical activity accompanying voluntary movements using an event-related beamforming approach. *Human Brain Mapping* 27:213–29.
- Classen J, Gerloff C, Honda M, Hallett M (1998) Integrative visuomotor behavior is associated with interregionally coherent oscillations in the human brain. *J Neurophysiol* 79:1567–73.
- Coles MGH, Rugg MD (1995) *Electrophysiology of Mind*, chapter Event-related brain potentials: An introduction., pp. 1–26 Oxford University Press, New York.
- Cuffin BN, Cohen D (1979) Comparison of the magnetoencephalogram and electroencephalogram. *Electroencephalogr Clin Neurophysiol* 47:132–46.
- da Silva FHL (1996) Biophysical issues at the frontiers of the interpretation of eeg/meg signals. *Electroencephalogr Clin Neurophysiol Suppl* 45:1–7.
- da Silva FL (1991) Neural mechanisms underlying brain waves: from neural membranes to networks. *Electroencephalogr Clin Neurophysiol* 79:81–93.
- Davare M, Montague K, Olivier E, Rothwell JC, Lemon RN (2009) Ventral premotor to primary motor cortical interactions during object-driven grasp in humans. *Cortex* 45:1050–7.
- Davis SW, Dennis NA, Buchler NG, White LE, Madden DJ, Cabeza R (2009) Assessing the effects of age on long white matter tracts using diffusion tensor tractography. *NeuroImage* 46:530–41.
- Diekmann V, Ern e SN, Becker W (1999) *Modern Techniques in Neuroscience Research*, chapter Magnetoencephalography., pp. 1025–1054 Springer Verlag, Berlin.
- Dujardin K, Bourriez JL, Guieu JD (1994) Event-related desynchronization (erd) patterns during verbal memory tasks: effect of age. *International journal of psychophysiology : official journal of the International Organization of Psychophysiology* 16:17–27.
- Dujardin K, Bourriez JL, Guieu JD (1995) Event-related desynchronization (erd) patterns during memory processes: effects of aging and task difficulty. *Electroencephalogr Clin Neurophysiol* 96:169–82.
- Engel A, Singer W (2001) Temporal binding and the neural correlates of sensory awareness. *Trends Cogn Sci (Regul Ed)* 5:16–25.
- Engel AK, Fries P, Singer W (2001) Dynamic predictions: oscillations and synchrony in top-down processing. *Nat Rev Neurosci* 2:704–16.

- Epstein CM, Schwartzberg DG, Davey KR, Sudderth DB (1990) Localizing the site of magnetic brain stimulation in humans. *Neurology* 40:666–70.
- Folmer RL, Carroll JR, Rahim A, Shi Y, Martin WH (2006) Effects of repetitive transcranial magnetic stimulation (rtms) on chronic tinnitus. *Acta oto-laryngologica Supplementum* pp. 96–101.
- Fries P (2005) A mechanism for cognitive dynamics: neuronal communication through neuronal coherence. *Trends Cogn Sci (Regul Ed)* 9:474–80.
- Fuggetta G, Pavone EF, Fiaschi A, Manganotti P (2008) Acute modulation of cortical oscillatory activities during short trains of high-frequency repetitive transcranial magnetic stimulation of the human motor cortex: a combined eeg and tms study. *Human Brain Mapping* 29:1–13.
- George MS, Nahas Z, Kozel FA, Goldman J, Molloy M, Oliver N (1999) Improvement of depression following transcranial magnetic stimulation. *Curr Psychiatry Rep* 1:114–124.
- Gerloff C, Braun C, Staudt M, Hegner YL, Dichgans J, Krägeloh-Mann I (2006) Coherent corticomuscular oscillations originate from primary motor cortex: evidence from patients with early brain lesions. *Human brain mapping* 27:789–98.
- Ghacibeh GA, Mirpuri R, Drago V, Jeong Y, Heilman KM, Triggs WJ (2007) Ipsilateral motor activation during unimanual and bimanual motor tasks. *Clin Neurophysiol* 118:325–32.
- Grady CL, Bernstein LJ, Beig S, Siegenthaler AL (2002) The effects of encoding task on age-related differences in the functional neuroanatomy of face memory. *Psychol Aging* 17:7–23.
- Grady CL, McIntosh AR, Craik FIM (2003) Age-related differences in the functional connectivity of the hippocampus during memory encoding. *Hippocampus* 13:572–86.
- Graziadio S, Basu A, Tomasevic L, Zappasodi F, Tecchio F, Eyre JA (2010) Developmental tuning and decay in senescence of oscillations linking the corticospinal system. *J Neurosci* 30:3663–74.
- Gross J, Timmermann L, Kujala J, Salmelin R, Schnitzler A (2003) Properties of meg tomographic maps obtained with spatial filtering. *NeuroImage* 19:1329–36.
- Halliday DM, Rosenberg JR, Amjad AM, Breeze P, Conway BA, Farmer SF (1995) A framework for the analysis of mixed time series/point process data—theory and

- application to the study of physiological tremor, single motor unit discharges and electromyograms. *Prog Biophys Mol Biol* 64:237–78.
- Hämäläinen M, Hari R, Ilmoniemi RJ, Knuutila J, Lounasmaa OV (1993) Magnetoencephalography - theory, instrumentation, and applications to noninvasive studies of the working human brain. *Reviews of Modern Physics* 65:413–497.
- Hansen PC, Kringelbach ML, Salmelin R (2010) *MEG: An Introduction to Methods* Oxford University Press, Oxford.
- Hayashi T, Ohnishi T, Okabe S, Teramoto N, Nonaka Y, Watabe H, Imabayashi E, Ohta Y, Jino H, Ejima N, Sawada T, Iida H, Matsuda H, Ugawa Y (2004) Long-term effect of motor cortical repetitive transcranial magnetic stimulation [correction]. *Ann Neurol* 56:77–85 Erratum in: *Annals of Neurology* 56(2): 311.
- Hebb DO (1949) *The Organization of Behavior* Wiley, New York.
- Helmholtz H (1853) über einige gesetze der vertheilung elektrischer ströme in körperlichen leitern mit anwendung auf die thierisch-elektrischen versuche. *Ann Phys Chem* 89:211.
- Herwig U, Fallgatter AJ, Höppner J, Eschweiler GW, Kron M, Hajak G, Padberg F, Naderi-Heiden A, Abler B, Eichhammer P, Grossheinrich N, Hay B, Kammer T, Langguth B, Laske C, Plewnia C, Richter MM, Schulz M, Unterecker S, Zinke A, Spitzer M, Schönfeldt-Lecuona C (2007) Antidepressant effects of augmentative transcranial magnetic stimulation: randomised multicentre trial. *The British Journal of Psychiatry: The Journal of Mental Science* 191:441–8.
- Hoffman R, Cavus I (2002) Slow transcranial magnetic stimulation, long-term depotentiation, and brain hyperexcitability disorders. *Am J Psychiatry* 159:1093–1102 Review.
- Holm S (1979) A simple sequentially rejective multiple test procedure. *Scand. J. Statist.* 6:65–70.
- Hubble JP (1998) Aging and the basal ganglia. *Neurol Clin* 16:649–57.
- Hummel F, Gerloff C (2005) Larger interregional synchrony is associated with greater behavioral success in a complex sensory integration task in humans. *Cereb Cortex* 15:670–8.

- Inuggi A, Amato N, Magnani G, González-Rosa JJ, Chieffo R, Comi G, Leocani L (2009) Cortical control of unilateral simple movement in healthy aging. *Neurobiol Aging* .
- Jernigan TL, Archibald SL, Berhow MT, Sowell ER, Foster DS, Hesselink JR (1991) Cerebral structure on mri, part i: Localization of age-related changes. *Biol Psychiatry* 29:55–67.
- Jing H, Takigawa M (2000) Observation of eeg coherence after repetitive transcranial magnetic stimulation. *Clin Neurophysiol* 111:1620–31.
- Jirsa KV, McIntosh AR (2007) *Handbook of Brain Connectivity* Springer, New York.
- Kalaska JF, Scott SH, Cisek P, Sergio LE (1997) Cortical control of reaching movements. *Curr Opin Neurobiol* 7:849–59.
- Kalbe E, Kessler J, Calabrese P, Smith R, Passmore AP, Brand M, Bullock R (2004) Demtect: a new, sensitive cognitive screening test to support the diagnosis of mild cognitive impairment and early dementia. *Int J Geriatr Psychiatry* 19:136–43.
- Kawashima R, Matsumura M, Sadato N, Naito E, Waki A, Nakamura S, Matsunami K, Fukuda H, Yonekura Y (1998) Regional cerebral blood flow changes in human brain related to ipsilateral and contralateral complex hand movements—a pet study. *Eur J Neurosci* 10:2254–60.
- Kay LM (2005) Theta oscillations and sensorimotor performance. *Proc Natl Acad Sci USA* 102:3863–8.
- Kay SM (1988) *Modern Spectral Estimation* Prentice Hall, Englewood Cliffs, New Jersey.
- Keil A, Gruber T, Müller MM (2001) Functional correlates of macroscopic high-frequency brain activity in the human visual system. *Neuroscience and biobehavioral reviews* 25:527–34.
- Kessler J, Calabrese P, Kalbe E, Berger F (2000) Demtect. ein neues screening-verfahren zur unterstützung der demenzdiagnostik. *Psycho* 6:343?347.
- Kido A, Tanaka N, Stein RB (2004) Spinal excitation and inhibition decrease as humans age. *Can J Physiol Pharmacol* 82:238–48.
- Klimesch W, Sauseng P, Hanslmayr S (2007) Eeg alpha oscillations: the inhibition-timing hypothesis. *Brain research reviews* 53:63–88.

- Kobayashi M, Hutchinson S, Théoret H, Schlaug G, Pascual-Leone A (2004) Repetitive tms of the motor cortex improves ipsilateral sequential simple finger movements. *Neurology* 62:91–8.
- Koch G, Franca M, Olmo MFD, Cheeran B, Milton R, Saucó MA, Rothwell JC (2006) Time course of functional connectivity between dorsal premotor and contralateral motor cortex during movement selection. *J Neurosci* 26:7452–9.
- Kolb B, Wishaw IQ (1996) *Fundamentals of human neuropsychology* Freeman, New York.
- Kolev V, Yordanova J, Basar-Eroglu C, Basar E (2002) Age effects on visual eeg responses reveal distinct frontal alpha networks. *Clin Neurophysiol* 113:901–10.
- Kopell N, Ermentrout GB, Whittington MA, Traub RD (2000) Gamma rhythms and beta rhythms have different synchronization properties. *Proc Natl Acad Sci USA* 97:1867–72.
- Labyt E (2003) Changes in oscillatory cortical activity related to a visuomotor task in young and elderly healthy subjects. *Clinical Neurophysiology* 114:1153–1166.
- Labyt E, Cassim F, Szurhaj W, Bourriez JL, Derambure P (2006) Oscillatory cortical activity related to voluntary muscle relaxation: influence of normal aging. *Clin Neurophysiol* 117:1922–30.
- Labyt E, Szurhaj W, Bourriez JL, Cassim F, Defebvre L, Destée A, Derambure P (2004) Influence of aging on cortical activity associated with a visuo-motor task. *Neurobiol Aging* 25:817–27.
- Lachaux JP, Rodriguez E, Martinerie J, Varela FJ (1999) Measuring phase synchrony in brain signals. *Hum. Brain Mapp.* 8:194–208.
- Lee L, Siebner HR, Rowe JB, Rizzo V, Rothwell JC, Frackowiak RSJ, Friston KJ (2003) Acute remapping within the motor system induced by low-frequency repetitive transcranial magnetic stimulation. *J Neurosci* 23:5308–18.
- Lehmann EL, Casella G (1998) *Theory of Point Estimation* Springer Verlag, New York.
- Leocani L, Cohen LG, Wassermann EM, Ikoma K, Hallett M (2000) Human corticospinal excitability evaluated with transcranial magnetic stimulation during different reaction time paradigms. *Brain* 123 (Pt 6):1161–73.
- Lutzenberger W, Elbert T, Rockstroh B, Birbaumer N (1985) *Das EEG* Springer Verlag, Berlin.

- Madden DJ, Spaniol J, Whiting WL, Bucur B, Provenzale JM, Cabeza R, White LE, Huettel SA (2007) Adult age differences in the functional neuroanatomy of visual attention: a combined fmri and dti study. *Neurobiol Aging* 28:459–76.
- Maestú F, Campo P, Gil-Gregorio P, Fernández S, Fernández A, Ortiz T (2006) Medial temporal lobe neuromagnetic hypoactivation and risk for developing cognitive decline in elderly population: a 2-year follow-up study. *Neurobiol Aging* 27:32–7.
- Maestú F, Fernandez A, Simos PG, López-Ibor MI, Campo P, Criado J, Rodriguez-Palancas A, Ferre F, Amo C, Ortiz T (2004) Profiles of brain magnetic activity during a memory task in patients with alzheimer’s disease and in non-demented elderly subjects, with or without depression. *J Neurol Neurosurg Psychiatr* 75:1160–2.
- Mars RB, Klein MC, Neubert FX, Olivier E, Buch ER, Boorman ED, Rushworth MFS (2009) Short-latency influence of medial frontal cortex on primary motor cortex during action selection under conflict. *J Neurosci* 29:6926–31.
- Mattay VS, Fera F, Tessitore A, Hariri AR, Das S, Callicott JH, Weinberger DR (2002) Neurophysiological correlates of age-related changes in human motor function. *Neurology* 58:630–5.
- May A, Hajak G, Gänsbauer S, Steffens T, Langguth B, Kleinjung T, Eichhammer P (2007) Structural brain alterations following 5 days of intervention: dynamic aspects of neuroplasticity. *Cereb Cortex* 17:205–10.
- Medendorp WP, Beurze SM, Pelt SV, Werf JVD (2008) Behavioral and cortical mechanisms for spatial coding and action planning. *Cortex* 44:587–97.
- Miltner WH, Braun C, Arnold M, Witte H, Taub E (1999) Coherence of gamma-band eeg activity as a basis for associative learning. *Nature* 397:434–6.
- Mima T, Hallett M (1999) Electroencephalographic analysis of cortico-muscular coherence: reference effect, volume conduction and generator mechanism. *Clin Neurophysiol* 110:1892–9.
- Minati L, Grisoli M, Bruzzone MG (2007) Mr spectroscopy, functional mri, and diffusion-tensor imaging in the aging brain: a conceptual review. *J Geriatr Psychiatry Neurol* 20:3–21.
- Moazami-Goudarzi M, Sarnthein J, Michels L, Moukhtieva R, Jeanmonod D (2008) Enhanced frontal low and high frequency power and synchronization in the resting eeg of parkinsonian patients. *NeuroImage* 41:985–97.

- Mognon A, Jovicich J, Bruzzone L, Buiatti M (2010) Adjust: An automatic eeg artefact detector based on the joint use of spatial and temporal features. *Psychophysiology* in press.
- Molins A, Stufflebeam SM, Brown EN, Hämäläinen MS (2008) Quantification of the benefit from integrating meg and eeg data in minimum l2-norm estimation. *NeuroImage* 42:1069–77.
- Montez T, Poil SS, Jones BF, Manshanden I, Verbunt JPA, van Dijk BW, Brussaard AB, van Ooyen A, Stam CJ, Scheltens P, Linkenkaer-Hansen K (2009) Altered temporal correlations in parietal alpha and prefrontal theta oscillations in early-stage alzheimer disease. *Proc Natl Acad Sci USA* 106:1614–9.
- Naccarato M, Calautti C, Jones PS, Day DJ, Carpenter TA, Baron JC (2006) Does healthy aging affect the hemispheric activation balance during paced index-to-thumb opposition task? an fmri study. *NeuroImage* 32:1250–6.
- Nichols TE, Holmes AP (2002) Nonparametric permutation tests for functional neuroimaging: a primer with examples. *Human Brain Mapping* 15:1–25.
- Niedermeyer E (1997) Alpha rhythms as physiological and abnormal phenomena. *International Journal of Psychophysiology* 26:31–49.
- Nunez P, Srinivasan R (2006) *Electric fields of the brain* Oxford University Press, New York.
- Oldfield RC (1971) The assessment and analysis of handedness: the edinburgh inventory. *Neuropsychologia* 9:97–113.
- Oliviero A, Strens LHA, Lazzaro VD, Tonali PA, Brown P (2003) Persistent effects of high frequency repetitive tms on the coupling between motor areas in the human. *Experimental Brain Research* 149:107–13.
- O’Reardon J, Solvason H, Janicak P, Sampson S, Isenberg K, Nahas Z, McDonald W, Avery D, Fitzgerald P, Loo C, Demitrack M, George M, Sackeim H (2007) Efficacy and safety of transcranial magnetic stimulation in the acute treatment of major depression: a multisite randomized controlled trial. *Biol Psychiatry* 62:1208–1216.
- O’Shea J, Sebastian C, Boorman ED, Johansen-Berg H, Rushworth MFS (2007) Functional specificity of human premotor-motor cortical interactions during action selection. *Eur J Neurosci* 26:2085–95.

- Palva S, Palva JM (2007) New vistas for alpha-frequency band oscillations. *Trends Neurosci* 30:150–8.
- Papadelis C, Poghosyan V, Fenwick PBC, Ioannides AA (2009) Meg’s ability to localise accurately weak transient neural sources. *Clin Neurophysiol* 120:1958–70.
- Pascual-Marqui RD (2002) Standardized low-resolution brain electromagnetic tomography (sloreta): technical details. *Methods and findings in experimental and clinical pharmacology* 24 Suppl D:5–12.
- Peinemann A, Lehner C, Conrad B, Siebner HR (2001) Age-related decrease in paired-pulse intracortical inhibition in the human primary motor cortex. *Neuroscience Letters* 313:33–6.
- Pfurtscheller G (1992) Event-related synchronization (ers): an electrophysiological correlate of cortical areas at rest. *Electroencephalogr Clin Neurophysiol* 83:62–9.
- Pfurtscheller G, Aranibar A (1977) Event-related cortical desynchronization detected by power measurements of scalp eeg. *Electroencephalogr Clin Neurophysiol* 42:817–26.
- Plewnia C, Reimold M, Najib A, Reischl G, Plontke SK, Gerloff C (2007) Moderate therapeutic efficacy of positron emission tomography-navigated repetitive transcranial magnetic stimulation for chronic tinnitus: a randomised, controlled pilot study. *J Neurol Neurosurg Psychiatr* 78:152–6.
- Plewnia C, Bartels M, Gerloff C (2003a) Transient suppression of tinnitus by transcranial magnetic stimulation. *Ann Neurol*. 53:263–6.
- Plewnia C, Lotze M, Gerloff C (2003b) Disinhibition of the contralateral motor cortex by low-frequency rtms. *Neuroreport* 14:609–12.
- Plewnia C, Rilk AJ, Soekadar SR, Arfeller C, Huber HS, Sauseng P, Hummel F, Gerloff C (2008) Enhancement of long-range eeg coherence by synchronous bifocal transcranial magnetic stimulation. *Eur J Neurosci* 27:1577–83.
- Pockett S, Bold GEJ, Freeman WJ (2009) Eeg synchrony during a perceptual-cognitive task: widespread phase synchrony at all frequencies. *Clin Neurophysiol* 120:695–708.
- Rao SM, Binder JR, Bandettini PA, Hammeke TA, Yetkin FZ, Jesmanowicz A, Lisk LM, Morris GL, Mueller WM, Estkowski LD (1993) Functional magnetic resonance imaging of complex human movements. *Neurology* 43:2311–8.
- Robinson S, Vrba J (1998) *Recent advances in biomagnetism*, pp. 302–305 Tohoku University Press, Sendai.

- Roelfsema PR, Engel AK, König P, Singer W (1997) Visuomotor integration is associated with zero time-lag synchronization among cortical areas. *Nature* 385:157–61.
- Roland PE, Zilles K (1996) Functions and structures of the motor cortices in humans. *Curr Opin Neurobiol* 6:773–81.
- Rossini PM, Forno GD (2004) Integrated technology for evaluation of brain function and neural plasticity. *Physical medicine and rehabilitation clinics of North America* 15:263–306.
- Rossini PM, Rossi S, Babiloni C, Polich J (2007) Clinical neurophysiology of aging brain: from normal aging to neurodegeneration. *Prog Neurobiol* 83:375–400.
- Rudiak D, Marg E (1994) Finding the depth of magnetic brain stimulation: a re-evaluation. *Electroencephalogr Clin Neurophysiol* 93:358–71.
- Schnitzler A, Gross J (2005a) Functional connectivity analysis in magnetoencephalography. *Int Rev Neurobiol* 68:173–95.
- Schnitzler A, Gross J (2005b) Normal and pathological oscillatory communication in the brain. *Nat Rev Neurosci* 6:285–296.
- Serrien DJ, Strens LHA, Oliviero A, Brown P (2002) Repetitive transcranial magnetic stimulation of the supplementary motor area (sma) degrades bimanual movement control in humans. *Neurosci Lett* 328:89–92.
- Singer W (1993) Neuronal representations, assemblies and temporal coherence. *Prog Brain Res* 95:461–74.
- Singer W, Gray CM (1995) Visual feature integration and the temporal correlation hypothesis. *Annu Rev Neurosci* 18:555–86.
- Singh KD, Barnes GR, Hillebrand A (2003) Group imaging of task-related changes in cortical synchronisation using nonparametric permutation testing. *NeuroImage* 19:1589–601.
- Singh KD, Barnes GR, Hillebrand A, Forde EME, Williams AL (2002) Task-related changes in cortical synchronization are spatially coincident with the hemodynamic response. *NeuroImage* 16:103–14.
- Smith CD, Umberger GH, Manning EL, Slevin JT, Wekstein DR, Schmitt FA, Markesbery WR, Zhang Z, Gerhardt GA, Kryscio RJ, Gash DM (1999) Critical decline in fine motor hand movements in human aging. *Neurology* 53:1458–61.

- Stefan K, Kunesch E, Cohen LG, Benecke R, Classen J (2000) Induction of plasticity in the human motor cortex by paired associative stimulation. *Brain* 123 Pt 3:572–84.
- Stoffers D, Bosboom JLW, Deijen JB, Wolters EC, Berendse HW, Stam CJ (2007) Slowing of oscillatory brain activity is a stable characteristic of parkinson's disease without dementia. *Brain* 130:1847–60.
- Strafella AP, Paus T, Fraraccio M, Dagher A (2003) Striatal dopamine release induced by repetitive transcranial magnetic stimulation of the human motor cortex. *Brain* 126:2609–15.
- Strens LHA, Oliviero A, Bloem BR, Gerschlagel W, Rothwell JC, Brown P (2002) The effects of subthreshold 1 hz repetitive tms on cortico-cortical and interhemispheric coherence. *Clin Neurophysiol* 113:1279–85.
- Talelli P, Ewas A, Waddingham W, Rothwell JC, Ward NS (2008) Neural correlates of age-related changes in cortical neurophysiology. *NeuroImage* 40:1772–81.
- Talelli P, Greenwood R, Rothwell J (2007) Exploring theta burst stimulation as an intervention to improve motor recovery in chronic stroke. *Clin Neurophysiol* 118:333–342.
- Talelli P, Waddingham W, Ewas A, Rothwell JC, Ward NS (2008) The effect of age on task-related modulation of interhemispheric balance. *Experimental brain research Experimentelle Hirnforschung Expérimentation cérébrale* 186:59–66.
- Tallon-Baudry C, Bertrand O (1999) Oscillatory gamma activity in humans and its role in object representation. *Trends Cogn Sci (Regul Ed)* 3:151–162.
- Terry K, Griffin L (2008) How computational technique and spike train properties affect coherence detection. *J Neurosci Methods* 168:212–23.
- Thoenissen D, Zilles K, Toni I (2002) Differential involvement of parietal and precentral regions in movement preparation and motor intention. *J Neurosci* 22:9024–34.
- Traub RD, Whittington MA, Stanford IM, Jefferys JG (1996) A mechanism for generation of long-range synchronous fast oscillations in the cortex. *Nature* 383:621–4.
- Vallesi A, McIntosh AR, Kovacevic N, Chan SCC, Stuss DT (2010) Age effects on the asymmetry of the motor system: Evidence from cortical oscillatory activity. *Biological Psychology* 85:213–218.
- Vallesi A, McIntosh AR, Stuss DT (2009) Temporal preparation in aging: a functional mri study. *Neuropsychologia* 47:2876–81.

- von Stein A, Sarnthein J (2000) Different frequencies for different scales of cortical integration: from local gamma to long range alpha/theta synchronization. *International Journal of Psychophysiology* 38:301–13.
- Vrba J (2001) Multichannel squid biomagnetic systems pp. 1–79.
- Vrba J, Robinson SE (2001) Signal processing in magnetoencephalography. *Methods* 25:249–71.
- Ward NS, Frackowiak RSJ (2003) Age-related changes in the neural correlates of motor performance. *Brain* 126:873–88.
- Wassermann EM (1998) Risk and safety of repetitive transcranial magnetic stimulation: report and suggested guidelines from the international workshop on the safety of repetitive transcranial magnetic stimulation, June 5-7, 1996. *Electroencephalogr Clin Neurophysiol* 108:1–16.
- Weiss S, Rappelsberger P (2000) Long-range eeg synchronization during word encoding correlates with successful memory performance. *Brain research Cognitive brain research* 9:299–312.
- Welford AT (1988) Reaction time, speed of performance, and age. *Annals of the New York Academy of Sciences* 515:1–17.
- Winterer G, Coppola R, Egan MF, Goldberg TE, Weinberger DR (2003) Functional and effective frontotemporal connectivity and genetic risk for schizophrenia. *Biol Psychiatry* 54:1181–92.
- Wise SP, Boussaoud D, Johnson PB, Caminiti R (1997) Premotor and parietal cortex: corticocortical connectivity and combinatorial computations. *Annu Rev Neurosci* 20:25–42.
- Wolters A, Sandbrink F, Schlottmann A, Kunesch E, Stefan K, Cohen LG, Benecke R, Classen J (2003) A temporally asymmetric hebbian rule governing plasticity in the human motor cortex. *Journal of Neurophysiology* 89:2339–45.
- Ziegler DA, Pritchett DL, Hosseini-Varnamkhasti P, Corkin S, Hämäläinen M, Moore CI, Jones SR (2010) Transformations in oscillatory activity and evoked responses in primary somatosensory cortex in middle age: A combined computational neural modeling and meg study. *NeuroImage* .

List of Figures

1.1	Examples of the Magnitude of various Magnetic Fields	9
2.1	Experimental Setup of the study on visuomotor integration	17
2.2	Pinch grip and visual feedback	17
2.3	Schematic representation of the xperimental procedure of one block of the study on visuo-motor integration	19
2.4	Example of performance of the visuo-motor integration task	20
2.5	Power spectra of rest, task, and rest-task activity for Group I and Group IV, condition VM	24
2.6	Mean coherence for left M1/ SI – left visual area of rest, task, and rest-task activity for all age groups, condition VM	25
2.7	Scalp positions of EEG electrodes and ROIs	26
2.8	Simulated data	28
2.9	Results of the group level analysis MEG source activity, Group I <i>vs.</i> Group IV	30
2.10	Mean Δ Power alpha and beta range at left and right M1/ SI conditions VM <i>vs.</i> V and V + M <i>vs.</i> V, Group I	31
2.11	Mean Δ Power alpha range at left parietal cortex Group I conditions VM <i>vs.</i> V and V + M	32
2.12	Mean Δ Power beta range at right parietal cortex Group I conditions VM <i>vs.</i> V and V + M	32
2.13	Mean Δ Power alpha and beta range at left and right M1/ SI conditions VM <i>vs.</i> V and V + M <i>vs.</i> V, Group IV	33
2.14	Mean Δ Power beta range at left and right prefrontal cortex Group IV condition VM	34
2.15	Mean Δ Power beta range at right parietal cortex Group IV conditions VM <i>vs.</i> V and V + M	35
2.16	Comparison Group I <i>vs.</i> Group IV mean Δ Power alpha and beta range at left and right M1/ SI condition VM	36

2.17	Comparison Group I <i>vs.</i> Group IV mean Δ Power beta range at left and right prefrontal cortex condition VM	37
2.18	Comparison Group I <i>vs.</i> Group IV mean Δ Power alpha range left SII conditions VM and V + M	37
2.19	Comparison Group I <i>vs.</i> Group IV mean Δ Power beta range left SII condition VM	38
2.20	Comparison Group I <i>vs.</i> Group IV mean Δ Coherence beta range left M1/SI – right visual area condition VM	38
2.21	Comparison Group I <i>vs.</i> Group IV mean Δ Coherence beta range left prefrontal cortex – left visual area condition VM	39
2.22	Mean Δ Power alpha range at FC3-CP3 and FC4-CP4 Group I conditions VM <i>vs.</i> V and V + M <i>vs.</i> V	40
2.23	Mean Δ Power beta range at P7-P3 Group I conditions VM <i>vs.</i> V and V + M <i>vs.</i> V	40
2.24	Mean Δ Power alpha range at FC3-CP3 and FC4-CP4 Group IV conditions VM <i>vs.</i> V and V + M <i>vs.</i> V	41
3.1	Stimulation locations and coil positions for bifocal stimulation	53
3.2	Schematic representation of the experimental procedure of the Study Asynchronous Bifocal Stimulation	54
3.3	Scalp positions of EEG electrodes and ROIs	55
3.4	Time Windows	56
3.5	Power spectra at FC3CP3 and O1Oz for the first sliding window (0-60 s) <i>vs.</i> an average across 150 s for condition 0 ms	56
3.6	Power Spectra Bipolar Channels Main Effect: Condition	59
3.7	Power Spectra Bipolar Channels Main Effect: Recordings	60
3.8	Power Spectra Bipolar Channels Significant Interaction: Channels \times Recordings	60
3.9	Coherence: bipolarized channels, averaged across subjects for all conditions, time range 0 to 150 s	62
3.10	Coherence: bipolarized channels, averaged across subjects for all conditions, time range 0 to 60 s	63
3.11	Coherence bipolar channels main effect Recordings	64
3.12	Short term effects for all conditions	65
3.13	Coherence bipolar channels main effect Time Windows: Condition random	66

List of Tables

2.1	Participants of the study on visuo-motor integration	16
2.2	Selected ROIs for the study on visuo-motor integration	22
2.3	Summary of the Results of the First Study: Visuo-motor Integration and Age Dependent Alterations. Comparisons of Conditions for Single Groups. MEG and EEG Data.	42
2.4	Summary of the Results of the First Study: Visuo-motor Integration and Age Dependent Alterations. Comparisons between the two extreme Groups. MEG Data.	43
3.1	Summary of the Results of the Second Study: Asynchronous Bifocal Stimulation	67

Personal Contribution to the Studies

First Study: Visuo-motor Integration Together with Prof. Dr. Christoph Braun, Dr. Albrecht Rilk, and Prof. Dr. Christian Plewnia I planned the study and designed the experimental setup for the original study on the first age group. I collected the data of the first age group with the help of Elke Buletta and Dr. Albrecht Rilk.

Prof. Dr. Christoph Braun, Prof. Dr. Gerhard Eschweiler and Dr. Surjo Soekadar helped me maturing the idea to investigate age dependent alterations using this experimental setup. Prof. Dr. Gerhard Eschweiler and the team of the Geriatisches Zentrum supported recruiting the fourth age group. The data of the three elderly age groups I collected alone. The structural MRIs of all subjects I obtained with the help of Dr. Anja Wühle, Sabine Frank, Dr. Ralf Veit, and Dr. Constantin Mänz. The principle strategy of the data analysis was developed by Dr. Christos Papadelis and these results of the first age group will be published separately in an article with Dr. Papadelis being first author. I adapted the analysis strategy, modified it and wrote the scripts and routines for running the analysis merely automatically. I compared the results of the manual performed data analysis by Dr. Christos Papadelis on the first age group with the results of running my scripts. The results of the data of the first age group reported in this thesis are the ones I performed for the comparison. I performed the analysis of all other age groups by myself. The part in the Method section of this study describing the details of the SAM beamforming analysis was written together with Dr. Christos Papadelis for the publication of the data of the first age group.

Second Study: Asynchronous Bifocal Stimulation I planned the study and designed the experimental setup together with Prof. Dr. Christian Plewnia. I collected the data with the help of Maren Reinl. The ocular artifact correction of the EEG data was done by Andrea Mognon in order to test the reliability of his recently introduced toolbox (Mognon et al. 2010). Together with my supervisor Prof. Dr. Christoph Braun I developed the routines for the data analyses. For the results reported here, I adapted the routines and performed the analysis.

Curriculum Vitae

Personal Profile

Name	Carola Renate Ilse Arfeller
Date of Birth	10/01/1980
Place of Birth	Leipzig, Germany
Nationality	German

Education

since 02/2008	PhD studies at the Graduate School of Neural and Behavioural Sciences (International Max Planck Research School and Eberhard Karls University Tübingen, Germany)
10/1999 – 03/2006	Studies in Biology, Psychology, Biological Anthropology (M. Sc.), Friedrich Schiller University Jena, Germany Degree: <i>Magistra Scientiarum</i> (grade: 1.8) Thesis (Magisterarbeit): „Frühe Diskriminierung hoch- vs. niedrig erregender Reize? Eine Untersuchung von Ereigniskorrelierten Potentialen während der Verarbeitung dargebotener schematischer Bilder in einem Rapid Serial Visual Presentation-Paradigma bei Spinnenphobikern, Sozialphobikern und Kontrollpersonen“
04/1999 – 09/1999	Studies in Law, Friedrich Schiller University Jena, Germany
1991 – 1998	Grammar School: Friedrichgymnasium Altenburg, Germany Degree: <i>Abitur</i> (grade: 2.3)
1990 – 1991	Secondary School: POS Karl Liebkecht Rositz, Germany
1986 – 1990	Primary School: Karl Liebkecht Rositz, Germany

Professional Experiences

- since 01/ 2010 Researcher at the CIMeC - Center for Mind/ Brain Science, University of Trento, Italy
- 04/ 2009 – 12/ 2009 PhD Student at the MEG Centre of the Eberhard Karls University Tübingen, Germany
- 01/ 2007 – 03/ 2009 Research Assistant in the Research Group Brainstimulation (Neurophysiology and Interventional Psychiatry) at the Department of Psychiatry of the Eberhard Karls University Tübingen, Germany
- 11/ 2006 – 12/ 2006 Training in neuronavigated TMS in the Research Group on Multimodal Brain Imaging by combining TMS and fMRI at the Max Planck Institute for Biological Cybernetics Tübingen, Germany
- 08/ 2006 – 12/ 2006 Research Internship in the Research Group Brainstimulation (Neurophysiology and Interventional Psychiatry) at the Department of Psychiatry of the Eberhard Karls University Tübingen, Germany
- 09/ 2004 – 09/ 2005 Student Assistant: Chair on Biological and Clinical Psychology, Institute of Psychology, Friedrich Schiller University Jena, Germany
- 04/ 2003 – 12/ 2003 Initiation of and participation in an interdisciplinary institute spanning project between the Junior Scientists Group on Cultural Ontogeny, Max Planck Institute for Evolutionary Anthropology Leipzig, and the Chair on Biological and Clinical Psychology, Friedrich Schiller University Jena, Germany
- 10/ 2002 – 03/ 2003 Student Assistant in Junior Scientists Group on Cultural Ontogeny, Max Planck Institute for Evolutionary Anthropology Leipzig, Germany
- 08/ 2002 – 10/ 2002 Internship in Junior Scientists Group on Cultural Ontogeny, Max Planck Institute for Evolutionary Anthropology Leipzig, Germany
- 09/ 1998 – 12/ 1998 Stay at Fiji Islands and Kiribati, meanwhile voluntary service: International School Suva, Fiji Islands

Grants and Fellowships

- 04/ 2009 – 03/ 2010 Scholarship from the Werner Reichardt Centre for Integrative Neuroscience (CIN) Eberhard Karls University Tübingen, Germany

Skills

Neuroscientific Methods	functional Magnetic Resonance Tomography Magnetoencephalography Transcranial Magnetic Stimulation (neuronavigated) Electroencephalography Behavioural Studies in Infants
Organizing	Autumn School at the MEG Center Tübingen, Germany in 2008 and 2009 (www.mp.uni-tuebingen.de) NeNa (Conference of the Junior Neuroscientists of Tübingen) in 2008 and 2009: advertising poster and abstract book (www.neuroschool-tuebingen-nea.de)
Raising Funds	Fast Oscillatory Activity in Human visual and auditory cortex Funding Period: 2009 – 2010 by the CIN (Werner Reichard Centre for Integrative Neuroscience - CIN University of Tübingen) Safety and Effectiveness of Repetitive Transcranial Magnetic Stimulation in the Treatment of Tinnitus Funding Period: 2007 – 2009 by the DFG (Deutsche Forschungsgemeinschaft), www.clinicaltrials.gov , NCT00518024
Management of Clinical Trial	Safety and Effectiveness of Repetitive Transcranial Magnetic Stimulation in the Treatment of Tinnitus

List of Publications

Articles

Cattaneo L, Barchiesi G, Tabarelli D, **Arfeller C**, Sato M, Glenberg AM (in press). One's motor performance predictably modulates the understanding of others' actions through adaptation of premotor visuo-motor neurons. *Social Cognitive and Affective Neuroscience*

Arfeller C, Vonthein R, Plontke S, Plewnia C (2009). Effectiveness and safety of bilateral continuous theta burst stimulation (cTBS) for the treatment of chronic tinnitus. *Trials*, 10: 74

Soekadar S, **Arfeller C**, Rilk A, Plontke S, Plewnia C (2009). Theta burst stimulation in the treatment of incapacitating tinnitus accompanied by severe depression. *CNS Spectrums*, 14(4): 208–211

Plewnia C, Rilk AJ, Soekadar SR, **Arfeller C**, Huber HS, Sauseng P, Hummel F, Gerloff C (2008). Enhancement of long-range EEG coherence by synchronous bifocal transcranial magnetic stimulation. *European Journal of Neuroscience* 27(6), 1577–1583

Conference Proceedings

Papadelis C, **Arfeller C**, Erla S, Nollo G, Plewnia C and Braun C (2010). Visuo-motor integration enhances coherent sources in the human brain. 17th International Conference on Biomagnetism 2010: T-II T6-9

Arfeller C, Papadelis C, Rilk AJ, Soekadar SR, Plewnia C, Braun C (2009). Coherent sources in the human brain during visuo-motor integration. 39th Annual Meeting SfN Chicago 2009: P853.7

Soekadar SR, Schwarz A, Schmid AC, Sinis N, **Arfeller C**, Bartels M, Plewnia C. Treatment of Complex Regional Pain Syndrom (CRPS) by neuro-navigated Theta Burst Stimulation (TBS). *Forschungskolloquium der Medizinischen Fakultät Tübingen* 2008: P11

Arfeller C, Braun C, Rilk AJ, Soekadar SR, Plewnia C. Oscillatory correlates of visuo-motor integration: Investigation of healthy controls and schizophrenic patients. 8. NeNa Freudenstadt 2007: P01

Soekadar SR, Rilk AJ, Bremme P, **Arfeller C**, Braun C, Plewnia C. Cortico-cortical coherence and performance in a visuo-motor integration task in schizophrenic patients. DGPPN Berlin 2007: P026–07

Soekadar SR, Rilk AJ, **Arfeller C**, Laske C, Plewnia C. Treatment of incapacitating tinnitus by theta burst stimulation (TBS). DGPPN Berlin 2007: P003–11

Plewnia C, **Arfeller C**, Rilk AJ, Soekadar SR, Huber H, Hummel F, Gerloff C. Modulation of long-range EEG coherence by bifocal transcranial magnetic stimulation. 37th Annual Meeting SfN San Diego 2007: P791.16

Soekadar SR, Braun C, Rilk AJ, **Arfeller C**, Bremme P, Plewnia C. EEG dynamics in visuo-motor integration of schizophrenic patients. 1st European Conference on Schizophrenia Research Düsseldorf 2007: P09–09

Kolassa IT, Musial F, **Arfeller C**, Trippe RH, Miltner WHR. Early discrimination of high- vs. low-arousing stimuli? A study of event-related potentials in a rapid serial visual presentation paradigm with spider phobics, social phobics and controls. 30. APM Freiburg 2004: P80

Talks

- | | |
|------|--|
| 2009 | Selected research and clinical applications of Transcranial Magnetic Stimulation. Institute Seminar CIMeC Trento |
| 2008 | Enhancement of long-range EEG coherence by synchronous bifocal transcranial magnetic stimulation. NeNa Ellwangen |